Rijksdienst voor Ondernemend Nederland

SUCCEED

Accelerating CCS Technologies

SUCCEED

Final Report for RVO

Public version

February 2024

Principal Researchers:
Dr. K-H.A.A. Wolf, Dr. R. de Kunder, Dr. A. Barnhoorn, Dr. D. Draganov, Dr. M. Janssen

TU Delft

seismic mechatronics

Within the SUCCEED ACT-program, the contracting parties are:

Partner	Abbrevation	Country
Imperial College London	**(ICL)**	United Kingdom
Middle East Technical University	**(METU)**	Turkey
Zorlu Enerji Elektrik Uretim AS	**(Zorlu)**	Turkey
Technische Universiteit Delft	**(DUT)**	Netherlands
Silixa Limited	**(Silixa)**	UK
Seismic Mechatronics BV)	**(SM)**	Netherlands
Orkuveita Reykjavíkur	**(OR)**	Iceland
OGS	**(OGS)**	Italy

For the Dutch part of the program, the contracting parties are:

Partner	Country	Status
Technische Universiteit Delft	Netherlands	Active participant
Seismic Mechatronics BV	Netherlands	Active participant
Veegeo BV **(Now Sproule BV)**	Netherlands	Observer for Dutch stakeholders

Final public report of the SUCCEED project

The confidential final report describes the activities and results of the project and includes the following topics:	
Theme	Page number
1. Gegevens project	
□ Projectnummer / Project codes □ Projecttitel / Project title □ Penvoerder en medeaanvragers / Project administrator and partners □ Projectperiode / Project period	
2. Inhoudelijk eindrapport	
□ Samenvatting / Summary	
□ Inleiding / Introduction	
□ Doelstelling / Goals	
□ Werkwijze / Methods	
□ Resultaten A) van het project zelf / Results A) of the RVO part of the project	
□ Resultaten B) mogelijkheden voor spin off en vervolgactiviteiten / Results B) opportunities for spinn off and continuation	
□ Discussie / discussion	
□ Conclusie en aanbevelingen / Conclusions and recommendation	
3. Uitvoering van het project	
□ Toelichting wijze van kennisverspreiding / Dissemination	
□ Toelichting PR project en verdere PR-mogelijkheden / Public relation activities	
□ Dankbetuigingen / Acknowledgements	
NOTE: because of the international nature of the partner's employees, researchers and research, this confidential report has been written in English. It will be followed by a public Dutch written resume.	

Acknowledgements

"Het project is uitgevoerd met subsidie van het Ministerie van Economische Zaken, Nationale regelingen EZ-subsidies, Topsector Energie uitgevoerd door Rijksdienst voor Ondernemend Nederland."

"The project was carried out with subsidy from the Ministry of Economic Affairs, National regulations for Economic Affairs subsidies, Top Sector Energy implemented by the Netherlands Enterprise Agency."

Acknowledgements II

SUCCEED is funded through the ACT programme (Accelerating CCS Technologies, Horizon 2020 Project No 294766). Financial contributions made by the Department for Business, Energy & Industrial Strategy UK (BEIS), ***the Rijksdienst voor Ondernemend Nederland (RVO)***, the Scientific and Technological Research Council of Turkey (TUBITAK), and our research partners Orkuveita Reykjavíkur/Reykjavik Energy Iceland (OR) and Istituto Nazionale di Oceanografia e di Geofisica Sperimentale Italy (OGS) are gratefully acknowledged.

Final public report of the SUCCEED project

1. Project information

Project codes	VO 18009 in the ACT - Era-Net Energycall Act ACT –Accelerating CCS Technologies" Project No: 299670
Project title	SUCCEED - Synergetic Utilisation of CO2 storage Coupled with geothermal Energy Deployment
Project administrator and partners	- Delft University of Technology – Administrator - Seismic Mechatronics - Veegeo BV – Observing Partner
Project period	01/09/2019 – 01/08/2022 and two times extended up to 01/03/2024

Table 1: Partner organizations, their contributing members and expertise.

Participating Project Members.	**Role**
Delft University of Technology	
Dr. K-H.A.A. Wolf DUT-CEG k.h.a.a.wolf@tudelft.nl	*Associate Professor for Petrophysics/Porous media* • Project Coordinator for the Netherlands. • Researcher for the petrophysics, petrography, geology, reservoir engineering and image analysis issues. • Communication with ICL, OR, METU, Zorlu and SM on Geotechnical Experimental work, fieldwork programs and field/lab data translations.
Dr. D. Draganov DUT-CEG d.s.draganov@tudelft.nl	*Associate Professor for Geophysics* • Responsible for the applied geophysics part of the fieldwork, i.e. the implementation and use of the landlines, cable planning and organization. • Main researcher for theory development and the data handling of the conventional seismic data and fiber optics data obtained during the fieldworks. • In cooperation with Dr. M. Janssen performing the large scale borehole simulator experiments. • Close communication regarding all geophysics activities with ICL, SM, Silixa and OGS.
Dr. A. Barnhoorn Associate Professor DUT-CEG auke.barnhoorn@tudelft.nl	*Associate Professor for Petrophysics/Rock-mechanics, director of the DUT-CEG geoscience and engineering laboratory.* • Responsible for rock sampling during the field sessions, sample preparation for lab work at DUT, ICL and METU. • In cooperation with Dr. M. Janssen, responsible for all laboratory experiments.
Dr. M. Janssen DUT-CEG	*PD and principal researcher* • Responsible for sample transport to Delft, sample preparation, distribution of plugs and samples to the relevant partners. • Responsible for all mechanic-acoustic experiments, preparation and use of the uni/tri-axial cells and borehole simulator. Performing all related experiments and data-validity practises. • Lead for all publications, presentations and reporting.
J. van den Berg, DUT-CEG	*Principal Technician* • Responsible for seismic fieldwork, i.e. preparing and implementing geophone lines, performing the communication with SM, Silixa, OGS and OR. • Taking care of the monitoring and data-acquisition.

	• DUT-field technician for the eVibe. • Lab support for sample preparations and experimental device constructions.
M.Friebel TU-Delft, CEG	*Principal Technician* • Responsible for development, construction and experimental support of all HP,T-equipment and set-ups used in the project. • Technical field support during the field seismics and monitoring.
Ing. K.Heller TU-Delft, CEG	*Principal Technician* • Responsible for petrophysical measurements and data validation.
Ing. J.van Meel and Ing. E. Meijvogel TU-Delft, CEG	*Principal Technicians* • Responsible for all CT-scanning and related data dissemination between the partners.
S. Hassing Elara Redondo Garcia	*MSc-students* • For passive monitoring and interferometry • For sample petrology on Icelandic rock
Seismic Mechatronics	
R. de Kunder MSc. SM r.de.kunder@seismic-mechatronics.com https://seismic-mechatronics.com/contact/	*CEO* • and coordinator for fieldwork activities, time frames, equipment, and monitoring. • Communication with ICL, DUT, OGS, OR and Silixa for the seismic monitoring infrastructure and type of measurements.
J. Bos SM	*CFO* • Responsible for equipment and material transport. • Budget controller and purchaser of parts for the newly developed and constructed eVibe.
W. Roefs SM	*Technician-developer* • Software designer for the new eVibe.
Ing. G. van Otten SM	*Construction and field technician* • Technical constructor of the Evibe. • Field engineer for the Evibe seismic source, source control, generator and telehandler supervision during monitoring.
L. Koorneef SM & MI-Partners BV	Principal technician • Senior source operator and equipment developer (E-design).

2. Principal final report

Summary

SUCCEED is and Accelerating CCS Technologies (ACT) and RVO funded multi-national research and demonstration program were CO_2 storage, monitoring of sub-surface CO_2 dissemination and utilization of CO_2 for reservoir performance improvement, have been the realized. The project accelerated innovative and newly developed CCUS technologies, regarding seismic source application, monitoring, imaging, and verification at field scale utilizing of previously mentioned methods and techniques.
In two high-enthalpy geothermal fields, i.e. Hellisheiði (Iceland) and Kizildere (Turkey), continuous base-line geophysical monitoring has been performed with novel types of helically winded tactical fiberoptic lines, both at the surface and in wells (**WP1, WP3, WP4**)

- On Iceland TU-Delft (DUT) has been supporting the fieldwork in Juli 2021 to acquire passive and active-source data. During the acquisition, when the active source was not used, we acquired passive-source data recording ambient-noise seismic signals, including local, regional, and global seismicity. As the main aim, active-source data was acquired using the eVibe seismic vibrator from Seismic Mechatronics (SM) and the fiber-optic helically wound cable from Silixa as receivers. For calibration and quality verification, active-source data was also recorded by two-component cabled geophones (10 Hz) along the helically wound cable, from and installed by DUT. Additional recording was also done along two perpendicular lines of three-component stand-alone geophones temporarily lent from the project DEEPEN.
  After the injection phase (10000 tons) into a 2 km depth porous basalt layer, the second active monitoring was done with reference measurements by DUT (July 2022). This series of shots along the paths of the first survey was done by using the 10kN eVibe P-waves. The combination of data over time is used for time lapse imaging of CO2-dissemination.
- In Turkey, the DUT and the project partners completed the third active-source monitoring campaign on the ZORLU company geothermal site in Kizildere. Here, fiberoptic cables have been installed for 3D monitoring, both as surface lines and in two monitoring wells. In November 2022, prior to implementation and use of equipment for CO_2 injection, the baseline or monitoring acquisition was conducted. The data was acquired using the 10kN eVibe from SM, the fiber-optic helically wound cable from Silixa as being the 'continuous' receivers and, again, as a reference the parallel running temporary two-component cabled geophones (10 Hz) from DUT. The target reservoir is at ca 2 km depth in a porous marble zone, which acts as being the main production reservoir of geothermal steam.
  The fourth active monitoring can be done when all requirements have been fulfilled for CO_2 injection over a considerable time span. However, Zorlu has not followed on its commitment until now. Negotiations are continuing.

During the preparatory meetings for both fieldworks in Iceland – Hellisheiði and in Turkey – Kizildere, geological field surveys have been made to investigate the nature of the target reservoirs and overburden strata. These surveys resulted into the collection of representative rock samples from outcrops for the determination of the petrological, petrophysical acoustic-rock mechanic and geochemical base line properties.

The collections have been prepared for small scale to large scale experiments at the partner laboratories of ICL, METU and DUT **(WP1, WP2, WP3).**

- In February 2020 a fieldwork around Kilzildere resulted into the collection of ca. 2 tons of characteristic small and large blocks. The larger blocks are for the large-scale borehole simulator experiments on reservoir rock. Here we acknowledge the support by ZORLU Energy.
- However, with the travel restrictions by TU Delft because of the two spikes of Covid-19 sample, collection from Iceland has delayed significantly. For modelling purposes, literature data from a large number of previous research on Hellisheiði and the CarbFix project were used. In the autumn of 2019,in a first batch hand-size samples have been obtained of reservoir rock and examples of overburden types. In June 2021, after the lock downs and all snow gone, the geological survey and rock sampling of larger blocks has been finalized. Here we acknowledge the support of OR.

For both sites, samples have been prepared by DUT at various scales for the determination or strength partly in combination with acoustic velocities; reservoir properties for multi-phase flow, and rock fluid interaction during CCUS. Samples, including the previously mentioned base-line qualification and quantification have been sent to the partner laboratories of ICL and METU for time lapse quantification.
The following scales bulk sample preparations were used:

- At chemical level, the most relevant rocks for reservoir purposes have been analyzed by XRD and XRF to get a base-line geochemical fingerprint.
- Small (5 $cm^3$to 50 cm^3) cores for acoustic and rock-mechanical tests under various P,T and fluid/gas conditions and triaxial flow experiments with acoustic velocity measurements.
- Medium sized cylindrical samples of ca 100 cm^3 to ca 250 cm^3 for rock mechanics and geochemical tests.
- Large cylindrical samples of ca 75*10^3 cm^3 have been prepared for HP,T acoustic measurements of fractured reservoir rock and multi-phase flow.
- Quantifying imaging was used for thin section analysis and for CT-scans. The CT-scans were made of the virgin cylindric samples of the geothermal experiments. Both the micro-CT scanner and Dual-beam scanner have been applied for the requested resolutions. After the experiments in the geochemical HP,T cells, postmortem imaging was done. Image resolution depended on the type of scanning in between ca. 5 – 250 micrometers.

The experimental result from DUT includes acoustic speed measurements under stress, resulting into a series of acoustic impedance values and speeds for both the reservoirs and overburden rocks. The results have been used for time-depth acoustic modeling of both the Hellisheiði and Kizildere sites synthetical seismic image have been created without and with CO2 injection in which various geophone and source spacings have been applied. Those results are used for the fieldworks in Iceland and in Turkey. All findings are extensively described in reviewed articles (Appendices). The acoustic experiments in the Borehole simulator were done on large cores consisting of reservoir basalt (Iceland) and marble (Turkey). Both samples have an artificial fracture for convection of water, supercritical steam, and CO_2. The marble showed changes in reflection with the change of fluid phases, however, the marble did not show a phase change.
All geochemical, petrology/mineralogy, acoustic and rock mechanic data have been handed over to ICL for geochemical leaching experiments; to METU for rock mechanics and modeling purposes, and Silixa, OGS, OR and SM for field data interpretation, imaging and modeling.

In WP4, the project is dedicated to field monitoring of CO_2 injection operations, site performance and reservoir behavior at pilot geothermal field sites - Kizildere in Turkey and Hellisheiði in Iceland. At the start, al partners were involved in the conventional monitoring of well instrumentation and downhole pressure and temperature measurements, fluid sampling, tracer breakthrough before, during, after the proposed CO_2 injection period. SM concentrated on the development and field implementation of a repeatable vibrator (eVibe) for semi-continuous seismic monitoring. In essence, the new apparatus has a vibration range relevant to the high-dynamic range iDAS system for semi-continuous seismic monitoring. Seismic monitoring data processing and interpretation using semi-continuous eVibe and iDAS monitoring campaigns pre-during-post injection were consucted and the Hellisheiði micro- seismic data processing for potential for injection induced seismicity. SM, together with DUT, did the initial field data analysis in cooperation with Silixa and OGS for comparison of the base-line monitoring results. Further, in cooperation with DUT's conventional seismic results, all seismic monitoring data have been processed and interpreted. Here we mean the pre- during and post- monitoring campaigns at Hellisheiði and the pre- injection campaign at Kizildere.

For **WP5,** limited activities have been performed. DUT and SM provided support to ICL and METU for the static model based on results from the baseline seismic activities, well information and petrophysics, as basic elements (WP1,3,4) for the determination of a reservoir configuration with in-situ conditions. Hence, the field calibration of the new eVibe, data acquisition of Silixa and petrophysical labwork by OGS, ICL, METU and DUT, created static reservoir models and defined the overburden. This description then is be used by ICL and METU as a set of initial conditions for history-matching, and for predictive time dependent calculations of the effects

of fluid production and reinjection upon the reservoir.

In WP6, the development of optimized field and regional scale fluids and CO_2 injection strategies for long-term reservoir pressure maintenance and CO_2 storage in the geothermal fields. Here DUT and SM provided their input during the project meetings in London (ICL) and in Kizildere (ZORLU), on quantification of spatial characteristics for the interpretation of reservoir properties, overburden properties, geophysical imaging of the geological structure, extension of the reservoirs and overburden properties. It was based on fieldwork, petrophysical lab work in WP1,3,4 and 5 and professional knowledge from previous (other) project activities. It contributed to the creation of static and dynamic reservoir models and were an added value for the well selection and injection rate optimization for long term pressure maintenance, geothermal fluids production and minimization of injected CO_2 production and maximization of CO_2 storage.

In WP7, DUT and SM, took care of the understanding of public perception, which was embedded in demonstration activities showing researchers working in this project and bringing industry in contact with our findings. For community service DUT developed SUCCEED websites with regular update of field activities, laboratory work, modeling, and summaries for dissemination. In addition, web movies and short interviews were produced for the people at all, for high school students and for media. For Stakeholders, presentations were prepared and organized during conferences, special topic meetings, information through the Chamber of Commerce and websites. For training and educational activities, two workshops have been organized during which representatives of the central and local authorities, geothermal and environmental industry, and public bodies representing green initiatives, were informed. In addition, DUT implemented results of the SUCCEED in Circextin, an Action2 ERASMUS+ program for innovation and exchange of good practices. A MOOC was made for higher education for post-graduates. It involves underground storage and circular storage of CO_2 and H_2 and waste storage and disposal.

In WP8, DUT took the coordination of the project for The Netherlands, was the liaison with the project coordinator ICL and the Dutch program provider RVO. DUT helped to coordinate project matters like; Project Management and Technical Committee Meetings, Progress Meetings, writing meeting minutes, Project Team meetings and meeting results throughout the project period. In addition, DUT prepared this final report for all involvements of the Dutch partners in the annual reports for RVO. All reports are publicly available through RVO and the SUCCEED program.

The detailed experimental work done in WP1, WP3, WP4 and interactions with other WP's are summarized in the ACT reporting, publications, and presentations, *and - for RVO specific - here below in the results.*

Introduction

The SUCCEED project is a targeted innovation and research activity which aims to facilitate the emergence of CCUS via transnational cooperation. It is an industrial CCUS project, which focuses on CO_2 utilization and storage. It benefits from the existing facilities of producing geothermal fields at Kizildere in Turkey and Hellisheiði in Iceland. The project aims at accelerating and maturing CCUS technology application by developing, testing, and demonstrating at field scale innovative measurement, monitoring and verification technologies that can be used in most CO_2 geological storage projects. Fieldwork and laboratory are strongly intertwined to develop and improve new and existing geophysical, techno-geological, and geochemical techniques on seismic sources and registration methods. Improvement of time lapse monitoring, data acquisition and data transfer to reservoir and environmental modeling procedures improve the resolution of – in this case – injection of CO_2 for storage and reservoir quality improvement of geothermal reservoirs. Cooperation between experts from industry and research institutes provided the knowledge to succeed in this program.

Objectives of the project

The Netherlands are involved in the "Italic" part of the objectives and achievements.

The objectives of the project are:

i) *To research and demonstrate the feasibility of utilizing produced CO_2 (currently vented to the atmosphere in many geothermal fields) for re-injection to improve geothermal performance, while also storing the CO_2,*

ii) To develop further, test and demonstrate innovative monitoring technologies:
a. new higher signal-to-noise ratio distributed fiberoptic acoustic sensing system (iDAS)
b. new permanent and highly repeatable vibratory-type (environmentally friendly) seismic monitoring electric seismic-vibrators (EM), and to provide semi-continuous seismic monitoring capability, which will complement the already installed local micro seismic monitoring network and geochemical and tracer monitoring programs implemented at the field sites,

iii) To test and demonstrate the industrial CCUS opportunity for geothermal field operators to:
a. maintain and enhance reservoir pressure as the driving mechanism for the geothermal fluid and improve geothermal performance,
b. increase reservoir permeability and productivity while suppressing scaling by artificial acidification,

iv) To utilize advantageous operational field environments, facilitated by thermally and hydrologically active geothermal fields which are currently in production, for accelerated testing of CO_2 utilization, supercritical and dissolved CO_2 injection, reactive transport, and storage,

v) *To use a real field environment for the testing of supercritical and dissolved CO_2 injection into a reservoir and provide the geothermal energy sector with the means to address the current climate change challenge through CO_2 utilization and storage.*

The main expected achievements of the project are as follows:

- *Field testing and implementation of a new higher signal-to-noise ratio iDAS system and a new and novel vibratory-type electric seismic sources to provide layer-specific seismic monitoring capability for CCUS and geothermal applications.*
- Accelerated testing and assessment of the effectiveness, and *validation of several CO_2 injection and plume monitoring techniques* in carbonate reservoirs in the main, which have so far been only tested in sandstone reservoirs and one pilot study in carbonate systems.
- Further insights into the potential for injection induced seismicity in geothermal fields through monitoring and evaluation of data from a local seismic network at the Hellisheiði field in Iceland and comparison with the new monitoring technologies tested in this project.
- *An understanding of the fundamentals of field scale behavior of injected supercritical and dissolved CO_2 in geothermal reservoirs, and critical assessment of the theories developed at laboratory scale so far.*

- Strategies for pressure management in geothermal reservoirs through supercritical and dissolved CO_2 injection and storage to extend the operational life of wells/fields with commercial benefits.
- Development of a reliable techno-economic assessment method to assess the economic benefits of CCUS implementation in geothermal energy production, enabling long term strategic system planning and decision-making for the industry.
- Development of a flexible and modular life cycle inventory model for geothermal CCUS implementation to enable the environmental assessment of the proposed technologies and support stakeholder communication for the industry and policy makers.
- Development and demonstration of an innovative CCUS technology to help accelerate CCS by opening it to an important CO_2 emitting power sector.

□ Method of approach

Here below we present the interaction between the activities and coordination structures for the entire program (Figure AP1). Thereafter, in short, the relevant contributions of TU-Delft (DUT) and Seismic Mechatronics (SM) will be explained. Other than in the original proposal, reciprocal Interaction between WP1 and WP3 to 5 and in between and WP3 and WP4 was needed to solve the logistic and lock-down problems of COVID. Delay problems were solved by changing activities in time, where needed and possible.

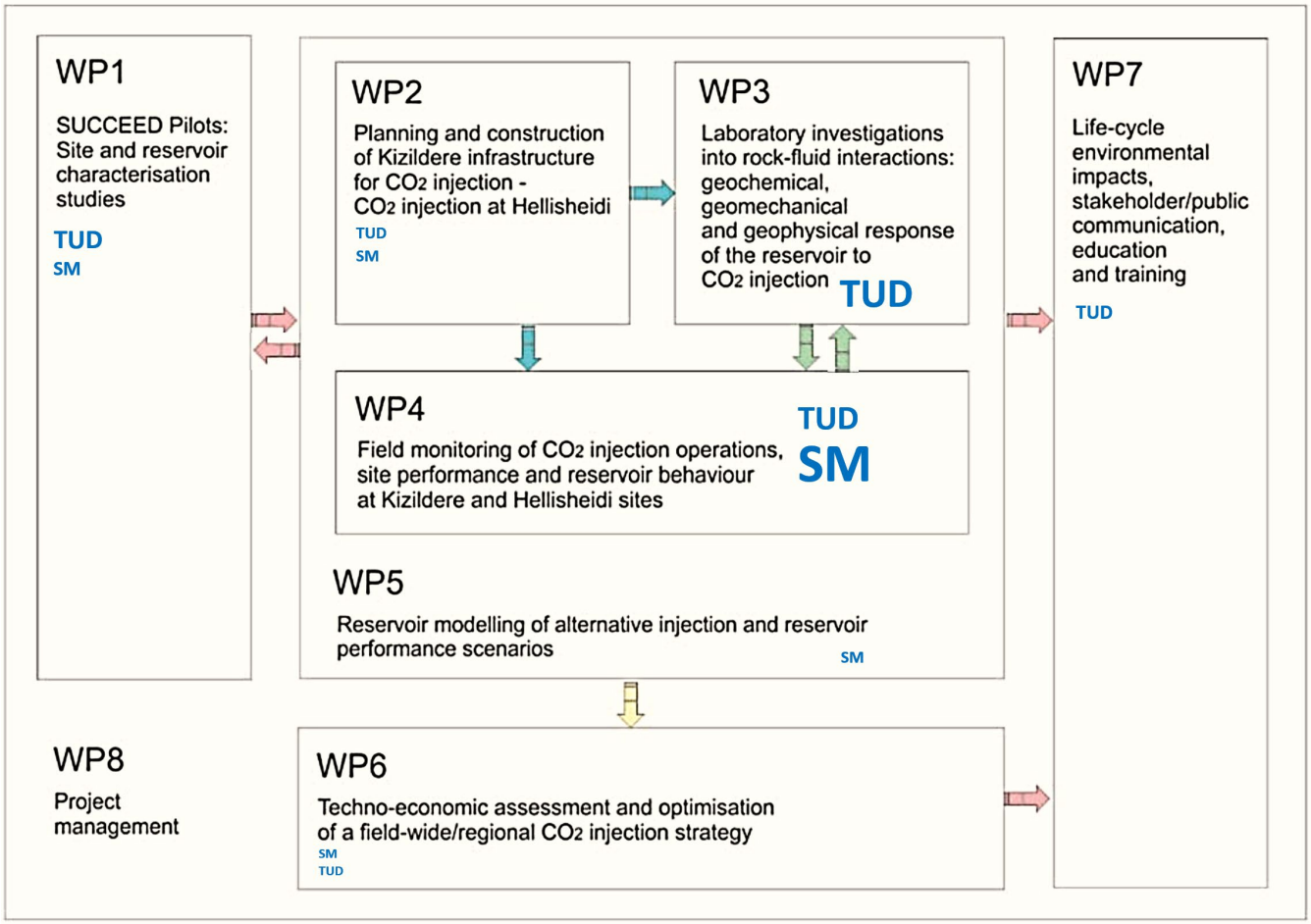

Figure AP 1:Schematic interactions of all work packages within SUCCEED. The size of the blue DUT/SM symbols represent the estimated time of involvement on the work packages.

Work Package 1 - SUCCEED Pilots: Site and reservoir characterization studies. We (mostly DUT) focused on the characterization of the field site and reservoir and constructing a static reservoir model for both sites. Rock and core sampling and a review of previous field-wide seismic and outcrop studies have been completed. During and after Covid, interrupted core analysis for reservoir rock characterization (petrophysical, petrological, geomechanical, and acoustic) is done for pre-injection monitoring of the geothermal performance as a baseline for geochemical, geophysical and reservoir modeling/interpretation.

Work Package 2 - Planning and construction of Kizildere infrastructure for CO_2 injection at Kizildere - CO_2 Injection at Kizildere - CO_2 Injection at Hellisheiði . Succeed concentrated on all technical, operational, and infrastructure issues necessary to enable safe and controlled CO_2 injection into the reservoir at Kizildere, i.e. selection of injection and monitoring wells layout; technical and operational procedures, infrastructure, and implementation of the CO_2 injection phase(s). The follow up of the CO_2 injection at the Hellisheiði site in Iceland in the CarbFix projects.

Work Package 3 - Laboratory investigations into rock-fluid interactions: Geochemical, geomechanical and geophysical response of the reservoir to CO_2 injection. We (mostly DUT) aimed to characterize on the response of marble and basalt, i.e., the supercritical CO_2 at in-situ reservoir conditions, seismic response; (wave velocities, wave attenuation), impact on flow properties, geochemistry and integrity of the reservoir rock on change in strength. The sample volume scales from 25 mm to 40 cm diameter cores, with resulting parameters as input for WPs 4 and 5, for interpretation, calibration of monitored data and numerical models. The results are used for the field performance evaluation pre-and post- CO_2-injection, as well as long-term injection strategies planning.

Work Package 4 - Field monitoring of CO_2 injection operations, site performance and reservoir behavior at Kizildere and Hellisheiði sites. The team aims were to study the induced changes in field parameters and in geochemistry and geomechanics of the geothermal field. In addition, the conduct of the CO_2 plume is surveyed, where possible, through different, site-adjusted surface and downhole monitoring activities. Standard monitoring technologies like pressure, temperature, and geochemical monitoring with tracers, are combined with a new and innovative seismic monitoring techniques and hardware eVibe from SM and an iDAS system (Silixa).

Work Package 5 - Reservoir modelling of alternative injection and reservoir performance scenarios. Pre- and post-CO_2 injection simulations are made of the changes in reservoir pressure, geochemistry and geomechanical reservoir properties. Models have been calibrated using historical and project-obtained monitoring data. Fault/fracture behavior and potential for induced seismicity at different injection/production scenarios are investigated.

Work Package 6 - Techno-economic assessment and optimization of a field-wide/regional CO_2 injection Strategy. The outcomes of WP 1-4 and identify strategies that optimize CO_2 injection as well as potential CO_2 storage performance and geothermal energy production in the field. Different CO_2 injection strategies, including injection-wells selection and injection rates, have been investigated to evaluate performance in terms of long-term pressure maintenance of the geothermal field while minimizing production of injected CO_2. This WP also considers the development and implementation of a regional scale CO_2 transport infrastructure for use in CO_2 injection along the Büyük Menderes Graben and the regional CCUS potential in the area.

Work Package 7 - Life-cycle environmental impacts, stakeholder/public communication, education, and training. First, a life-cycle assessment (LCA) model reflects the engineering processes to assess the scalability of enhanced geothermal and CCUS systems considering environmental and resource constraints. Second, DUT focus on stakeholder and public communication and education activities with regards to the CCUS technology blueprint developed and the validation of monitoring, modelling, and verification methodologies applicable to these systems.

***Work Package 8 - Project coordination and management*.** The overall technical coordination of the project is the responsibility of IMPERIAL. METU has been responsible for coordinating the field-based activities providing effective links within the consortium, as reflected in the previous figure.

In effect, DUT has been the regional coordinator for the Netherlands. The responsibilities have been:

- Site characterization studies in Turkey and Iceland. Handling the fieldwork rock sampling, core preparations and petrophysical, petrographic/mineralogic, and image characterization in WP1.
- In WP3 as lead it carried out the small and large-scale HPHT borehole-simulator experiments on the seismic response and imaging alteration of the reservoir rocks with CO2/brine-saturated flow in Task 3.1
- Support OGS in the coordination of WP4, responsible for the seismic fieldworks in Iceland and Turkey, as well as sharing most seismic monitoring data and processing and interpretation in Task 4.4
- DUT contributed to the Planning of CO2 injection at Kizildere in WP2, as well as the tasks in WP6 and WP7.

SM responsibilities:

- Carrying out substantial work in the Netherlands, in their facilities manufacturing the systems for use, i.e. developing, and constructing the new eVibe as the seismic active source.
- Responsible of the source, field monitoring of CO2 injection operations in Kizildere and Hellisheiði sites and carrying out research elements of the work.
- Contributed to the work of WP2, WP5 and WP6 from their research base when developing and constructing the new source and contributing the resulting knowledge into the modelling activities and determination of wells and seismic lines for monitoring purposes.

□ Results of the project (A)

In General

All project parts have been completed or almost realized, which means for the Netherlands, i.e. DUT and SM that:

In WP 1, mostly *DUT with SM*, performed all geotechnical fieldwork on the sites of Hellisheiði and Kizildere have been surveyed. At the surface, the locations for the by two-component cabled geophones (10 Hz) along and the helically wound cable have been determined. Where possible, options for additional recording was also prepared with two perpendicular lines of three-component stand-alone geophones (Iceland) and fiber optics cables in two monitoring wells. In addition, geological surveys in the vicinities of the test sites made it possible to characterize the reservoir and overburden rocks. For Turkey, two tons of representative samples have been collected and transported to Delft. *For Iceland, the sampling and transport of rocks was delayed by 16 months and done after the Covid lock downs and snow period.* All samples have been cored and petrographically. geomechanically, geophysically and petrophysically analyzed and also sent to partners in METU and ICL for further research win WP2 and WP3. Further, a part of the DUT samples was used for uni-axial acoustic measurements under high P,T for the determination of acoustic speed in the reservoirs and overburden. The results have been shared with the partners involved in geophysical imaging and fieldwork activities. In addition, the outcomes were used for the first imaging of the static profile for determination of source and receiver spacings of the 1st seismic field work.

In WP2, *SM and DUT*, in interaction with the partners, reviewed for both sites the geomorphological situation for the choices to be made for outlays of the surface monitoring lines in Hellisheiði and on the first choice for surface lines and monitoring wells in Kizildere. Regarding the development of technical and operational procedures, it was decided to implement the additional two-component cabled geophones (10 Hz) and place those along the fiber optics lines. To get cost neutral as possible, SM and DUT merged the shipping activities for both, the vibrator and monitoring equipment and implemented it in the operational procedures, monitoring lay-outs and infrastructure planning.

In WP3, *DUT* has contributed to the rock mechanics and geochemical rock characterizations by the preparation and quantification of the provided cores. In addition, pre-, syn-, and post- analysis CT-scanning quantified the volumetric alterations of the ICL geochemical experiments. In addition, (DUT and ICL) determined the effects of injected CO_2 on the reservoir rock at Kizildere and Hellisheiði, and mobility of the geothermal fluid in the wellbore region/reservoir, and the enhancement of the production conditions such as pressure and mobility. Reservoir and overburden rocks have been triaxially tested under stress with P_{pore}, high T, alternating H_2O/CO_2 saturations. With artificial fractures we recognized changes in seismic signatures and permeability. In the meantime, and parallel to the small-scale experiments (*and with many months of Covid delays*), the large-scale HPHT borehole-simulator has been reconstructed with existing and renovated parts, borrowed peripheral data acquisition equipment and additional need for techtime. Experiments have been performed by using seismic response in an changing basalt and a marble reservoir rock when fractures were saturated by alternating CO_2/brine compositions at different P,T and Sw/Sg. Seismic interferometry have been used to follow the replacement of brine by CO_2. The results of all laboratory experiments are used for the construction of vertical seismic profiles from the surface to reservoir depth, both in original conditions and after reservoir saturation. In addition, the outcomes were used for the first imaging of the static profile for determination of source and receiver spacings of the 2nd seismic field work.

In WP4, *SM* built a repeatable eVibe. The apparatus has been developed, built, and tested in the workshop and field. Thereafter it was successfully used during the two field campaigns in Iceland and in Turkey. Since the Silixa-iDAS system also was innovative, it was decided to add reference measurements by *DUT* in all fieldworks, by using two-component cabled geophones in all monitoring activities. As part of this WP, the seismic-data

acquisition campaigns were carried out. During the 2021 acquisition, whenever the active source was not utilized, the stand-alone three-component geophones (temporarily lent from the DEEPEN project) also acquired passive-source data (i.e., ambient-noise seismic signals such as local, regional, and global seismicity). Student Sverre Hassing used the passive data for his MSc thesis. He created a passive image of the subsurface, by using seismic interferometry. This is especially relevant for the crossline. As the active source was only located along the inline, no high-quality active image could be obtained for the crossline. *DUT* tried to fill this gap with the construction of a passive image. In November 2022 the baseline, i.e., prior to CO_2 injection, monitoring acquisition was conducted at Kizildere, Turkey. The data was acquired using the seismic vibrator from SM as a source and the fiber-optic helically wound cable from Silixa as 'continuous' receivers. Moreover, conventional geophones from *DUT* were also used, to verify the results obtained with the fiber-optic cable. The goal of this monitoring acquisition is to have a baseline, which we can compare later with data acquired when substantial amounts of CO_2 have been injected. The field data has been disseminated between all partners involved in geophysical monitoring activities. Here, intensive input by *DUT and SM* and in close cooperation with OR, ZORLU, ICL, OGS and Silixa, two successful seismic fieldworks for the Hellisheiði and one for Kizildere. The data-acquisition resulted into good (micro-) seismic data processing for injection induced seismicity (Hellisheiði)and progress of CO_2 injection in the reservoir. For Kizildere, only the baseline activities have been monitored and processed.

In WP5 and WP6, the results of WP1, 2, 3 and 4 produced by *DUT and SM* have been used for reservoir modeling of alternative injection and reservoir performance scenarios. *DUT* and OGS prepared the Kızıldere subsurface model for which the velocity model was taken from our earlier work (Janssen et al. 2021). Now the 3rd marble layer (shown by the blue outline in figure WP4.12), for which CO_2- and brine-saturated velocities from the laboratory measurements can be used with the visualization of the CO_2 dissemination. Thereafter, all previous results have been applied to techno-economic assessment and optimization of a field-wide or regional CO_2 injection strategies, where possible, for the Kizildere region.

In WP7, *DUT and SM* contributed to stakeholder involvements in Denizli and Ankara (Turkey) and The Hague (Netherlands), through the Dutch CATO-program and through public communication such as the Newsletters of DUT and newspapers. Furthermore, various conferences and reviewed publications with regards to the CO_2 injection/storage have been integrated with geothermal technology. In cooperation with the partners, a blueprint was developed and applied to validation of monitoring, modelling and verification methodologies applicable to other high enthalpy geothermal systems.

In WP8, *DUT* was responsible for the project planning, monitoring, and execution, in close cooperation with ICL and participated in the Project Management by the preparation of Project Periodic Meetings, minutes, and periodical reports. Periodical reports were prepared. through ICL, for ERA-ACT on monitoring the time planning, progress and tracking of deliverables, milestones, and dissemination activities through the monitoring tool; Deviations from the work description and implement remedial processes are explained. By *DUT and SM*, similar activities have been reported for RVO. They do involve the Dutch part of the activities that has been supported by RVO. *DUT* cooperated with the organization of steering and meeting events mostly through TEAMS or ZOOM sessions with Work Package Leaders for the technical progress in the laboratory, for fieldwork, for interpretation, modeling and scenario building and particularly the development, construction, calibration and implementation of the eVibe by *SM*. In addition, the Dutch dissemination of results via websites, interviews, (conference) presentations, stakeholder meetings and reviewed publications, have been monitored and processed through the procedures of the SUCCEED program.

Work package 1: SUCCEED Pilots: Site and reservoir characterization studies

- **Task 1:1: Review of previous field-wide seismic and outcrop studies at Kizildere and Hellisheiði sites.**
- **Task 1.2 Reservoir rock and fluid characterisation for geochemical, geomechanical, and petrophysical baseline properties at field sites.**

Petrophysical characterization of reservoir and overburden samples of Kizildere.

The results presented are summaries of the progress reports for ACT. Most of the work is performed by Dr. M. Janssen and Dr. A. Barnhoorn in the DUT Geoscience and Engineering Laboratories and described in the literature and presentations which are summarized in the section “References”. The acoustic imaging work was supported by Dr. D. Draganov.

First sample collection at Kizildere

On February 26, 2020, ZORLU, METU, DUT, and IMPERIAL sourced multiple rock samples from various fresh outcrops at the Kizildere site. These included limestones, claystones, quartzites, quartschists, marbles, calcschists, siltstones, mudstones, and micaschists. The figures here below present the sampling locations at the Kızıldere site and several examples of samples that were collected, respectively.

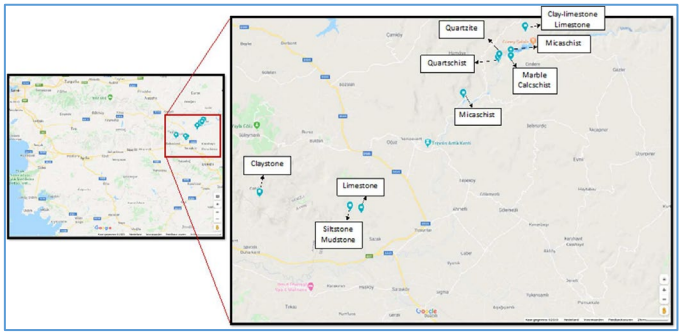

Figure WP1.1: Sampling locations near Kızıldere, Turkey (source: Google Maps).

Figure WP1.2a: Left: Quartzite, Middle: Marble and Right: Calcschist samples collected from the Igdecik formation from the outcrops around Kizildere.

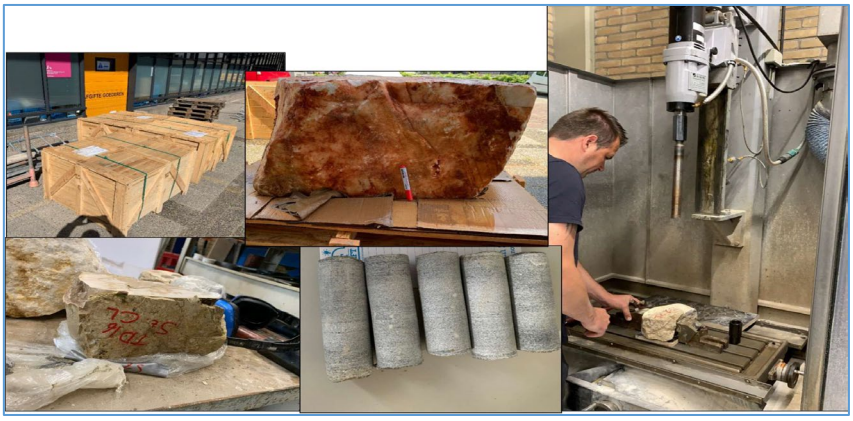

Figure WP1.2b: Arrival of Kizildere samples at DUT and preparation of the first cores.

Seismic-response characterization

For Kizildere

The rock samples arrived at DUT on May 19, 2020 (previous figure). As soon as the first cores were drilled from the rock samples, they were cut and dried for 24 hours in an oven at 60 °C. Prior to performing the seismic-response characterization experiments, first the physical properties (i.e., porosity and density) of each of the cores were determined. Porosities were measured using an Ultra Pycnometer 1000 (Quantachrome Corporation). All cores have lengths and diameters of 6.20±0.15 cm and 2.97±0.02 cm, respectively. Each core is drilled perpendicular to any potential layering.

Table WP1.1: Properties of the cores of series A: UCS. For each rock type, all cores were drilled from one block.

UCS	Experiment													
Sample origin	Kizildere													Hellisheidi
Type	Calcschist		Marble		Limestone			Quartzite			Siltstone	Quartschist	Mudstone	Basalt
Code	TD12-CS4	TD12-CS5	TD1-M2	TD1-M3	TS2-SZL2	TS2-SZL4	TS2-SZL5	TD20-QZ-1	TD20-QZ-2	TD20-QZ-4	TK-B1-2	TD-23-QMS1	TK-B2-1	I.B2
Length (mm)	61.6±0.1	61.5±0.1	62.9±0.1	61.9±0.1	58.9±0.1	60.8±0.1	61.4±0.1	62.8±0.1	62.5±0.1	60.8±0.1	62.7±0.1	62.5±0.1	63.7±0.1	59.3±0.1
Diameter (mm)	29.8±0.1	29.8±0.1	29.8±0.1	29.8±0.1	29.1±0.1	29.8±0.1	29.0±0.1	29.8±0.1	29.8±0.1	29.8±0.1	29.8±0.1	29.6±0.1	29.7±0.1	29.9±0.1
Porosity (%)	4.14±0.10	2.42±0.03	3.01±0.13	2.27±0.03	5.33±0.13	10.48±0.24	7.54±0.16	2.77±0.16	2.57±0.03	3.65±0.05	22.55±0.01	1.71±0.29	16.60±0.15	23.59±0.14
Porosity at failure point (%)	5.93±0.10	-	-	4.20±0.07	-	-	-	-	-	4.21±0.03	-	-	-	-
Permeability (mD)	-	-	-	-	-	-	-	-	-	-	97±6	-	-	-
Pore Volume (mm^3)	1779±58	1038±22	1321±68	980±21	2088±69	4444±140	3058±92	1213±81	1120±23	1548±34	9861±87	735±132	7326±127	9822±142
Matrix density (g/cm^3)	2.78±0.01	2.75±0.01	2.76±0.01	2.75±0.01	2.73±0.01	2.75±0.01	2.75±0.01	2.89±0.01	2.90±0.01	2.92±0.01	2.78±0.01	2.80±0.01	2.82±0.01	3.12±0.01
Bulk density (g/cm^3)	2.67±0.02	2.68±0.02	2.68±0.02	2.69±0.03	2.59±0.03	2.47±0.03	2.55±0.03	2.81±0.02	2.82±0.02	2.82±0.03	2.15±0.01	2.76±0.03	2.36±0.02	2.38±0.02

Table WP1.2 presents averaged properties per rock type. UCS experiments are performed in order to (i) obtain relevant static elastic properties of the various samples, and (ii) study the effect of axial stress on seismic velocities at atmospheric radial stress.

Table WP1.2 List of averaged properties per rock type utilized in this study.

UCS	Experiment						
Type	Calcschist	Marble	Limestone	Quartzite	Siltstone	Quartschist	Mudstone
Number of samples	2	2	3	3	1	1	1
Length (mm)	61.6±0.1	62.4±0.7	60.4±1.3	62.0±1.1	62.7±0.1	62.5±0.1	63.7±0.1
Diameter (mm)	29.8±0.1	29.8±0.1	29.3±0.4	29.8±0.1	29.8±0.1	29.6±0.1	29.7±0.1
Porosity (%)	3.28±1.22	2.64±0.52	7.78±2.58	3.00±0.57	22.55±0.01	1.71±0.29	16.60±0.15
Matrix density (g/cm^3)	2.77±0.02	2.76±0.01	2.74±0.01	2.90±0.02	2.78±0.01	2.80±0.01	2.82±0.01
Bulk density (g/cm^3)	2.68±0.01	2.69±0.01	2.54±0.06	2.82±0.01	2.15±0.01	2.76±0.03	2.36±0.02

After the samples were prepared, they are placed on a pressure bench, in between two aluminum pistons, with a 500 kN load frame. A hydraulic ram provides the axial stress. Axial strain and radial strain are recorded by two linear variable displacement transformers (LVDTs) and an extensometer chain, respectively. Active-source acoustic measurements are taken over the course of the experiment, where attention is paid on how the seismic signal varies as a function of axial stress. Next to studying the effect of axial stress on seismic velocities, static elastic properties, such as the static Young's modulus (E) and Poisson ratio (v), were obtained from the UCS experiments. All rock samples were deformed until they reached their respective ultimate strength (i.e., the maximum axial stress that the sample can withstand before it fails). The variable in all UCS tests is the axial stress. It is increased using a constant axial displacement rate of 0.0005 mm/s until the rock sample starts to fail. Figure WP1.3 presents a schematic of the experimental set-up used for conducting the UCS experiments. All UCS experiments are performed at ambient temperature.

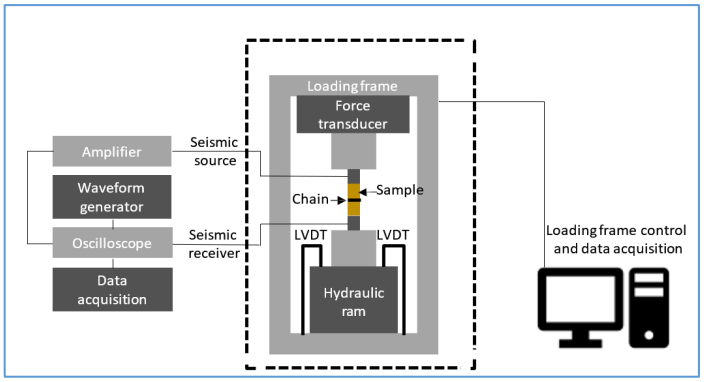

Figure WP1.3: Schematic of the experimental set-up used for performing the unconfined compressive strength (UCS) tests. Note that the seismic source and receiver are being placed inside the two aluminum pistons.

In all experiments conducted, a seismic source is placed at the top of the rock sample whereas a seismic receiver is located at the bottom (Figure WP1.3). For both the receiver and source, a single-element normal-incidence shear wave transducer from OLYMPUS is used. The source signal is characterized by a sinus wave with a frequency of 1 MHz and an amplitude of 800 mV. A burst period of 5 ms is used, and the signal is averaged over a total of 512 shots. An active-source acoustic measurement is taken every 10 s.
Experimental series A consists of a total of 13 UCS experiments on the various rock types present in the Kizildere geothermal field and 1 UCS test on a basalt sample from Iceland.

Table WP1.3 presents an overview of the static elastic properties resulting from the abovementioned experiments.

The results related to samples obtained from the Kizildere field show in figure WP1.4 the axial stress-strain behavior for the 13 UCS experiments performed. It is obvious that limestone sample TS2-SZL2 is the stiffest material compared to the other rock types; the steep trend between 0.2-0.3 % axial strain yields the relatively high Young's modulus presented in Table WP1.3. On the other hand, it is apparent that the tested siltstone sample (TK-B1-2) is the weakest compared to the other samples; note the very gentle slope.

Table WP 1.3: Static elastic parameters obtained from the UCS experiments.

UCS	Experiment													
Sample origin	Kizildere													Hellisheidi
Type	Calcschist		Marble		Limestone			Quartzite			Siltstone	Quartschist	Mudstone	Basalt
Code	TD12-CS4	TD12-CS5	TD1-M2	TD1-M3	TS2-SZL2	TS2-SZL4	TS2-SZL5	TD20-QZ-1	TD20-QZ-2	TD20-QZ-4	TK-B1-2	TD-23-QMS1	TK-B2-1	I.B2
Ultimate strength (MPa)	44.4	45.6	57.0	51.1	145.4	72.5	43.7	82.0	48.3	88.8	15.5	75.4	22.2	51.8
Static Young modulus – E (GPa)	22.2	26.5	40.1	29.5	52.9	33.9	27.9	35.0	38.5	38.0	3.8	43.1	10.5	30.3
Static Poisson ratio – v	0.14	0.14	0.17	0.14	0.39	0.19	0.09	0.11	-	0.17	0.27	0.18	0.16	0.28
Bulk modulus (GPa)	10.3	12.3	20.3	13.7	80.2	18.2	11.3	15.0	-	19.2	2.8	22.4	5.1	23.0
Shear modulus (GPa)	9.7	11.6	17.1	12.9	19.0	14.2	12.8	15.8	-	16.2	1.5	18.3	4.5	11.8

The steep trend, at axial strain values of >0.2%, related to limestone sample TS2-SZL2 suggests that the material undergoes relatively little deformation before failure at σ1=145.5 MPa. It implies a more brittle-like behavior of the limestone compared to the other rock samples. This conclusion is supported by the fracture pattern observed in the sample after its failure (Figure WP1.5). It indicates axial splitting, an indication of brittleness, whereas the other rock samples show a clear shear failure pattern. However, it is crucial to note that this is not always the case for the limestone samples. As shown by the bottom graph within Figure WP1.4, other limestone samples (TS2-SZL4 and TS2-SZL5), drilled from the same block as the original sample, show a different stress-strain behavior: lower static Young's modulus and ultimate strength (i.e., less brittle-like behavior). It is believed that heterogeneity, due to diagenesis processes, within the limestone yields different axial stress-strain patterns of the three limestone samples studied.

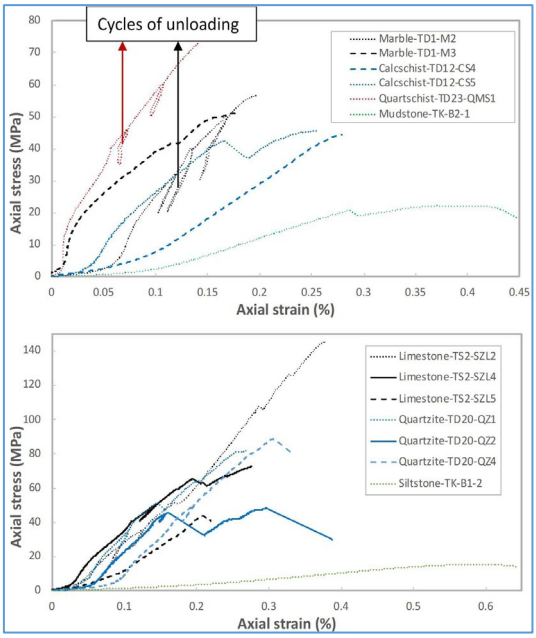

Figure WP1.4: Axial stress-strain behavior of 13 UCS experiments. For some of the UCS tests also unloading cycles were performed. For the limestone samples (black trends in bottom graph); note the difference in ultimate strength and stress-strain slope due to heterogeneity because of diagenesis.

Figure WP1.6, shows the compressional wave (P-wave) velocity as function of axial stress, i.e., depth below surface. The shear wave (S-wave) velocity as function of axial stress is shown in Figure WP1.7. The soft siltstone reveals significantly lower seismic velocities compared to the other 6 rock types assessed. Since the siltstone undergoes a lot of deformation prior to its failure (Figure WP1.4), compaction within the rock itself occurred, which led directly to an increased seismic velocity as function of increasing axial stress. For all samples studied, the largest increment in seismic velocity took place at the lowest absolute stress values. The latter is potentially due to closure of microcracks within the samples, leading to an increased seismic velocity.

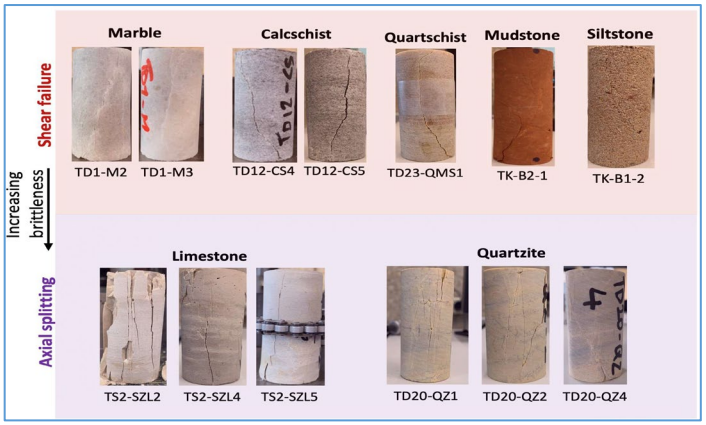

Figure WP1.5: 13 Kizildere rock samples after failure. Note the presence of axial splitting patterns within the limestone (especially TS2-SZL2) and quartzite (mainly TD20-QZ1 and 2) samples. All marble, calcschist, quartschists, mudstone, and siltstone samples show clear shear failure characteristics.

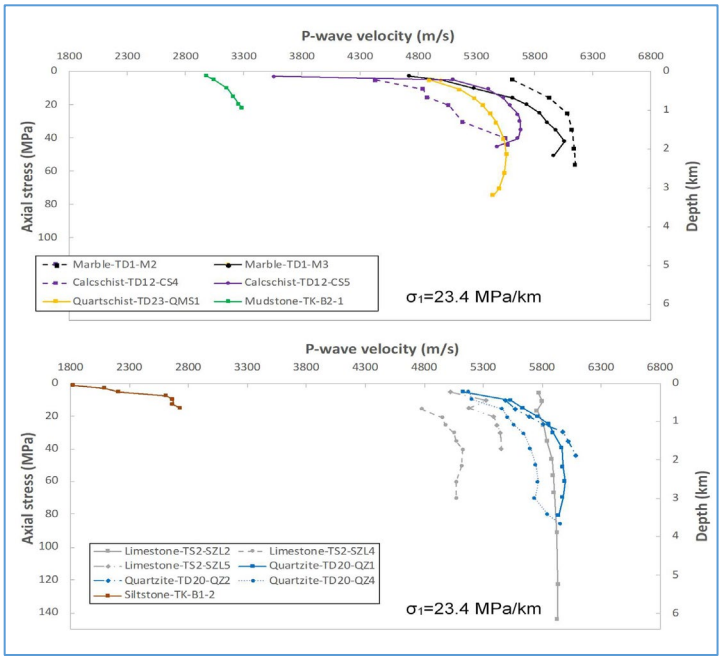

Figure WP1.6: P-wave velocity as function of axial stress, and thus depth below surface, for all 13 UCS experiments performed. Axial stress-depth relationship is taken from Çiftçi (2013).

Limestone sample TS2-SZL2 (continuous grey line in Figure WP1.6) show a somewhat different trend compared to the other rock types: its seismic velocity does not change significantly with increasing axial stress. This can be explained by the fact that this limestone sample shows a more brittle-lake behavior compared to the other rock samples (Figure WP1.5).

Thin section analyses on samples obtained from Kizildere

Several rock samples, that were collected at Kizildere, Turkey, were shipped for thin section preparation. Table 4.4 presents the image analyses results and mineralogy obtained from thin sections analyses. For the image analyses an area of interest was identified for each of the thin sections assessed. The area of interest does not include edges of the thin sections. The 2D area and 2D perimeter, of the connected pores within an area of interest, are implemented in the 2D Carman-Kozeny equation.

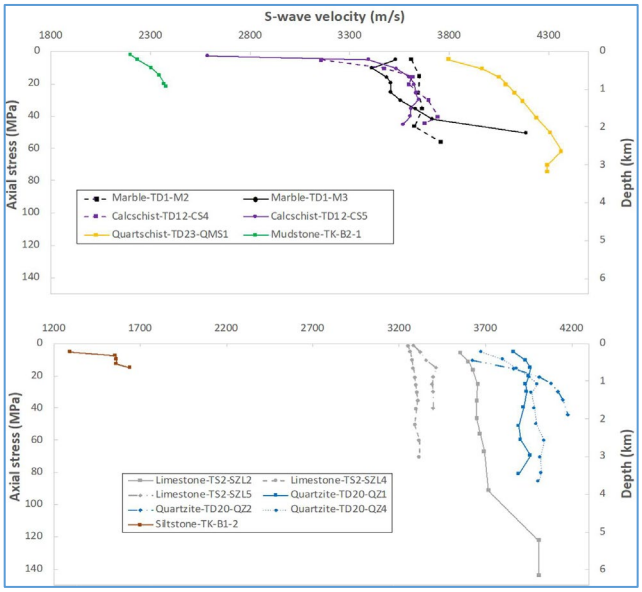

Figure WP1.7: S-wave velocity as function of axial stress, and thus depth below the surface, for all 13 UCS experiments performed. Axial stress-depth relationship is taken from Çiftçi (2013).

Table WP1.4: Image analyses results and mineralogy from thin section analyses on Kizildere samples.

Type	Calcschist		Marble		Limestone		Micaschist		Claystone[d]		Quartschist	
Code	TD11-B		TD1-B		TS1-B5		TD24-B		TKK1-B		TD23-B	
Area porosity (%)	Incl. fracture: 1.3 Excl. fracture: 0.4		Total: 1.6 Effective: 0.4		Effective: 1.5		Total: 8 Effective: 2.3		Effective: 6.6		Incl. fracture: 16.7 Excl. fracture: 10.5	
2D Carman-Kozeny permeability (D) [a,] Incl. fracture: [b,] Matrix: [c] Best guess compacted	• 25*10^{-3} D • 3*10^{-3} D • << 10^{-3} D		• 2.2 D • 7*10^{-4} D • < 10^{-4} D		• 12 D • - • <1 D		• 26*10^{-3} D • - • <10^{-2} D		• 0.12 D • - • < 10^{-3} D		• 0.24 D • 0.06 D • < 10^{-2} D	
Mineralogy (area %)[e]	-Calcite & dolomite (recrystallised) -Muscovite / Sericite -Quartz or feldspar	98% 1% <1%	-Calcite & dolomite (recrystallised) -Smectites (Haloysite?)	99% 1%	-Calcite & dolomite -Organic matter & oxides	89% 1%	-Calcite & dolomite with organic matter -Angular quartz and Feldspar -Smectites (vermiculite?) -Accessories incl. Biotite remnants)	89% 8% 2% <1%	-Calcite & dolomite with organic matter -Disperse angular quartz and feldspar -Smectites (vermiculite?)	83% 8% 8% <1%	-Calcite, dolomite. Ankerite -Mica, i.e. muscovite and sericite -Quartz, feldspar	30% 45% 45%

[a] Permeability is related to intergranular pore connected micro-porosity from up to 100 pixels pores including the matrix and fractures (if available). [b] Permeability is related to intergranular pore connected micro-porosity from up to 100 pixels pores, i.e., the matrix permeability. [c] 2D permeability ⍰ at least one order of magnitude overstated because of stress-free matrix and preparation damage. [d] Claystone represents here a compacted mixture of a vaguely layered limestone matrix with angular quartz/feldspar grains and dispersed clay minerals. [e] Mineral composition is based on random point counting of 100 points in the image texture.

Together with the XRD and XRF analysis carried out on the same sample, a more detailed description of the thin section analysis results for the TD1-B marble sample is presented in publications of Prakla et al, 2022.

Conclusion for the Kizildere experiments

As part of WP1, sampling collection from fresh outcrops at the Kizildere site was conducted in February 2020. After the samples were shipped to The Netherlands, multiple cores were prepared and subsequently used for obtaining the baseline seismic response on dry and saturated samples. Studied samples include limestones, quartzites, marbles, calcschists, siltstones, and quartschists. Our experimental results show that the rate of velocity increase, as function of increasing stress and is largest at low absolute stresses. This most probably reflects the closing of microcracks at low stress values, resulting in increased velocities. Moreover, preliminary laboratory results suggest that some marble samples behave more brittle-like compared to the other rock types, including other limestone samples, collected at Kizildere.

Petrophysical rock characterization for Hellisheiði reservoir and overburden rock.

The results, here presented, are a summary of the work of Dr. A. Barnhoorn and E. Redondo García in the DUT Geoscience and Engineering Laboratories and described in the MSc-thesis "Petrophysical and Mechanical Characterization of the Volcanic Rocks in the Hellisheiði Geothermal Field and implications of Thermal Fracturing in CO_2 mineralization" (http://repository.tudelft.nl/). Most of the work for the translation to seismic images have been performed by Dr. M. Janssen and Dr. Draganov. The results presented are summaries of the progress reports for ACT.

Seismic-response characterization for Hellisheiði

During the first site meeting at Hellisheiði, some small basalt samples were collected from the site and one UCS test was performed on a representative basalt core. In July 2021, various larger samples have been collected and analyzed by E. Redondo García for use in WP4, the results from this experiment are also reported in her MSc-thesis "Petrophysical and Mechanical Characterization of the Volcanic Rocks in the Hellisheiði Geothermal Field and implications of Thermal Fracturing in CO_2 mineralization" and is publicly available in the DUT library MSc-repository (https://repository.tudelft.nl/islandora/object/uuid%3A641e5df2-c411-450d-9095-342673a225a7?collection=education).

Figure WP1.8 presents the axial stress-strain curve for the first sample. The presented data shows that the sample started to fail at around 51.8 MPa axial stress. The resulted fracture pattern showed characteristics related to axial splitting, like the limestone sample discussed earlier. Figure WP1.9, P- and S-wave velocity as function of axial stress results indicate a reasonably constant P- and S-wave velocity as functions of increasing axial stress, suggesting that the sample undergoes little deformation/compaction before it fails. It is a sign of brittleness and falls in line with the observations made regarding the fracture pattern (Figure WP1.8).

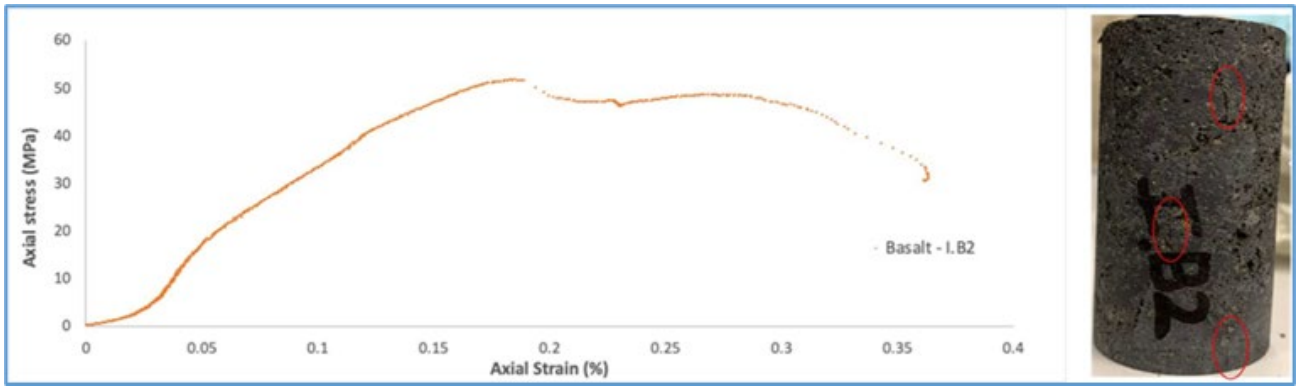

Figure WP1.8: Axial stress-strain behavior of the single UCS experiment conducted on a basalt sample from Hellisheiði. The picture on the right shows the sample after failure occurred. Note the presence of multiple vertical 'splitting' patterns; highlighted in red.

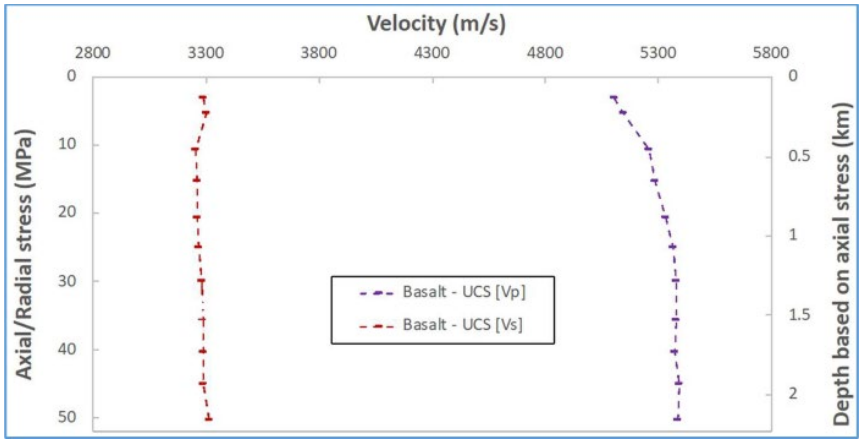

Figure WP1.9: P- and S-wave velocity as function of axial stress, thus depth below surface, for the single UCS experiment conducted on a basalt sample from Iceland. Axial stress-depth relationship is taken from Batir et al. (2012).

Petrophysical results from the 2nd sample series

During a field campaign, samples were collected in different outcrops, ensuring that the samples were of high quality and sufficiently diverse to enable comprehensive analysis. Four samples per block and rock type have been prepared from the collected blocks, and they have been subjected to different laboratory tests to evaluate their petrophysical properties, such as porosity, density, and permeability, and their geomechanical behavior, using Unconfined Compression Test (UCS), Active-Source Acoustic Test, and Splitting Tensile Strength Test.

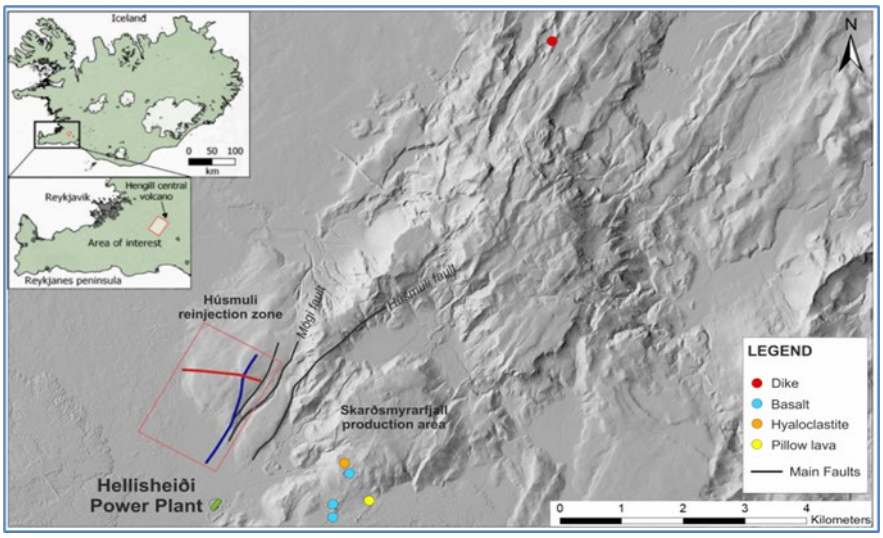

Figure WP1.10: Map of the vicinity of the Hellisheiði Power Plant and area of interest (red square). The blue and red lines are the established seismic lines. The dots are sample locations.

The location of the sampled outcrops show that several rock types were collected.. The main geological formations that make up the subsurface were identified in the outcrops and sampled, i.e. hyaloclastite, various types of basalts, and intrusive rocks (dikes). Pillow lavas from specific levels within the hyaloclastites were sampled but not included in this study and considered not relevant for the research purposes. Figure WP1.11 showcases some of the sampled outcrops.

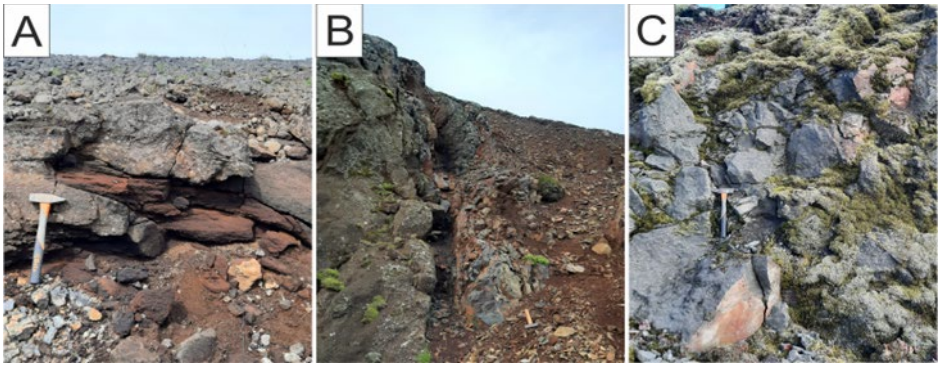

Figure WP1.11: Outcrops sampled for hyaloclastite (A), dike (B) and basalt (C)

Petrophysical results: Density, porosity, permeability

Cylindrical pores have been drilled from the previous mentioned reservoir and overburden types (Figure WP1.12).

The porosity values of various rock samples were analyzed using a *helium pycnometer*, giving the effective porosity or the connected porosity. However, it is possible that some of these pores may not be connected *in situ*, meaning that the effective porosity values may have been overestimated to some degree. Porosity values are strongly varying, however, the overall, minimal variation in porosity was observed across most samples. The basalt HBA-18 exhibits the highest porosity values, ranging from 42.20% - 51.37%. The hyaloclastite HH-1 has a porosity range of 40.99% - 47.03%, and the basalt HPB-23 in between 36.54% - 46.87%. The basalt HB-4 porosity ranges from 23.34% - 26.66%, and basalt HBimp-9 between 18.19% - 20.31%. The dike ND-6 has a lower porosity ranging from 7.90% - 9.45%, as also gabbro G, between 0.18% and 0.92%.

Through an analysis of the porosity measurements, sample weight and volume of the samples, the *bulk densities* of the samples were determined. Going from high to low density, the values are Dike sample ND-6, 2.74 - 2.78 g/cm$_3$; gabbro G, 2.67 - 2.72 g/cm^3; Basalts HBimp-9 and HB-4 with respectively 2.38 - 2.49 g/cm^3 and 2.30 - 2.40 g/cm^3; basalt HPB-23, 1.67 - 2.00 g/cm^3, and; HBA-18, 1.53 - 1.8 g/cm^3. The hyaloclastite HH-1 has the lowes values, i.e. 1.49 - 1.68 g/cm^3.

The Ruska permeameter was used to measure the *permeability* of the different sets of basalt samples from the series HBA18, HB4, HBimp9 and, ND6, resulting in permeabilities of respectively; 22.70 - 28.58 mD; 4.82 - 7.86 mD; 0.11 - 0.17 mD, and; 7.76 mD.

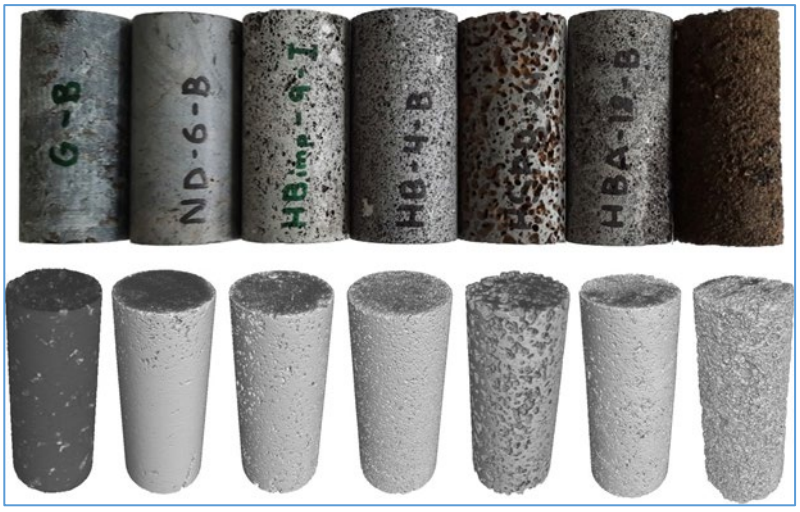

Figure WP1.12: Sample cylinders as used for the experiments. Micro CT scans visualization images (bottom) and reference sample picture (top).)

Table WP1.5: Comparison of porosity, density, and permeability of Icelandic rock samples.

	HBA - 18	HH - 1	HPB - 23	HB - 4	HBimp - 9	ND - 6	G
Porosity [%]	46.38	44.68	40.34	24.99	21.53	8.71	0.44
Bulk density [g/cm3]	1.68	1.56	1.87	2.36	2.38	2.76	2.7
Permeability [mD]	26.33	>33	>33	6.23	0.14	<7.76	-

Comparing the rock types that represent the basalt/gabbro reservoirs and overburden, it can be stated that an increase in porosity a negative correlation with density. However, differences in matrix density and the presence of non-connecting pores gives variations in results compared to the trend. Hence, additional CT-scans have been produced to verify the signature of the pores i.e., connected, or non-connected (FigureWP1.13).

Hence, *microcomputed tomography* (micro-CT) with 3D image analysis is used for analyzing porosity of samples measuring 30 mm in diameter and 60 mm in length. The micro-CT images have a resolution of 60 micrometers. The software Avizo© was used to determine the total porosity, as well as connected and unconnected porosity (Figure WP1.13). The software DragonFly© was applied to measure the pore-wall surface and plot the pore size distribution of connected and unconnected porosity for all the samples. In conclusion, the basalt with the largest pore size, for both connected and unconnected porosity, is HPB-23-B, followed by HB-4-B and HBA-18-B, and lastly with only unconnected porosity, HBimp-9-I. However, in general, the pore size distribution in basalt samples is similar for all analyzed samples, except for HPB-23-B, which has much larger pores. The ND-6-B dike has a pore size mode value of 0.78 mm, which is like most basalts. On the other hand, the HH-1-B hyaloclastite has a mode value of 0.47 mm for connected porosity and 0.81 mm for unconnected porosity (Table WP1.5).

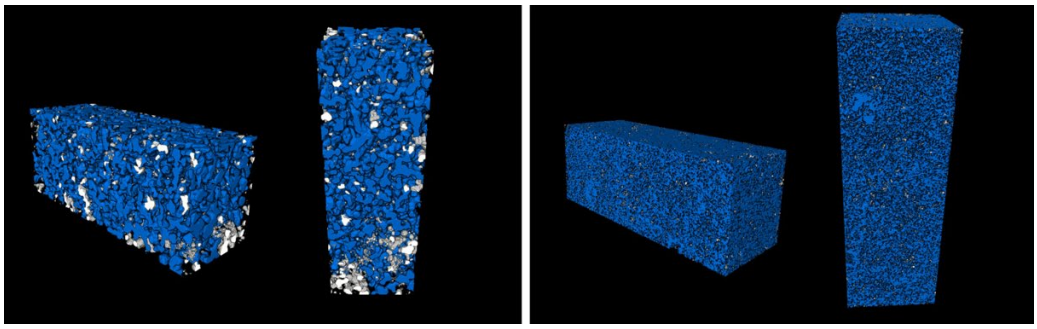

Figure WP1.13: Examples of pore-structure visualization from micro CT scans (resolution of 60 µm). Connected porosity in blue, unconnected porosity in white. Left, sample HPB3 with large pores and right sample HH1 with pores an order of magnitude smaller.

Table WP1.5: Summary table of micro CT scans analysis results.

	Cropped Volume [cm³]	Pycnometer Φ [%] *	Total Φ [%]	Connected Φ [%]	Unconnected Φ [%]	Surface of connected pores [cm²]	Surface of unconnected pores [cm²]
ND – 6 – B	23.28	8.44	2.68	0	2.68	0	132.96
HBimp – 9 – I	21.90	21.8	13.19	0	13.19	0	297.24
HBA - 18 – B	22.09	42.2	22.61	19.23	3.38	499.12	150.12
HB – 4 – B	21.49	25.71	19.16	15.98	3.18	478.12	135.97
HPB – 23 – B	19.07	36.89	29.06	27.91	1.15	213.01	18.47
HH – 1 – B	17.46	47.03	32.25	31.68	0.56	787.63	29.90

* In sample volume of 42.4 cm³.

Geomechanical Properties of Hellisheidi samples

The Unconfined Compression Test (UCS) is used to get the unconfined compressive strength and it stands for the maximum axial compressive stress that a specimen can bear under zero confining stress. In addition to measuring axial load, this test also measures axial and radial strain, which is used to calculate the sample's Young's modulus and Poisson's ratio. Figure WP1.3 shows a scheme of the experimental setup. In this type of experiment, a cylindrical sample of 30 mm All tests have been performed at room temperature and both

acoustic and steel strain calibration for the axial strain corrections have been done to obtain more accurate results.

Acoustic measurements are obtained by accurate measurements of first arrival times and by tat give the acoustic wave velocities. The transducers have been placed in steel cups surrounding the source and receiver. To achieve this, the first arrival times of the P and S waves were plotted under varying stresses,

The Brazilian Test is used for determining *the tensile strength.* Cylindrical samples with a diameter of 30 mm and a height of 15 mm are placed between two hardened steel plate with a semicircular groove that acts as a stress concentrator. A compressive load is applied causing the sample to split diametrically along the groove. In this experiment, the movement of the pistons is constant at a steady strain rate of 10^{-5} s^{-1}. The tensile strength of the rock sample is calculated based on the magnitude of the applied load and the dimensions of the rock sample.

Thermal Shock Test are performed to determine the degree of spalling and cracking because of sudden decrease of in-situ temperatures by cold water and CO_2-injection at 60°C in a reservoir at a temperature between 260°C - 285°C. Rapid cooling generates differential thermal expansion, which may result in the formation of cracks and fractures in the rock matrix, thereby impacting the permeability of the reservoir. The samples are gradually heated to the desired temperature and then rapidly brought back to the target temperature. The shock experiments were performed on samples of 30 mm diameter and 60 mm height of HBimp-9 basalt samples, which have similar textural characteristics to those observed in CarbFix mineralized CO_2 basalt cores.

Unconfined Compression (UCS)

Testing results Table WP1.6 is a summary of the results obtained from the Unconfined Compression Test, including Maximum Stress the samples can withstand; Young's Modulus; Poisson's ratio; the average S and P wave velocities, and the Vp/Vs ratio for each sample. In addition to the data collected in the table, the results per sample and rock have been plotted in Figures WP1.14 and WP1.15. They show examples of "stress vs strain" and "axial strain vs radial strain" plots respectively. This facilitates the analysis and comparison between the different samples.

Table WP1.6: Summary Table of Unconfined Compression Test Results.

	Φ [%]	Max Stress [MPa]	Young Modulus	Poisson's Ratio	Vp [m/s]	Vs [m/s]	Vp/Vs ratio
HBA – 18 – A	51.37	12.58	7.61	0.23	2006	2872	1.43
HBA – 18 – B	42.20	13.95	7.66	0.40	1935	2942	1.52
HBA – 18 – C	50.36	11.76	5.84	0.22	2956	1830	1.62
HBA – 18 – D	45.05	26.71	6.69	0.11	4312	2742	1.60
HH – 1 – B	47.03	2.37	2.23	0.05	-	-	-
HH – 1 – C	44.90	3.23	0.56	0.03	-	-	-
HH – 1 – D	40.98	1.49	0.34	0.02	-	-	-
HH – 1 – E	45.91	2.42	0.62	0.01	-	-	-
HPB – 23 – A	36.54	29.51	7.31	0.16	3017	1806	1.67
HPB – 23 – B	36.89	21.92	6.81	0.12	3166	1833	1.73
HPB – 23 – C	41.75	20.32	6.03	0.18	3057	1795	1.70
HPB – 23 – D	46.87	9.64	3.10	0.17	2817	1727	1.63
HB – 4 – A	24.87	74.82	15.31	0.15	3899	2423	1.60
HB – 4 – B	25.71	81.72	18.32	0.22	3710	2306	1.61
HB – 4 – C	23.34	101.67	18.84	0.21	3923	2462	1.59
HB – 4 – D	26.66	75.56	18.96	0.23	3962	2563	1.55
HBimp – 9 – A	20.31	65.22	16.80	0.33	3762	2332	1.61
HBimp – 9 – B	22.10	59.70	13.36	0.25	3514	2154	1.63
HBimp – 9 – C	20.97	58.45	14.99	0.26	3405	2105	1.62
HBimp – 9 – D	18.19	95.20	20.89	0.24	3733	2316	1.61
ND – 6 – A	8.44	193.26	28.54	0.16	4646	3065	1.52
ND – 6 – B	9.45	130.14	27.23	0.33	4541	3208	1.42
ND – 6 – C	7.90	161.21	32.30	0.27	4621	3335	1.39
ND – 6 – D	8.64	121.24	24.82	0.15	4664	3253	1.43
G – A	0.18	108.27	47.35	0.18	5897	4042	1.46
G – B	0.27	71.58	29.98	0.19	5501	3422	1.60
G – C	0.92	119.60	49.89	0.10	5855	4058	1.44
G – D	0.4	74.36	40.68	0.24	5714	3875	1.47

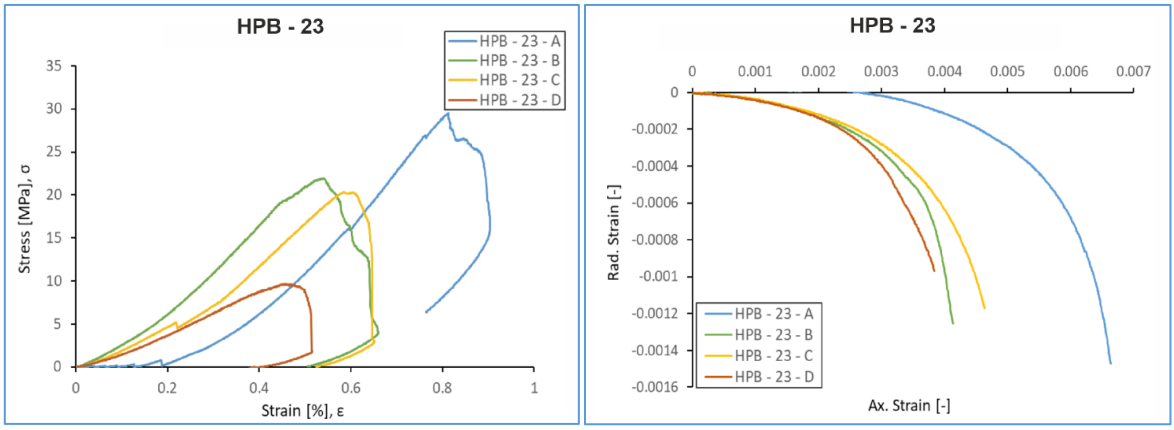

Figure WP1.14: For basalts, left; Stress vs Strain Plots per sample, per rock, and right; Radial Strain vs Axial Strain Plots per sample, per rock.

After comparing the different samples within each rock, the samples were compared with each other across all rocks. Two plots with all the results were generated and they compare "stress vs strain" and "axial strain vs radial strain" together (Figure WP1.15). In these graphs, five units can be identified, i.e. the Gabbro unit, the ND-6 unit, the HBimp-9, the HB-4 unit, the HPB-23, the HBA-28 unit, and the HH-1 unit. The gabbro (G) is the stiffest of the materials and deforms less axially.

However, it does not get the high maximum stresses of ND-6 dyke material. ND-6 has the lowest Young's modulus of the group, meaning it deforms slightly more, although less than the basalts. The basalts HBimp-9 and HB-4 have similar petrophysical and mechanical properties, although HB-4 is slightly more porous. The basalts with the lowest Young's modulus are HBA-18 and HPB-23, with the latter being more porous and reaching lower maximum stress values but similar Young's modulus values to HBA-18. However, HBA-18 reaches higher Poisson's ratios and deforms more radially. The hyaloclastite HH-1 is the rock that reaches the lowest maximum stress and has the lowest Poisson's ratio, indicating that it deforms very easily radially compared to the other lithologies. Additionally, this rock also has a very low Young's modulus, indicating that it undergoes significant axial deformation.

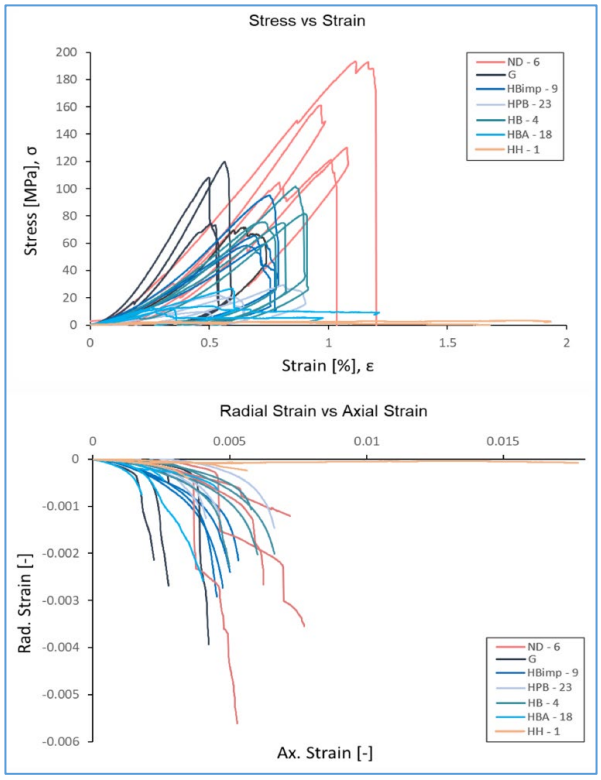

Figure WP1.15: Comparison of 'Stress vs Strain' & 'Radial Strain vs Axial Strain' Plots of all samples.

Active-Source Acoustics Testing results

During the Unconfined Compression Test, the P-wave and S-wave velocities were measured by using an active-source. An example of the results plotted has been displayed in Figure WP1.15. The highest average P-wave velocity is with the gabbro (G), ranging from 5501 - 5897 m/s, followed by the basalt HB-4, ranging from 3710 - 3962 m/s. The dike (ND-6) has a narrow range of P-wave velocities, from 4541 - 4664 m/s. The basalt HBimp-9 has a lower P-wave velocity of 3405 - 3762 m/s, while the basalt HPB-23 has lower velocities from 2817 - 3166 m/s, followed by basalt HBA-18 with the lowest P-wave velocity from 1935 - 4312 m/s. The reduction of speed is different for the S-waves, where the gabbro once again has the highest range, from 3422

- 4058 m/s, followed by the basalt HBA-18, from 1830 - 2942 m/s. The other rocks have lower S-wave velocities, as for the dike (ND-6) ranging from 3065 - 3335 m/s, the basalt HB-4 from 2306 - 2563 m/s, the basalt HBimp-9 at 2105.19 - 2332.27 m/s, and the basalt HPB-23 ranging from 1727 - 1833 m/s. For most of the rocks most of the Vp and Vs values are in the same range of velocities with a Vp >> Vs. The wave velocity rises with increase of the applied stress and especially considering the velocity of P waves.

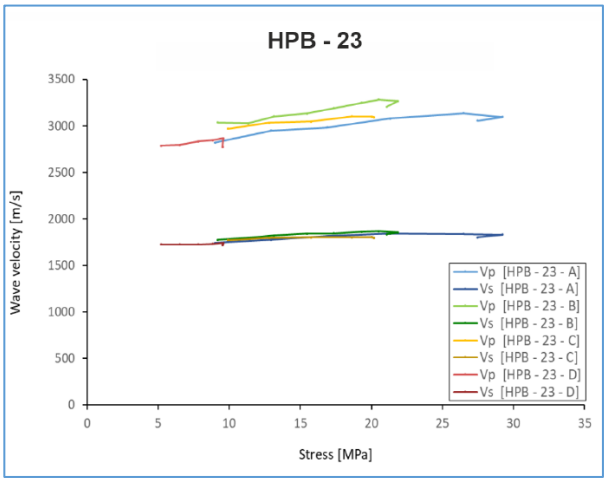

Figure WP1.16: Active-Acoustic Test results for rock under axial stress conditions. The graphs display the P- and S-wave velocities for Basalt HPB-23, measured at different levels of axial stress in MPa. Each line in the plot corresponds to a different sample measurement.

Tensile Strength Test Results

The Splitting Tensile Strength Test has been performed on all rocks hard rocks and the results are visualized as average values per rock in Table WP1.7. The maximum tensile strength values for different types of rocks have been determined through laboratory experiments. The dike (ND-6) has the highest tensile strength values, ranging from 10.2 to 12.17 MPa. The basalt HB-4 follows with a maximum tensile strength range of 5.2 to 8.17 MPa, while the basalt HBimp-9 has a range of 4.23 to 6.83 MPa. The basalt HPB-23 has a maximum tensile strength range of 3.22 to 4.39 MPa, and the basalt HBA-18 has a range of 2.95 to 4.4 MPa. The hyaloclastite HH-1 has the lowest maximum tensile strength range among the rocks, varying between 0.78 and 3.79 MPa.

Table WP1.7: Average Maximum Tensile Strength values per rock.

	HBA - 18	HH - 1	HPB - 23	HB - 4	HBimp - 9	ND - 6	G
Max. Tensile Strength [MPa]	3.68	0.87	3.77	6.94	5.84	11.21	-

Thermal Shock Experiment Results

Observed *changes* in porosity and mechanical properties.

Six samples have been subjected to thermal shock and measured with a helium pycnometer before and after the experiments. The results by sample are in the work of Redondo, 2023.. *The average porosity* of the tested Icelandic sample before the test is 20.91% and after the test 21.41%. Some results of related the UCS tests are presented in Figure WP1.17. After the thermal shock, there is an increase in porosity of 0.5% on average with respect to the values measured before the test. This is caused by:

- Differential thermal expansion in texture and mineral concentrations causing loss in texture coherence.
- Quenching, causing irregular contraction and increase of microcracks.
- Mineral phase changes, causing mineral alterations and by that changing matrix volumes.

The mechanical properties of the control group have an average maximum stress value, Young's modulus and Poisson's ratio before the thermal treatment of 69.64 MPa, 16.51 Gpa, and 0.27 respectively. After thermal treatment and quenching those are respectively 64.76 MPa, 16.02 Gpa, and 0.3. Thus, the mean maximum

stress has decreased by around 4.88 MPa, the Young's modulus has decreased by 0.49 Gpa and the Poisson's ratio has increased by 0.03. So, thermally treated rock has a porosity increase and is mechanically weakened.

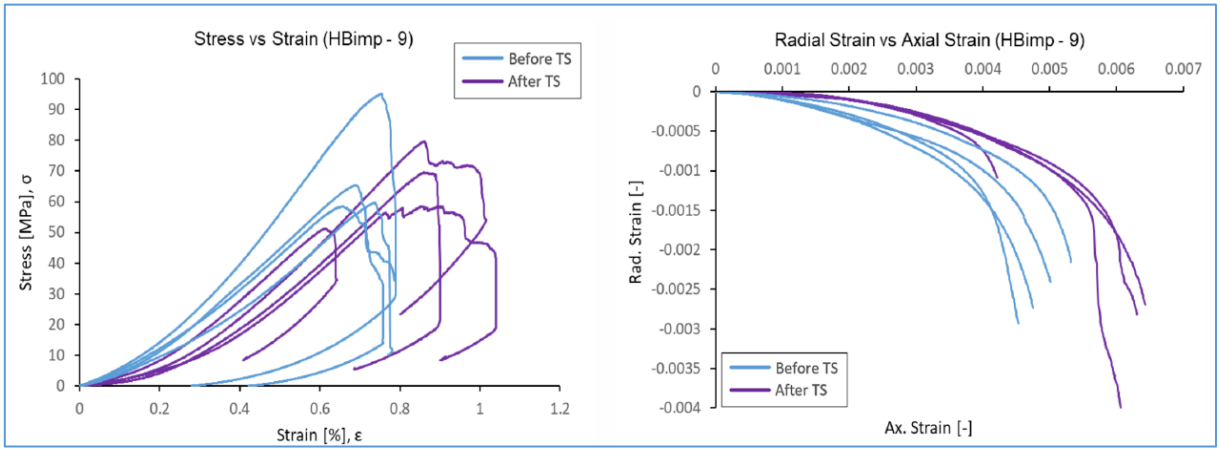

Figure WP1.17: Stress vs Strain & Radial Strain vs Axial Strain Plots of HBimp9 before and after thermal shock.

Wave velocities before and after Thermal Shock

In Figure WP1.18, the acoustic measurements during the UCS test show that the average velocity of P- and S-waves before and after thermal treatment are 3977 m/s and 2300 m/s, respectively. In other words, the thermal shock resulted into a relative increase of 10% in the P-wave velocity (from 3603 m/s to 3977 m/s), and a relative increase of 3% in the S-wave velocity (from 2227 m/s to 2300 m/s).

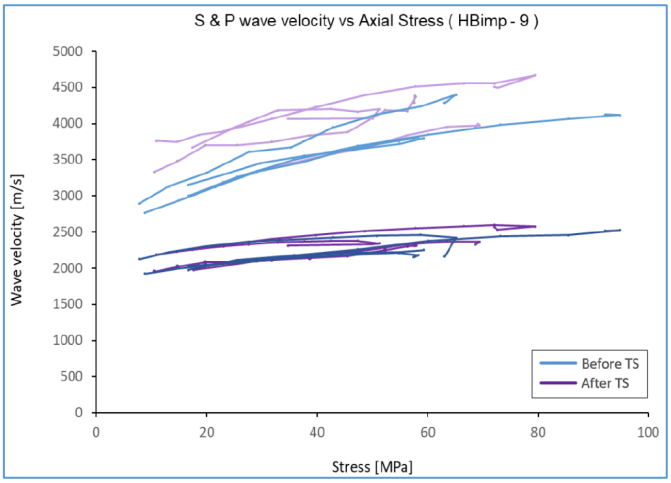

Figure WP1.18: Active-Source Acoustics Test results for P & S e velocity of Control group and Thermal Shock group after the test.

Conclusion for the Hellisheiði experiments

As part of WP1, sampling collection from outcrops near the Hellisheiði site was conducted in Juli 2022, after a delay of 18 months due to Covid. After the samples were shipped to The Netherlands, multiple cores were prepared and subsequently used for obtaining the baseline rock mechanics and seismic-response on dry and saturated samples, shock heated and under ambient conditions. The studied samples include several a gabbro, several basalts, a basalt dyke, and a hyaloclastite.

- *Density/porosity relation.* a consistent trend was observed: samples with lower porosity values tended to have higher bulk density values. However, matrix densities may vary and cause deviations from the trend line. Moreover, a minor effect of the presence of non-connecting pores may also create a minor change in

matrix densities. In line with what can be expected, the gabbro's and dykes had the lowest porosities (<10 vol.%) and the various basalts a hyaloclastites a wide range from ca. 20 v0l.% to 55 vol.%.

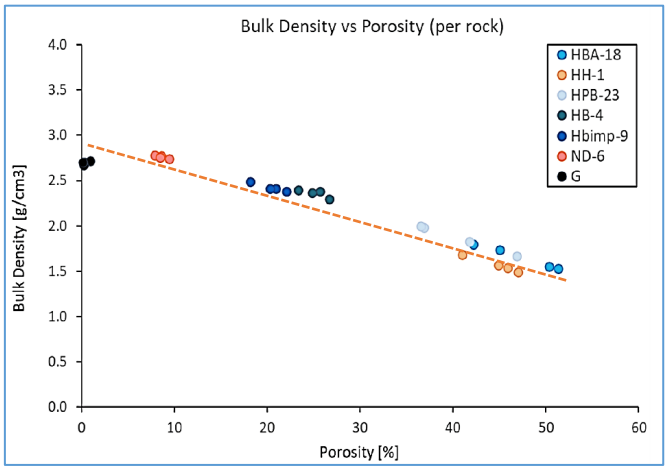

Figure WP1.19: Comparing the relationship between Density and Porosity of all samples together with a trendline.

- The obtained *permeability data* did not a significant relationship between permeability and density or porosity. Pore connection, presence, or absence of micro-cracks between the vacuoles and presence of erratic weathering products are the most logic explanation.
- There is an inverse connection between *porosity and the ultimate compressive strength.* The low porous hard rocks (gabbro and dykes) have the highest strength, which decreases with the in crease the vacuoles in the basalts and hyaloclastites (Figure WP1.20).

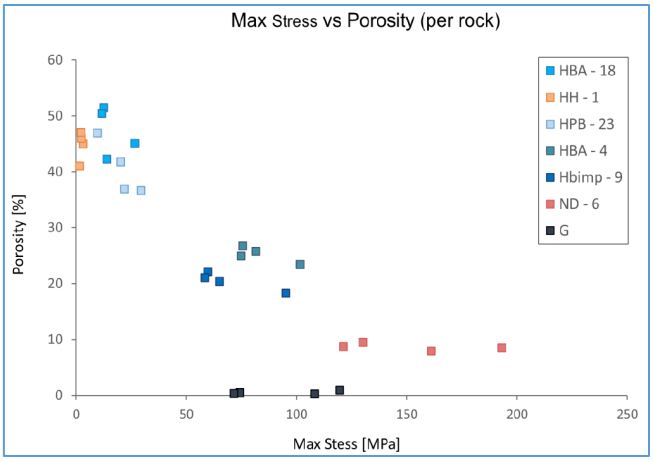

Figure WP1.20: Maximum stress versus porosity of all treated samples.

- A positive correlation between *the ultimate compressive strength and the Young's modulus* when considering all samples (Figure WP1.21-left), shows the highest modulus values for the highest Yield stresses. However, the *Poisson ratio* does not show a straight correlation (Figure WP1.21-right). Usually, higher Poisson's ratios indicate more brittle rock types, less capable of withstanding deformation, while lower ratios correspond to ductile rocks that endure more deformation before failure.

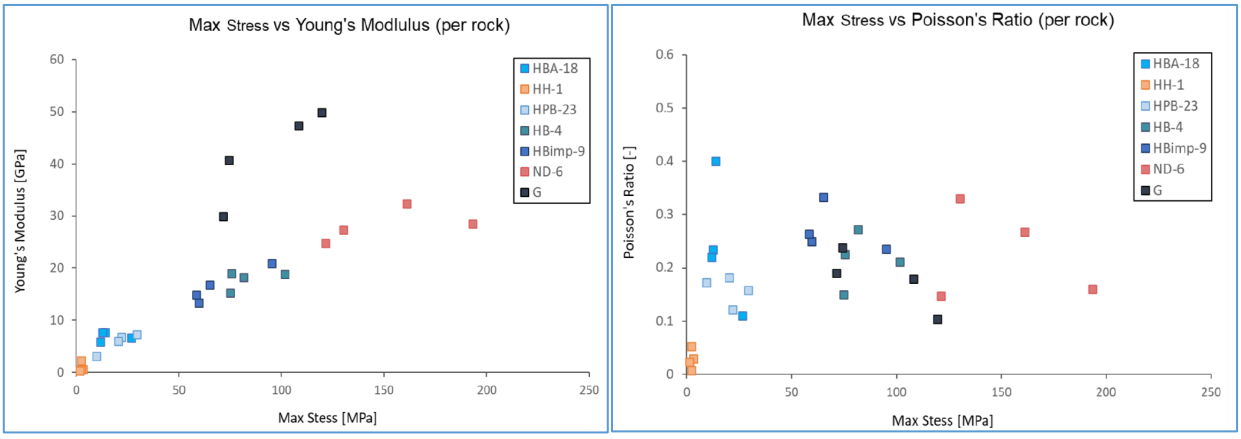

Figure WP1.21: Maximum stress versus Young's modulus (left) and Poisson's ratio (right).

- The results of *a thermal shock* conducted to simulate reservoir temperature conditions (270ºC) and injection temperature (60°C) showed no significant texture changes. It resulted into microfractures generation and by those slight changes in the mechanical properties of the TS group. The acoustic data. However, show an inconsistent velocity increases instead of decreasing. Despite this, the results of the control group (220 and 357 m/s for S and P waves) are comparable. Hence, the acoustic results of this thermal shock are inconclusive since if changes are not significant, when considering the natural variability of the rock. Translating those observations to field conditions and injection conditions at temperature, the effect that a combination of overburden stress and injection pressure can induce thermal shock and generate fractures in the vicinity of well. However, it should be noted that a drastic increase in this temperature difference may compromise the integrity of the reservoir, and as such, the use of thermal shock as a method to increase CO2 storage capacity should be studied in greater detail in the future.

Translation of the results to depth profiles for WP2, WP4 and WP5

Conversion to depth Kizildere and model

The previous displayed uni-axial laboratory measurements (Figure WP1.22), and at a later stage the bi-axial and CO_2-measurements (WP3,4,5) have been applied to prepare acoustic models of the Kizildere sub-surface. The dry scenario was followed by a brine saturated scenario. Then, brine was replaced by various degrees CO_2, saturation. This exercise has been used to define the geophone distance of the reference lines and the shot distance with the new eVibe (see WP4).

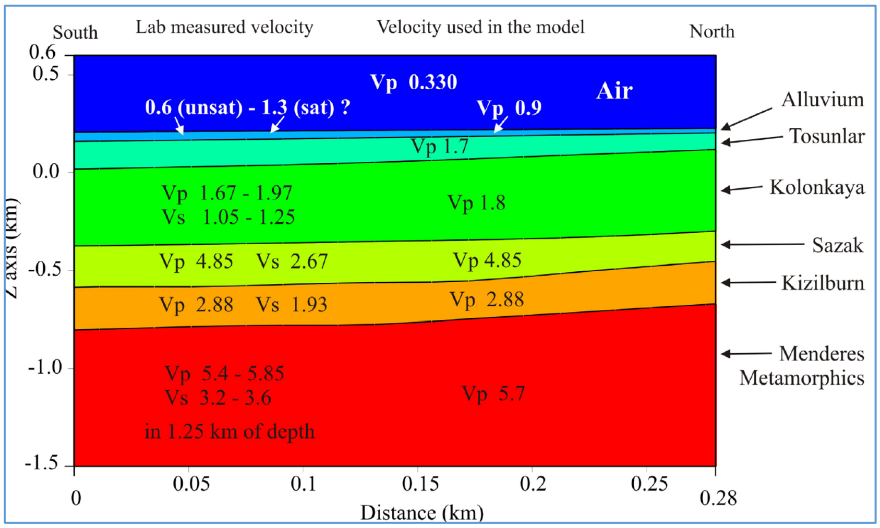

Figure WP1.22: Kizildere velocity model in the 2D section along the 2D HWC line.

The previous displayed uni-axial laboratory measurements (Figure WP1.22), and at a later stage the bi-axial and CO_2-measurements (WP3,4,5) have been applied to prepare acoustic models of the Kizildere sub-surface. The dry scenario was followed by a brine saturated scenario. Then, brine was replaced by various degrees CO_2, saturation. This exercise has been used to define the geophone distance of the reference lines and the shot distance with the new eVibe (see WP4). In the imaging examples here presented, we used for modelling seismic reflection source and responses of different distances the following distances:

- With sources at surface every 25 m for the dry scenario, 50 m for the brine saturated scenario and 100 m for the CO_2 saturated scenario.
- Receivers at surface every 5 m
- Ricker wavelet with peak fequency of 50 Hz
- Number of time samples equals 4096 at 0.09 ms
- The model edges are tapered and by that suppressing reflections from the sides of the model.

It was found that changing the pore-fluid from dry to brine saturated yields increase absolute velocities, however, they do not imply that reflectors will be brighter as reflections are controlled by the contrast in acoustic impedance. The presence of CO_2 in the reservoir changes the absolute velocity, however, the effect of presence of CO_2 is hard to observe in the migrated image, though confirmed by subtracting separate gathers. In WP3, we discuss the follow-up activities of the WP1 laboratory work to include different combinations of pore-fluids (i.e. brine - CO_2 combinations) and compare results with Gassmann 'ubstitution findings and study the effect of temperature on seismic velocities. In addition, we discuss modelled reflection data in relation to frequency and amplitude spectrum analysis.

As an example, for modelling seismic reflection responses of 50% CO_2 saturated vs. 100% brine saturated, we took the difference between two single shots gather, i.e. a CO_2 case – brine saturated case. No direct waves were applied. Note in figure WP1.23D the presence of some clear reflectors that show the effect of CO_2 addition.

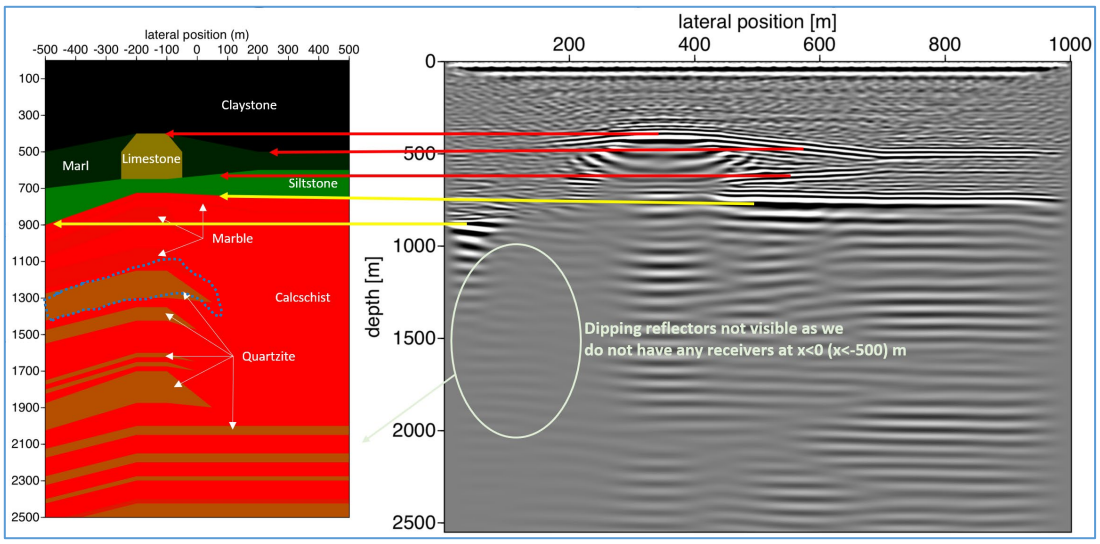

Figure WP1.23.A: Result of the pre-stack depth migration – dry case. Kizildere subsurface model for which the velocity model was taken from Janssen et al. 2021, except for the third marble layer (shown by the blue outline), for which CO_2- and brine-saturated velocities from labwork in WP3 was used (Figure WP1.23C).

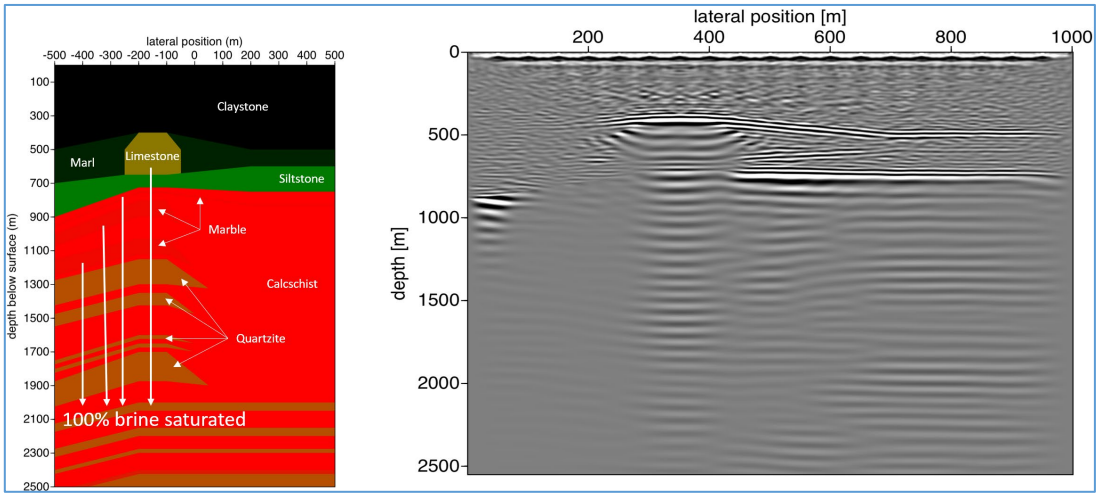

Figure WP1.23.B: Result of the pre-stack depth migration – 4 layers saturated with brine.

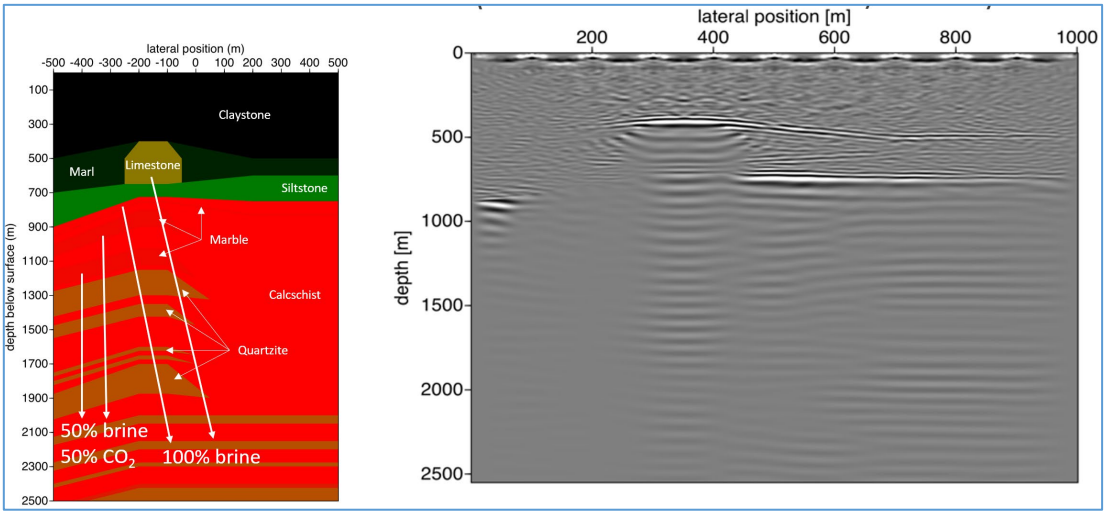

Figure WP1.23.C: Result of the pre-stack depth migration –2 layers saturated with brine, 2 layers saturated with 50% brine and 50% CO_2.

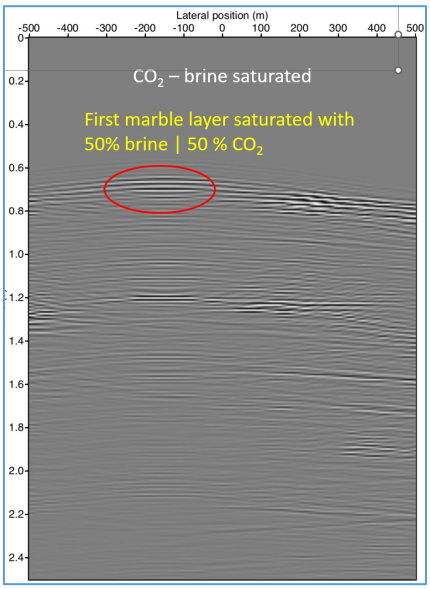

Figure WP1.23D: Single shot gather in time domain in the center of the model

Conversion to depth for Hellisheiði

After analyzing the geomechanical and petrophysical properties of the rocks, 5 units have been implemented in a stress-depth profile: Unit 1, hyaloclastite HH-1; Unit 2, basalts HBA-18 and HPB-23; Unit 3, basalts HB-4 and HBimp-9-; Unit 4, dike ND-6; Unit 5, gabbro G. Using the mechanical properties of these surface-collected samples, we presume that they maintain the same properties as if been buried at the depths of the main feed zones. Note that the experiments were conducted without confining pressure. The vertical stress (σv) in the zone of interest has been considered based on Batir et al. (2012), i.e. integrated weight of overburden on the lithologic model from the mud log of the well HN-16 and bulk densities (Gudfinnsson et al., 2010). The conclusions are conservative since the maximum stress that rocks can withstand with increasing confining pressure results in considerable higher yield strengths. In Figure WP1.24, the main feed zones found in the Húsmuli wells are represented by horizontal dashed lines (from ca. 900 m to 2180 m). The vertical-colored lines represent the average maximum stress of the unit rocks. The ultimate strengths of some basalts (HBimp-9, HB-4), the gabbro (G) and dike (ND-6) are far above the σv for the given depth. Other basalts (HBA-18) and the hyaloclastite (HH-1) lower ultimate strengths than σv for the subsurface region where the feed zones are located. Up to a depth of 1700 m, one basalt (HPB-23) has its ultimate strength being higher than σv.

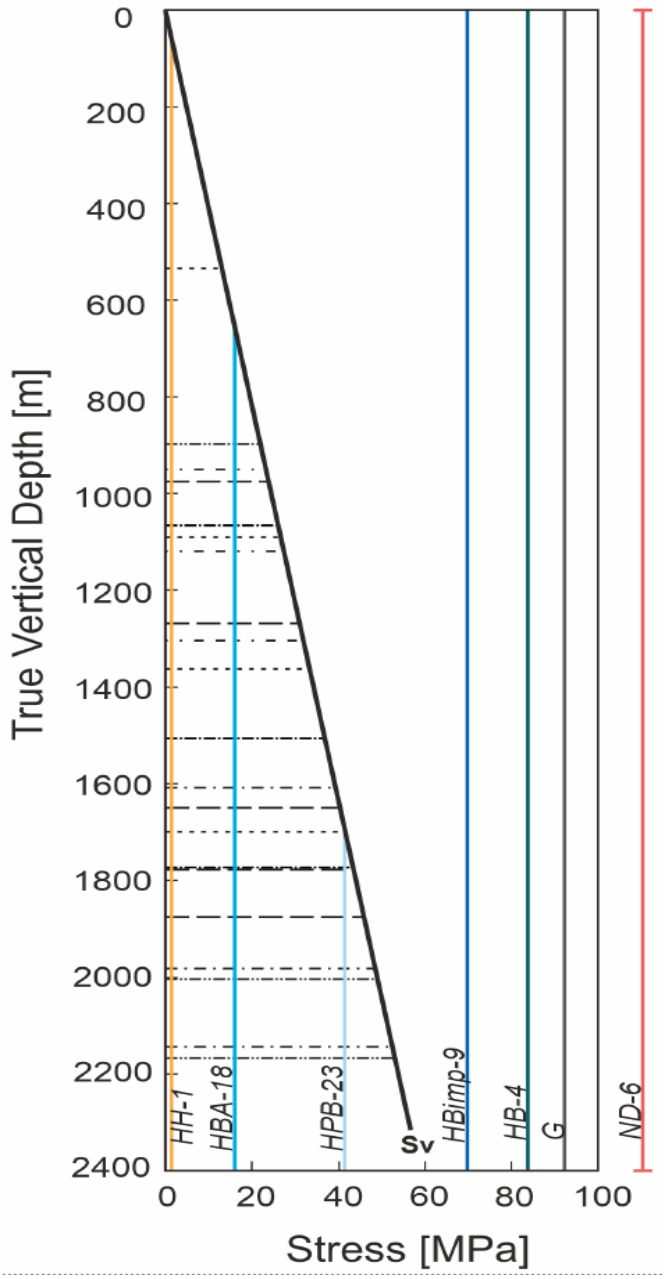

Figure WP1.24: Vertical stress (σv) profile with depth in Húsmuli and feedzone depth locations, overlaid with maximum stress of the rocks. σv increases with depth to 50 MPa at 2200 m. The main feed zones are in between 900 and 2200 m.

This extensive laboratory study on the effect of stresses on seismic velocities and related literature data are used for a base-case scenario of the Hellisheiði field monitoring in a situation prior to and after CO_2 injection. These results serve as a reference for WP4 and WP5. By using fluid substitution according to Gassmann's theory (Gassmann, 1951), seismic reflection responses are modelled for the case after CO_2 injection. They are significant for deciding on the acquisition configuration in the field, and by that will help with the interpretation of the field data. Figure WP1.25 and Figure WP1.26

show examples of modelling results, obtained for the Hellisheiði geothermal site and showing an increased acoustic impedance contrast.

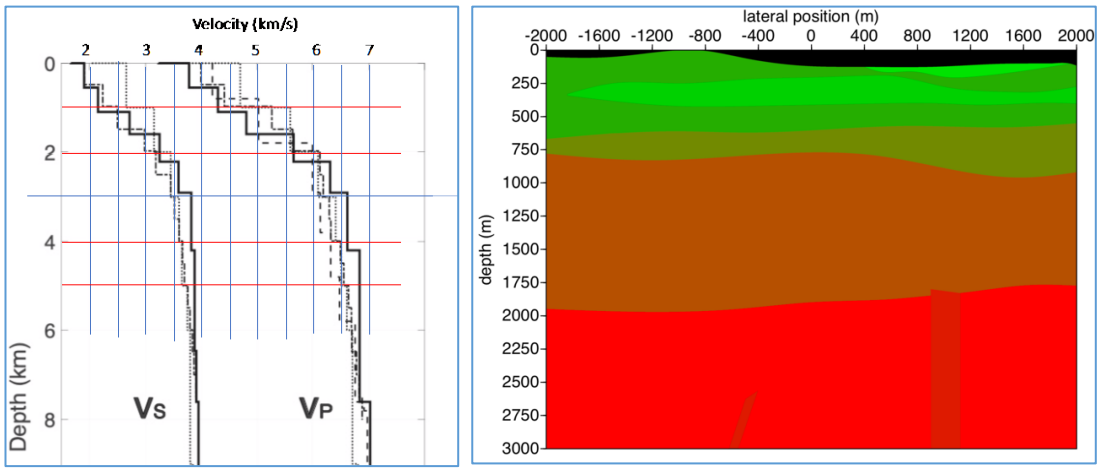

Figure WP1.25: Example of a subsurface model as prepared for the Hellisheiði site

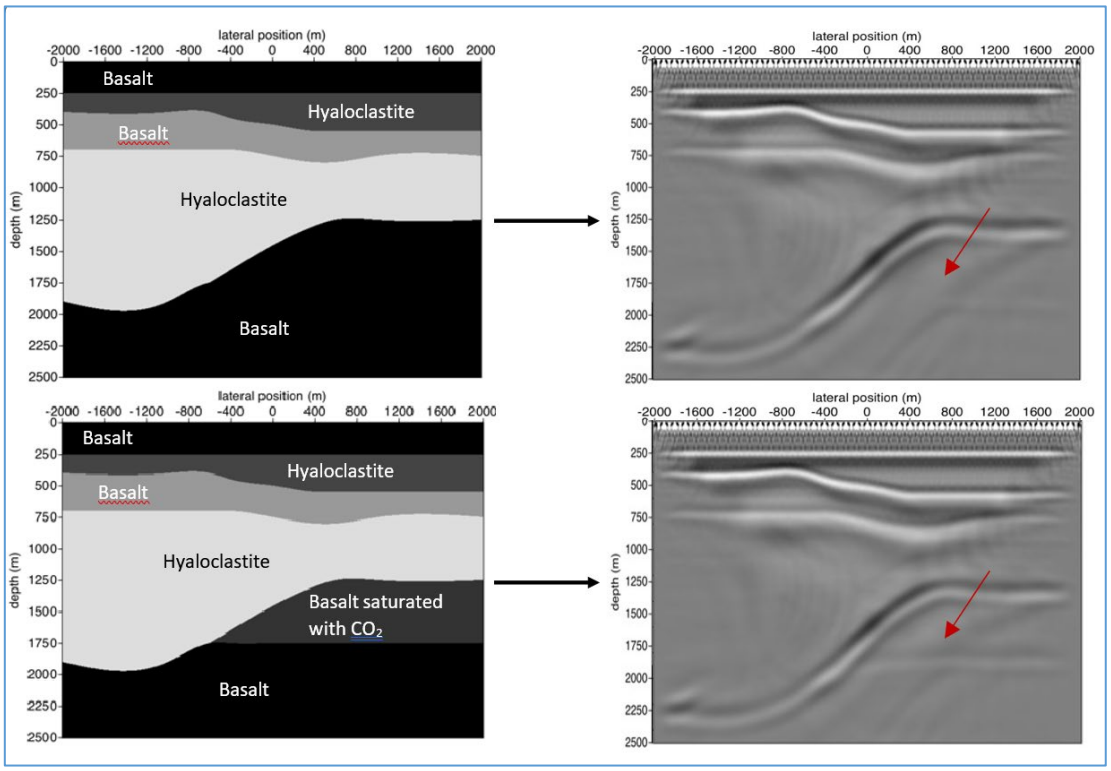

Figure WP1.26: Modelling results obtained for the Hellisheidi (Iceland) site. A total of 801 receivers were placed at the surface, one every 5 m. Also at the surface, 41 active seismic sources were located at every 100 m. The left-hand side displays two subsurface models: 1) prior to CO_2 injection, i.e. the base-case (top), and 2) after CO_2 was injected in the bottom basalt layer (bottom). The right-hand side presents the corresponding imaging results from pre-stack depth migration of the modelled reflections for both cases. Note the effect of the presence of CO_2 on the imaged impedance contrasts (red arrow). Results shown were obtained using literature data and in the final stage with lab data.

Literature referred to and created through WP1

- Gudfinnsson, G., H. Helgadottir, C. Feucht, and H. Ingólfsson (2010). "Húsmúli – well HN-16: Drilling, 1st and 2nd stage. Drilling for surface casing at 95 m, production casing at 660 m and production part in 2204 m depth". REPORT In: Icelandic. Iceland GeoSurvey, Reykjavík. Janssen, M.T.G, Barnhoorn, A., Draganov, D.,

Wolf, K. H. A., & Durucan, S. (2021). Seismic Velocity Characterisation of Geothermal Reservoir Rocks for CO2 Storage Performance Assessment. Applied Sciences, 11(8), 3641.

- Janssen, M.T.G., Russel, J., Barnhoorn, A., Draganov, D., Wolf, K., & Durucan, S. (2020, November). Seismic Velocity Characterization and Modelling for Synergetic Utilisation of CO2 Storage Coupled with Geothermal Energy Extraction. In 1st Geoscience & Engineering in Energy Transition Conference (Vol. 2020, No. 1, pp. 1-6). European Association of Geoscientists & Engineers.
- Parlaktuna, M., Durucan, Ş., Parlaktuna, B., Sinayug, Ç., Janssen, M.TG., Şenturk, E., Tongic, E., Demircioglu, Ö., Poletto, F., Bohm, G. and Bellezza, C., 2021. Seismic velocity characterisation and survey design to assess CO2 injection performance at Kızıldere geothermal field. Turkish Journal of Earth Sciences, 30(9), pp.1061-1075.
- Redondo García, E., 2023. Petrophysical and Mechanical Characterization of the Volcanic Rocks in the Hellisheiði Geothermal Field and implications of Thermal Fracturing in CO_2 mineralization.. MSc-thesis TU Delft. https://repository.tudelft.nl/islandora/object/uuid%3A641e5df2-c411-450d-9095-342673a225a7

Work Package 2: Planning and construction of Kizildere infrastructure for CO_2 injection at Kizildere, CO_2 injection at Kizildere and, continuous long-term CO_2 Injection at Hellisheiði.

Task 2.1: Review and selection of injection and monitoring wells layout at Kizildere.
Task 2.2: Development of technical and operational procedures, infrastructure planning, construction of injection facilities at Kizildere..

In WP2, DUT and SM, in interaction with the partners, reviewed for both sites the geomorphological situation for the choices to be made for outlays of the surface monitoring lines in Hellisheiði and on the first choice for surface lines and monitoring wells in Kizildere. Regarding the development of technical and operational procedures, it was decided to additionally implement the DUT two-component cabled geophones (10 Hz) and place those along the fiber optic lines. To get cost neutral as possible, SM and DUT merged the shipping activities for both, the vibrator and monitoring equipment and implemented it in the operational procedures, monitoring lay-outs and infrastructure planning. For both Kizildere and Hellisheiði, it was possible to use the preliminary seismic imaging results, made with the outcomes of WP1 and WP3 and preliminary seismic modeling results based on literature related to the EU funded CarbFix project.

Figure WP2.1: Kizildere, September 2019. First discussions for the selection of monitoring and injection wells at the Zorlu geothermal site.

SM and DUT contributions were needed to define the choices for:

- The first definition of the monitoring lines in Iceland and the monitoring lines and monitoring wells in Turkey. The layout in Kizildere has been changed at a later stage.
- The definition of the monitoring spacings of all sensors.
- The definition of the spacing of the sources, i.e. position of the eVibe during signal generation.
- Data-acquisition and synchronization parameters for triggering sources and receivers.

All details of spacing, source characteristics and data-acquisition are extensively explained by SM in WP4.

For more details, we refer to the Final Report and Periodical Reports with ERA-ACT and the SUCCEED website.

Work Package 3 - Laboratory investigations into rock-fluid interactions: geochemical, geomechanical and geophysical response of the reservoir to CO_2 injection

Task 3.1: Large-scale HPHT borehole-simulator experiments on the seismic response and alteration of the reservoir rocks with CO_2/brine-saturated flow.

Task 3.2: Long-term HPHT treatment of cores from Kizildere and Hellisheiði sites, impacts of CO_2 injection on petrophysical and seismic properties of reservoir rocks during the CO2-injection process.

Preamble

Experimental work has been performed to determine the effects of injected CO_2 on the reservoir rock at Kizildere and Hellisheidi. For Delft University (DUT) it aims at studying:

- WP3.1. The reconstruction and use of the Large-scale HPHT borehole-simulator. Experiments on the seismic response and alteration of the of the reservoir rocks with CO_2/brine-saturated flow.
- WP3.2. the response of carbonate rocks to the injection of supercritical CO_2 at high-pressure/temperature reservoir conditions, seismic response (wave velocities, wave attenuation), impact on flow properties, and integrity of the reservoir rock on change in strength.

Due to Covid restrictions, delays in rock sampling and the impossibility to purchase durables and consumables for experimental work, the pre-studies for the Borehole simulator in WP3.1, have been performed at smaller scale samples and included into the experiments of WP3.2.However, all the work still has has been performed at various volume scales, from 40mm diameter cores to 0.4 m^3 large blocks.

The Icelandic and Turkish seismic velocity data on plug-scale cores were shared with our SUCCEED partners who utilized it as an input to create a velocity model of the Icelandic and Turkish demonstration site.

This work connects to:

- WP1.2: Reservoir Rock Characterization Studies. This task was mostly completed in the first half of 2022.
- WP3.2: Long-term HPHT treatment of cores from Kizildere and Hellisheiði sites, impacts of CO2 injection; the geochemical experimental work.
- WP4: Seismic fieldwork related modeling, monitoring, and data interpretation.
- WP5: Interpretation and calibration of monitored data and numerical models used in field performance evaluation pre-and post- CO2 injection, as well as long-term injection strategies planning.

Lab experimental work

A: Small Scale preliminary HP/HT experiments on marble: introduction

The results as described here below are mostly discussed in detail in: Janssen, M.T.G, Draganov, D., Barnhoorn, A. and Wolf, K.H.A.A., 2023. Storing CO2 in geothermal reservoir rocks from the Kizildere field,

Turkey: Combined stress, temperature, and pore fluid dependence of seismic properties. Geothermics, 108, p.102615.

As requested, this task has been completed for the Turkish marble.

Based on the outcomes in WP1, Kizildere plugs with and without fractures have been acoustically measured under P, T with a fracture filling of air, brine and CO2. The acoustic responses have been compared. In this follow-up, a plug with a fracture connected to an in- and outlet was prepared for the triaxial cell. This preliminary work was used for the preparations of the large sample experiments in the borehole simulator. The results have been used for the decisions regarding fracture preparation; the injection and production line configuration; P,T-schemes for pore pressures and tri-axial stresses on the rock, brine and CO2; and acoustic measurements.

Figure WP3.1 shows the schematics of the experimental set-up. In the bottom left, a sketch of the artificial fractured marble sample (Marble-frack) is shown. It was created by cutting the sample in two, creating a fracture plane presented in brown. In addition, in- and outlet holes were drilled from each side of the core sample (red arrows displays the flow path). The fractured marble sample was fully saturated with a Kizildere type brine having 0.41 wt.% NaCL.

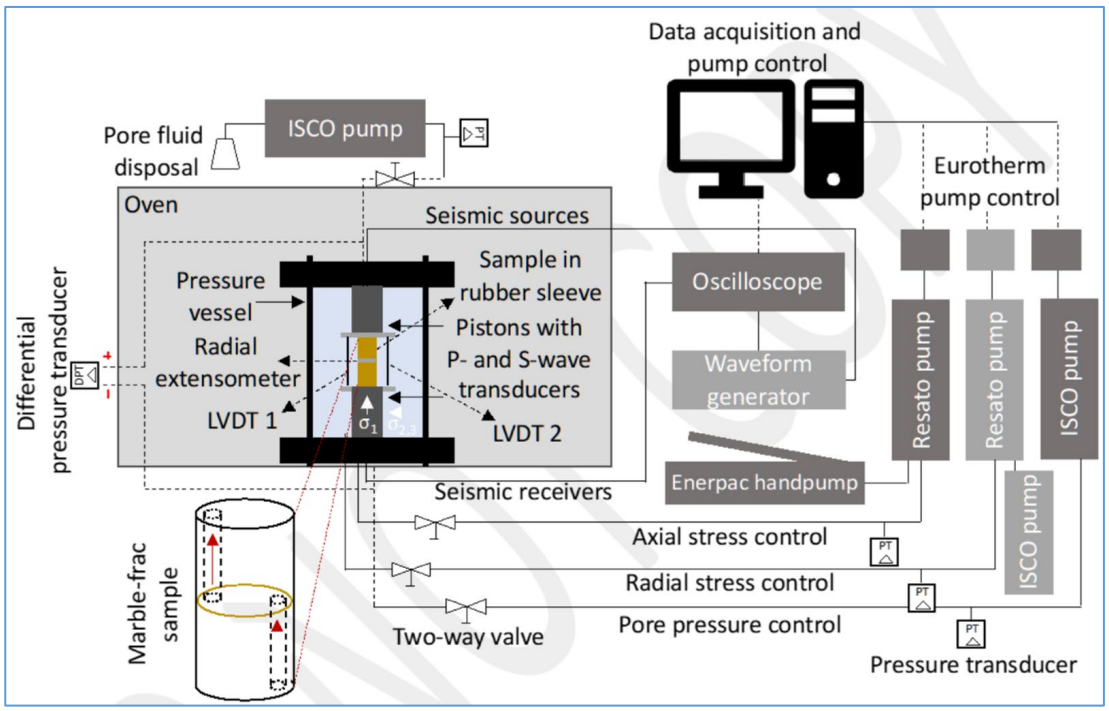

FigureWP3.1: The triaxial set-up for acoustic measurements on Kizildere plugs with a fracture.

B: Effect of temperature and pore fluid on seismic properties of the Kizildere plugs.

This paragraph presents the results related to tests performed at field-representative stress conditions. For the mechanical tests on plugs, relevant values for σ1 and σ2 (= σ3), that prevail in the Kızıldere reservoir, were obtained from the local geological literature and results of WP1.

Besides conducting the active-source acoustic-assisted CCS tests on the dry marble and calcschist samples, it was also carried out on an artificially fractured marble sample, where its fracture was either 100% saturated with Kızıldere type brine or supercritical CO2. Figure WP3.2 shows Vp as function of the axial stress, σ1, at a fixed radial stress, (σ2 = σ3) of 16.9±0.1 MPa, for both the dry calcschist and marble core samples. Vp is also shown as function of temperature for fixed magnitudes of σ1 of 17.0, 25.5, and 41.7 MPa. Vp/Vs ratios are shown as function of temperature for fixed σ1 of 17.0 and 41.7 MPa.

The Vp values show an increasing speed with increasing σ1, at which the higher density marbles give the faster results when compared to the calcschist. The elevated initial stress level causes that potential closure of micro-cracks, which yields increasing Vp, already occurred prior to performing the first active-source acoustic transmission measurement. The velocities shown in the two top graphs of figure WP3.2 correspond well with the velocity results obtained earlier in the WP1 reporting (i.e., uniform stress conditions). Hence, the original uniaxial UCS results show that radial stresses (σ2 = σ3) most likely have a negligible impact on Vp as long as it is higher than the atmospheric pressure. The loading phase has mostly happened within the elastic regime since there is no visual sign and measurement evidence of permanent deformation; the data points are approximately the loading-related trend.

In terms of temperature dependency, similar observations can be made: Vp reduces as function of increasing temperature and its impact is larger on Vp-marble compared to Vp-calcschist. Within a temperature range of 21-80°C, for a σ1 of 25.5 MPa, Vp decreased with 6.8% and 2.6% for the marble and calcschist, respectively. Compared to the reduction in Vp, within the same temperature range, at isotropic stress conditions of σ1,2,3, = 25 MPa (5.4% and 1.2% for the marble and calcschist, respectively), we may conclude that the temperature effect is.

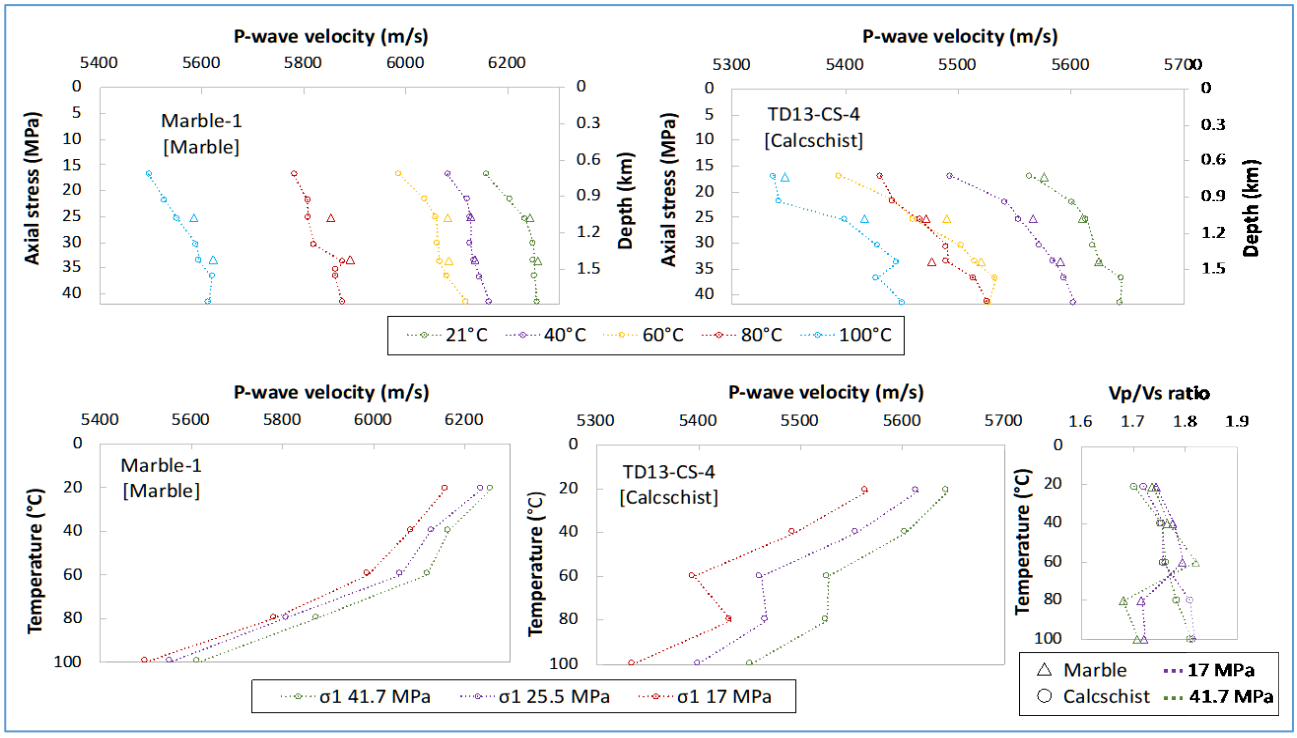

Figure WP3.2: Vp as function of σ1, and thus depth below surface, for marble (top-left) and calcschist (top-right) samples. Vp is plotted against T for σ1 of 17.0, 25.5, and 41.7 MPa (bottom-left). Bottom-right shows Vp/Vs ratios for marble and calcschist at fixed value for a σ1 of 17.0 and 41.7 MPa. The triangular data points in the top graphs are acoustic measurements during unloading (for a potential hysteresis check).

Like the observations made in previous sections, the stress σ1 (17.0 or 41.7 MPa) shows a negligible effect on the resulting Vp/Vs ratios. For the calcschists, the averaged Vp/Vs ratio as function of temperature, shows similar behavior to the uniform stress conditions, i.e.; a gradual increase from 1.71±0.01 (21±1°C) to 1.81±0.01 (100±1°C). For the marble, no distinctive trend was recognized.

C: Effect of temperature and pore fluid on seismic properties of fractured Kizildere marble plug.

Besides investigating the combined temperature and stress effect on seismic properties, the effect of pore the Kızıldere type brine and pore pressure were also assessed. It was done by using an artificially fractured marble

sample. Figure WP3.4 shows Vs, Vp, and the Vp/Vs ratios as function of increasing σ1 and Pp, at a fixed σ2,3 of 16.9±0.1 MPa for a 100% brine-saturated fracture. Increasing Vp values, as function of increasing σ1 and Pp, are observed. In terms of absolute velocities, Vp of the fractured marble, fully saturated with brine, is higher than the Vp data shown in figure WP3.3 (i.e., the velocities related to a dry, intact, marble). The trend related to Vs differs from the observations made regarding Vp, since Vs shows a slight reduction as function of increasing σ1 and Pp. The latter is most likely related to the pore fluid, and corresponding Pp, as in earlier work by Janssen et al. 2021, i.e. increasing Vs as function of increasing σ1 for dry samples. The Vp/Vs ratios presented show a slightly increasing ratio as function of increasing σ1 and Pp, which can be explained by the abovementioned behaviour of Vs and Vp. Moreover, the Vp/Vs ratios exhibit higher magnitudes when compared to similar experiments on a dry marble (figure WP3.2). It is a consequence of the higher Vp due to the presence of brine.

At a temperature of 80±1°C, and σ1 between 18 - 40 MPa, Vp increased with 1.8%. However, for the same range in σ1, but at a temperature of 40±1°C, Vp increased just with ca. 0.6%. As discussed before, at higher temperatures, minerals expand more and by that increases compaction, thus an increasing Vp.

Subsequent to the fully brine-saturated fractured marble experiments, two additional tests were performed on a 100% supercritical CO2-saturated fracture. These experiments were conducted at 40±1°C and 80±1°C.

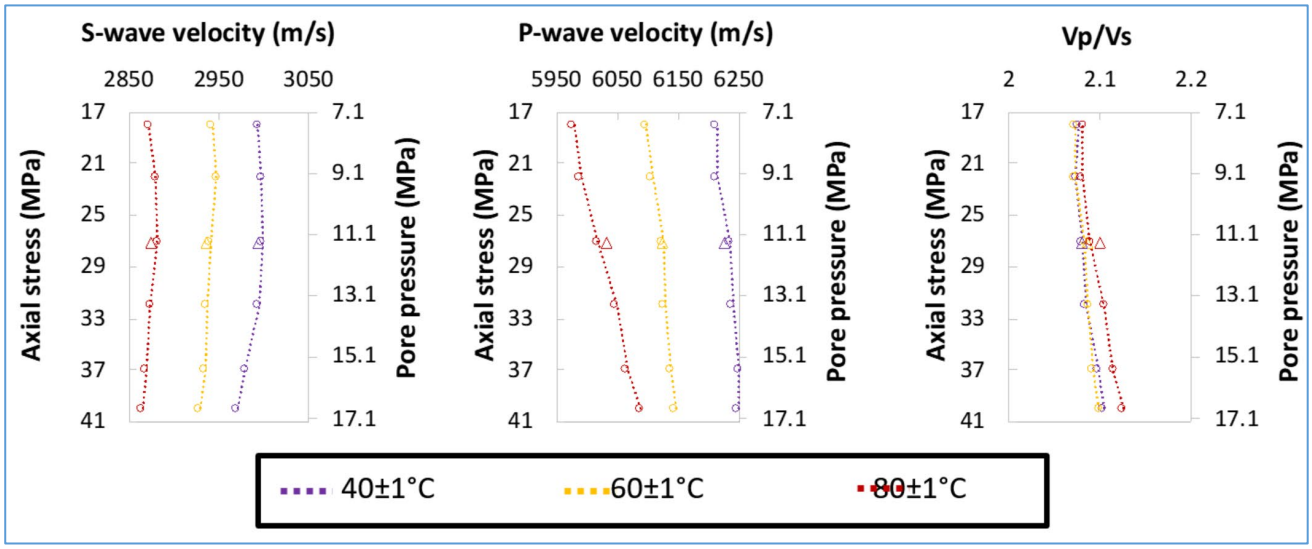

Figure WP3.3: Artificially fractured marble at 100% brine-saturated fractures. Vs (left), Vp (center), and the Vp/Vs ratios (right) as function of vertical stress (σ1) and pore pressure (Pp), and thus depth below surfaced. Field-representative values for σ1 and Pp were taken from the results of WP1. The triangular data points represent acoustic measurements done during unloading of the sample for a potential hysteresis check.

So far, we mainly focused on first arrivals, i.e., Vp and Vs. However, to differentiate between a supercritical CO2-filled fracture and a fully brine-saturated crack, first arrival analyses might be less. Figure WP3.4.A, B show that the first arrivals, for both the P- and S-wave, are very similar in wavelength. Figure WP3.4.A shows the recorded signal (P-wave) for both the brine- and CO_2-case at temperatures of 40±1°C and 80±1°C and for varying σ1 and Pp. We assume that the aperture diameter of the prepared fracture is too small to observe any effect in transmission arrival times. However, we do observe discrepancies in amplitude levels for both temperatures studied. When the fracture is filled with supercritical CO_2, the recorded maximum and minimum amplitude levels are lower compared to the situation where the fracture is fully saturated with brine. The same observation has been with the recorded transmitted S-waves (Figure WP3.4.B). We conclude that the fracture filled with supercritical CO_2, has a higher impedance difference (between the marble itself and the fracture) when, compared to the brine-saturated case.

It directly implies that, when filled with CO_2, more energy is reflected, hence less energy is left for the transmitted wave, which results in lower maximum and minimum amplitude levels being measured in transmission.

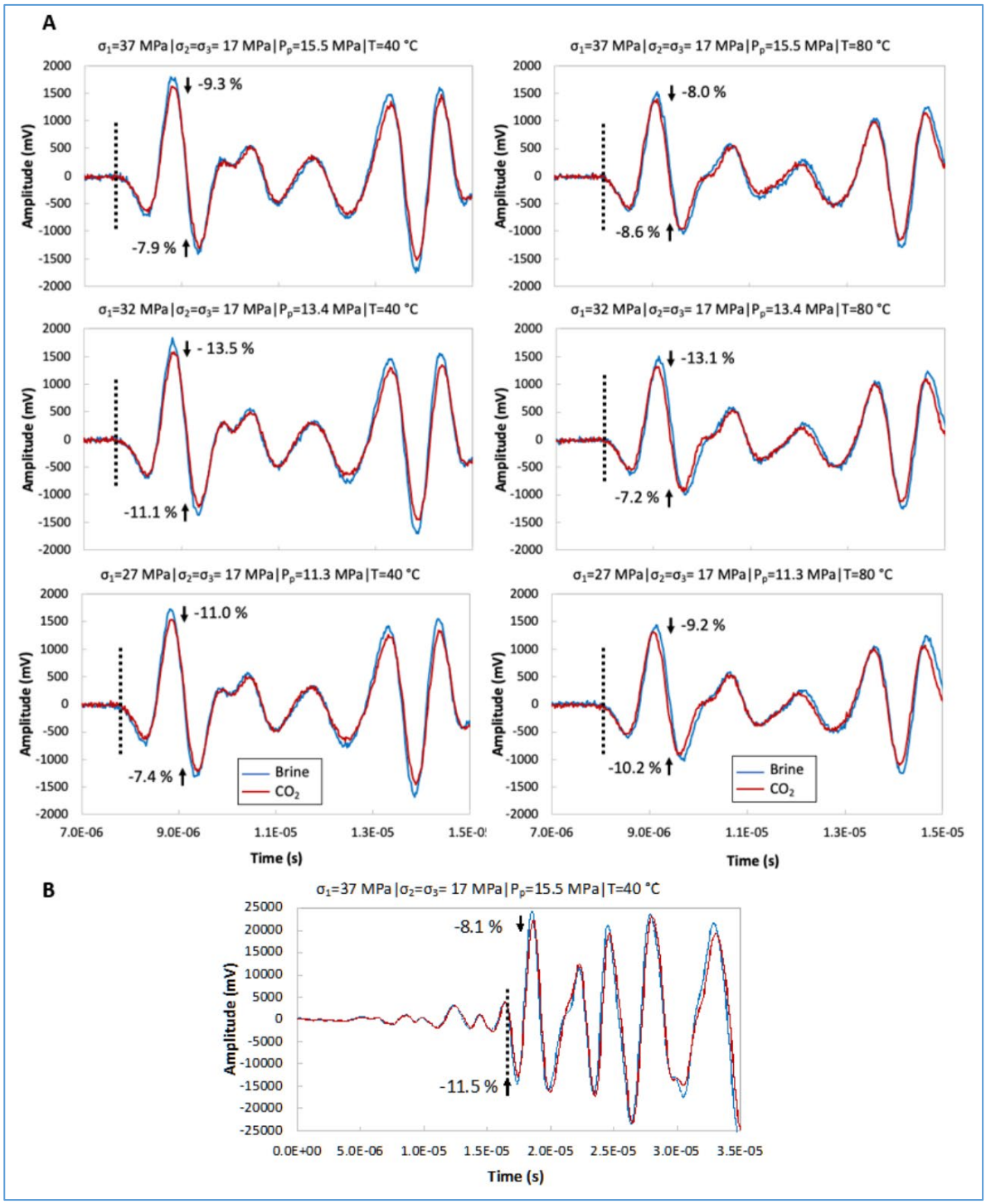

Figure WP3.4: Recorded P-wave (a) and S-wave (b) signals in active-source transmission for the brine-saturated fracture (blue) and the fully supercritical CO_2 saturated fracture (red). Both σ1 and Pp were varied according to field-representative conditions taken from WP1. Two temperatures were assessed: 40±1°C (left) and 80±1°C (right). The black-dashed lines indicate the first arrival times, which are almost identical for both situations investigated. For the first peak and second trough the reduction in amplitude (in %), between brine- and CO2-saturated, is shown. Note that for the S-wave only one situation is highlighted (b), which is representative for the entire stress range studied.

D: Large Scale HP/HT Borehole-Simulator Experiments

Most of the Icelandic work has been explained in the abstract and presentations of Janssen, M., Draganov, D,. Bos, J., Farina, B., Barnhoorn, A., Poletto, F., van Otten, G., Wolf, K-H., and Durucan, S., 2022. Monitoring CO2 Injection into Basaltic Reservoir Formations at the Hellisheiði Geothermal Site in Iceland: Laboratory Experiments. EAGE Annual Conference, Madrid.

This task has been completed for both the Icelandic basalt and Turkish marble. The results have been used in WP5 and WP6.

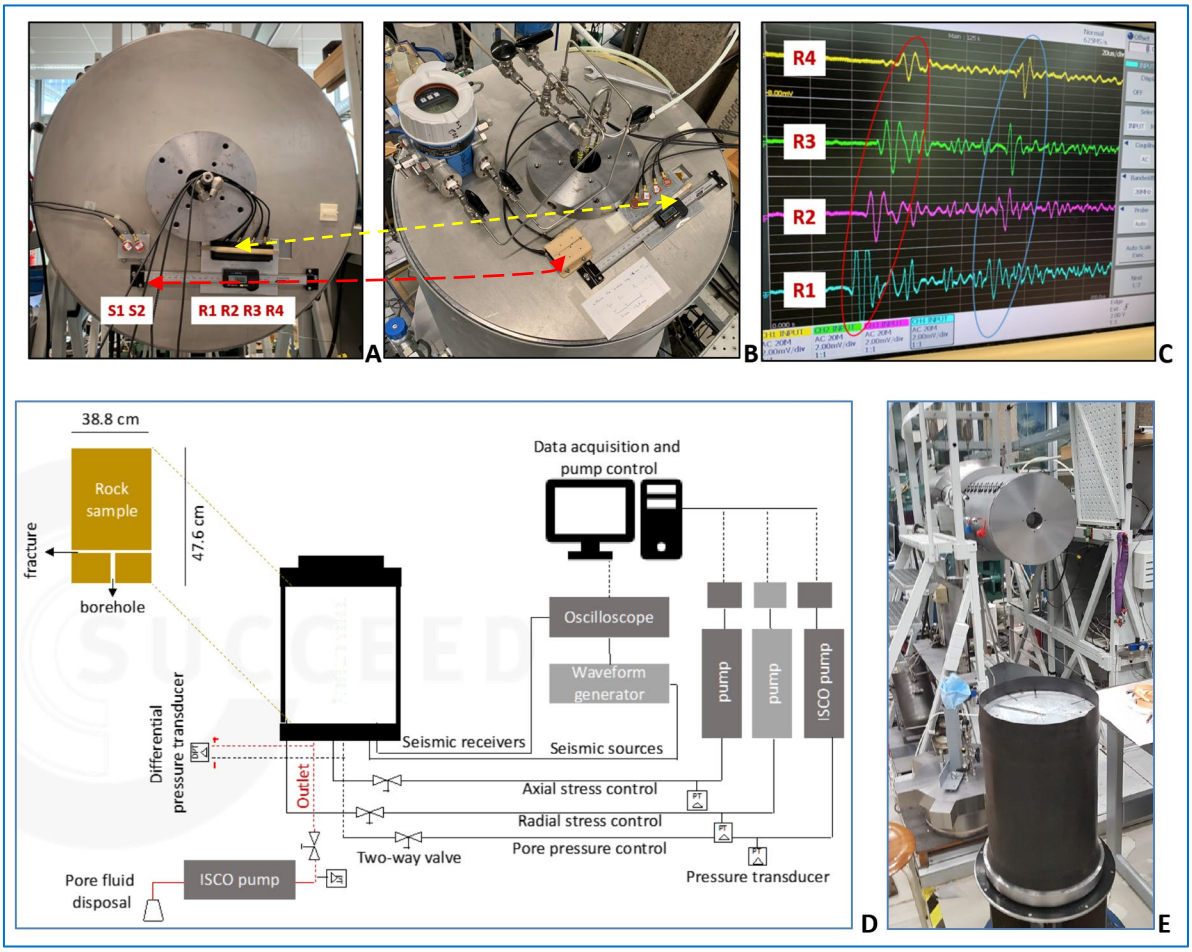

Figure WP3.5: TOP. Configuration of a) the transducers and sources of the receivers were used on 21 positions, b) Injection/production liners for evacuation and saturation with brine and/or CO2, c) Resulting acoustic reflections with resulting events of interest, representing relevant comparable layers and fractures for dry, brine saturated and CO2-saturated pore/fracture space. BOTTOM. The triaxial set-up for acoustic measurements on the Hellisheidi and Kizildere large cylindrical samples. d) Schematic representation of the experimental set-up, e) configuration of the sample in it the rubber sleeve.

The large 400mm diameter and 600mm length samples have been prepared from large blocks collected at the field sites. Those have been placed in the borehole simulator. It can hold an independent radial stress and axial stress of up to 45MPa and a pore pressure at a maximum of 140 bar and at 110°C. The sample is placed in a sleeve and prepared with a small injector where CO_2 and brine are injected after primary brine saturation (Figure WP3.5). During the saturation process and the injection procedures, the refraction and reflection properties, as well as the deformation characteristics, have been monitored. Seismic interferometry analysis have been used (Figure WP3.5 A,B,C) to assess the measurements from empty pore space until full saturation with brine that was stepwise replaced by CO_2. Since both the basalt and marble samples are very isotropic in texture and do not show significant tectonic and sedimentary layering, the experiments have been performed in cylinders with the axis perpendicular to possible signs of layering, schistosity, and former fracture zones of weakness.

The Icelandic Basalt Large Diameter Cylindrical Sample

A complete cycle experiment was conducted on Icelandic basalt. The sample was cut perpendicular to the cylinder axis to create an artificial fracture (Figure WP3.5.D). Then in the central axis of the shorter part, a tubing system was installed to evacuate the pore system; saturate it with brine and finally; replace the brine by CO2-injection. All fluid and gases have been removed via a porous metal sheet in the annular rubber sleeve. Herewith, a closed system was ensured. Thereafter, the wave-propagation parameters obtained during preliminary plug tests as described previously and measured in WP1 (e.g., optimal central frequency of 600 kHz), were used for the seismic characterization. Active-source seismic reflection measurements were performed by utilizing two separate transducers as seismic sources with a total of 21 transducers spots acting as receivers (Figures WP3.5 A,B,C). Reflection measurements were done at 1) dry, 2) brine-saturated, and 3) CO2-saturated fracture conditions. A suite of 8 measurements were taken as function of the saturation amount of supercritical CO2 (80 bar and >33°C) injected.

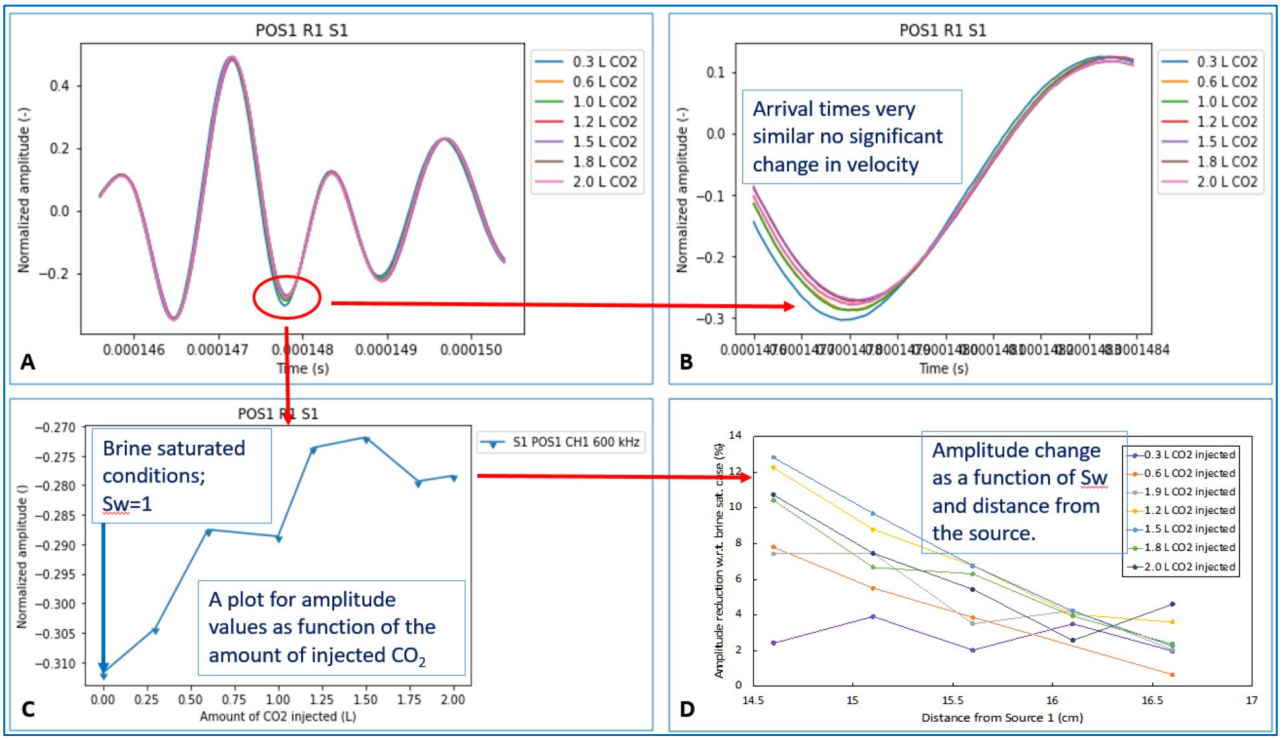

Figure WP3.6: Basic experimental results of acoustic measurements examples as in Figure WP3.5.A: The reflection pulse for source 1 (S1) to receiver 1 (R1) during the replacement of brine (Sw=1) with CO2. B:Detail of showing the minor increase in wavelength and significant increase in amplitude with CO_2 injection. C: Normalized increase of amplitude with increase of CO_2 injection as the replacement of brine. D: For different CO_2 saturations, reduction of amplitude with increase of distance between source and receiver.

Results indicate that the velocity decreases as function of an increasing amount of CO_2 injected, that replaces the brine. In Figure WP3.6.A, the velocity shows no significant change. However, the amplitude values of the brine/CO_2-saturated fracture reflector, shows to be more sensitive to pore fluid changes (Figure WP3.6.B). Overall, amplitude values reduce as function of injected CO_2, reaching maximum reductions of 12±1% when compared to fully brine-saturated amplitude value at near offset (Figure WP3.6.C). Moreover, amplitude reductions (compared to the brine-saturated case) decrease as function of increasing offset (Figure WP3.6.D).

In the second analysis, reflection results were analyzed in line with the field active-source seismic data from Iceland. We detect the velocity changes in specific layers, i.e., CO_2-injection layers and compare those with layers that are not changing. This is based on application of seismic interferometry for retrieval of non-physical reflections from within a target layer from correlation of a primary reflection from the top of the layer and from the bottom of the layer (Draganov et al., 2012,2013, 2023; Ma et al., 2022; Shirmohammadi et al., 2023). The correlation is performed trace by trace in common-source gathers or common-receiver

gathers. The correlation result is then summed over the receivers, in the former case, or over the sources, in the latter case. The result is a retrieved arrival that is kinematically equivalent to a reflection that has propagated only inside the target layer from a source and receiver placed directly at the top of the layer. Because such a reflection cannot be recorded with surface sources and receivers, it is called non-physical (ghost) reflection.

Figure WP3.5.A,B shows the setup geometry for recording a reflection survey (at ultrasonic frequencies) to monitor for changes in the reflections from the fractured sample when injecting CO2 at reservoir conditions inside the fracture. To avoid damage to the ultrasonic transducers, they are installed at the outer metal cover. We use two transducers as sources placed at fixed locations spaced at 20 mm from each other (the yellow arrows). We use four transducers fixed with 20 mm between them in a solid construct (red arrows). The solid construct can slide along the micrometer.

Between the transducers and the basalt sample are two disks of steel and one disk of aluminum. The reflection signals must pass through the disks before and after they pass through the basalt to reflect from the fracture. This could potentially introduce non-repeatability due to temperature changes in the metal disks. Using retrieved ghost reflections for monitoring eliminates this kinematic uncertainty.

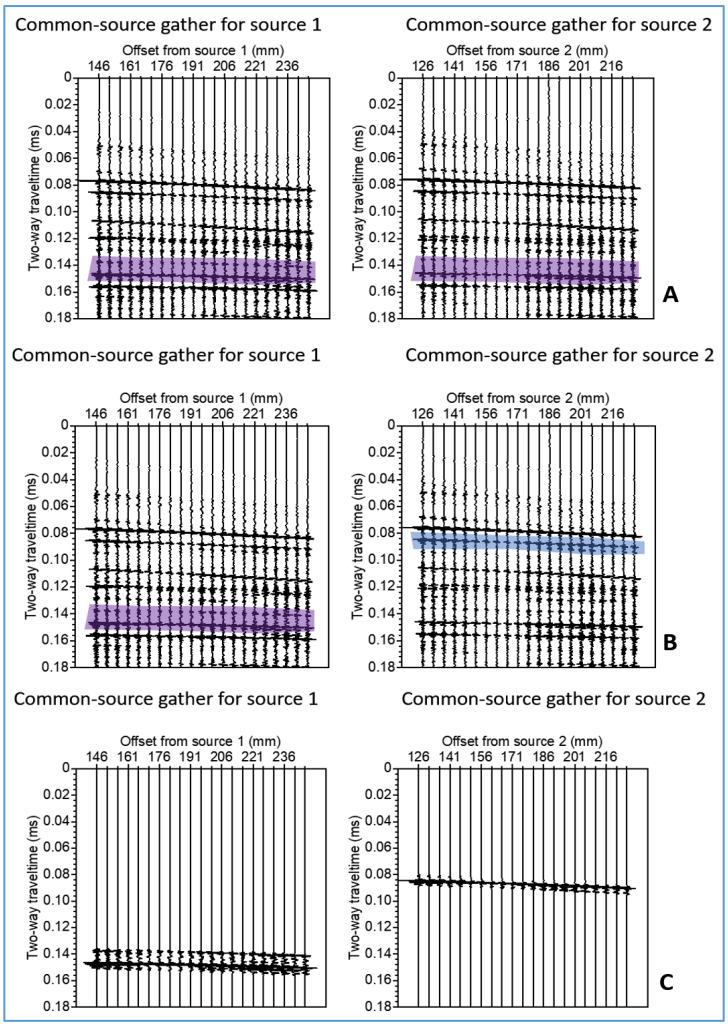

Figure WP3.7: Representation of various common source gathers summarized for source 1 and source 2.

Method of approach

In figure WP3.7.A, the recorded common source gathers from source 1 (left) and source 2 (right) are shown for a compressed dry sample. The first receiver in the solid construct with the four receivers was 126 mm from source 2 and 146 mm from source 1. First, one of the sources was ignited and the signals from it recorded by the solid construct. Then, the other source was ignited, and its signals were recorded. After that, the solid construct was moved away from the sources by 5 mm, and a new recording from each source was made. The solid construct was moved 5 times, resulting in 21 non-repeated recording points per source. Here, we see recordings for central frequency of the two sources of 600 kHz. The gathers are recorded when the basalt sample was dry and under 96 bar axial pressure and 36 bad radial pressure. The violet color in figure WP3.7.A indicates the region of expected arrival time of the reflection from the fracture, which is estimated from comparison with numerical modelling using the velocities estimated from transmission measurements on small samples (Janssen et al. 2022). We repeated the dry measurements described in WP3.7.a at the expected reservoir pressure, i.e., at 233 bar axial and 147 bar radial pressure. After that, we performed measurements at seven levels of injected CO_2: 275 ml, 605 ml, 955 ml, 1225

ml, 1495 ml, 1765 ml, and 2085 ml. During the injection, the axial pressure was 233 bar, the radial pressure was 147 bar, and the pore pressure was 78 bar (supercritical).

In the resulting figure WP3.8 the reflection arrivals between 0.135 ms and 0.143 ms exhibit small time differences. These can be caused by non-repeatability issues (e.g., temperature changes in the metal disks) or they might indicate velocity changes in the basalt above the fracture due to injection of CO_2. If ghost reflections are retrieved, the non-repeatability issued from the metal disks will be eliminated and thus a conclusion whether velocity changes are observed could be drawn.

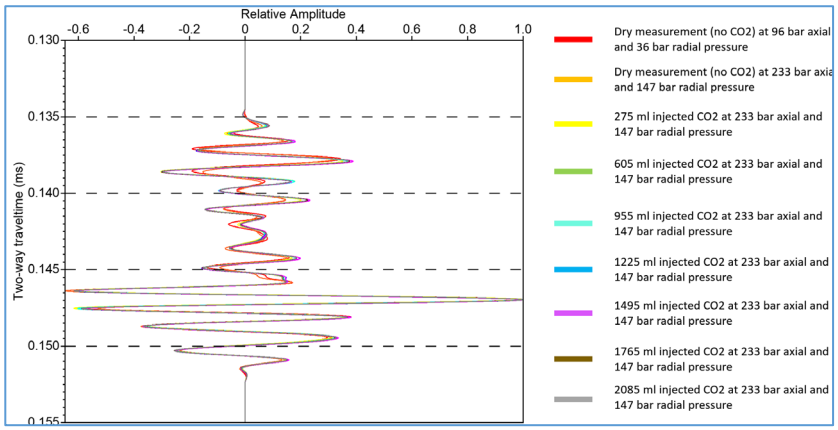

Figure WP3.8: The recordings from source 1 at the receiver closest to it inside the transducer region in figure WP3.5A,B. This specific signal configuration has been compared for all radial- and annular pressures and amount of CO_2 injected.

To retrieve a ghost reflection between the aluminum/basalt interface and the fracture in the basalt, we correlated the primary reflection arrival from the aluminum/basalt interface (figure WP3.7.B) in the recordings from source 1 (indicated with the blue color in the right panel) with the primary reflection arrival from the fracture in the recordings from source 2 (indicated by the violet color in the left panel). The expected arrival time of the blue arrival was also estimated from comparison with numerical modelling using the velocities estimated from transmission measurements on small samples (Janssen et al. 2022). The clearest result is achieved when only the two arrivals on interested are correlated. For this, we extract those from their corresponding common-source gathers (figure WP3.7.C). In order to ensure that in the summation after the correlation, all signals contribute to the summation, we also normalized the arrivals at each receiver to their maximum.

The results in Figure WP3.9.A , shows that the main contribution in the summation comes from the stationary-phase regions, i.e., the regions in the left panel where the arrivals appear at the same or nearly the same time (the orange regions). To avoid artefacts due to the finite and open aperture of the receiver array, we reduce gradually to zero the right traces in the left panel. The summation result, representing the retrieve ghost reflection between the aluminum/basalt interface and the fracture, is shown in the right panel. The ghost reflection represents a reflected arrival from the fracture recorded between a ghost source and ghost receiver placed directly at the aluminum/basalt interface spaced at a distance equal to the distance between the two fixed sources at the top plate of the borehole simulator, i.e., 20 mm. The fracture is at around 67 mm. Then, using a P-wave velocity of the basalt of 2548 m/s (WP1), the expected two-way travel time of the ghost reflection is 0.053 ms. This arrival is indicated with the magenta ellipse in the right panel.

In figure WP3.9.B. we see the results for the retrieval of the ghost reflection for dry conditions but at 233 bar axial pressure. Comparing to figure WP3.9.A, we can see that the retrieved ghost reflection arrives at exactly the same time, as expected. It proves that the application of ghost-reflection retrieval has succeeded in eliminating possible non-repeatability issues. Note that the magenta pointer indicated the maximum of the retrieved ghost reflection, which kinematically coincides exactly with the maximum in figure WP3.9.A.

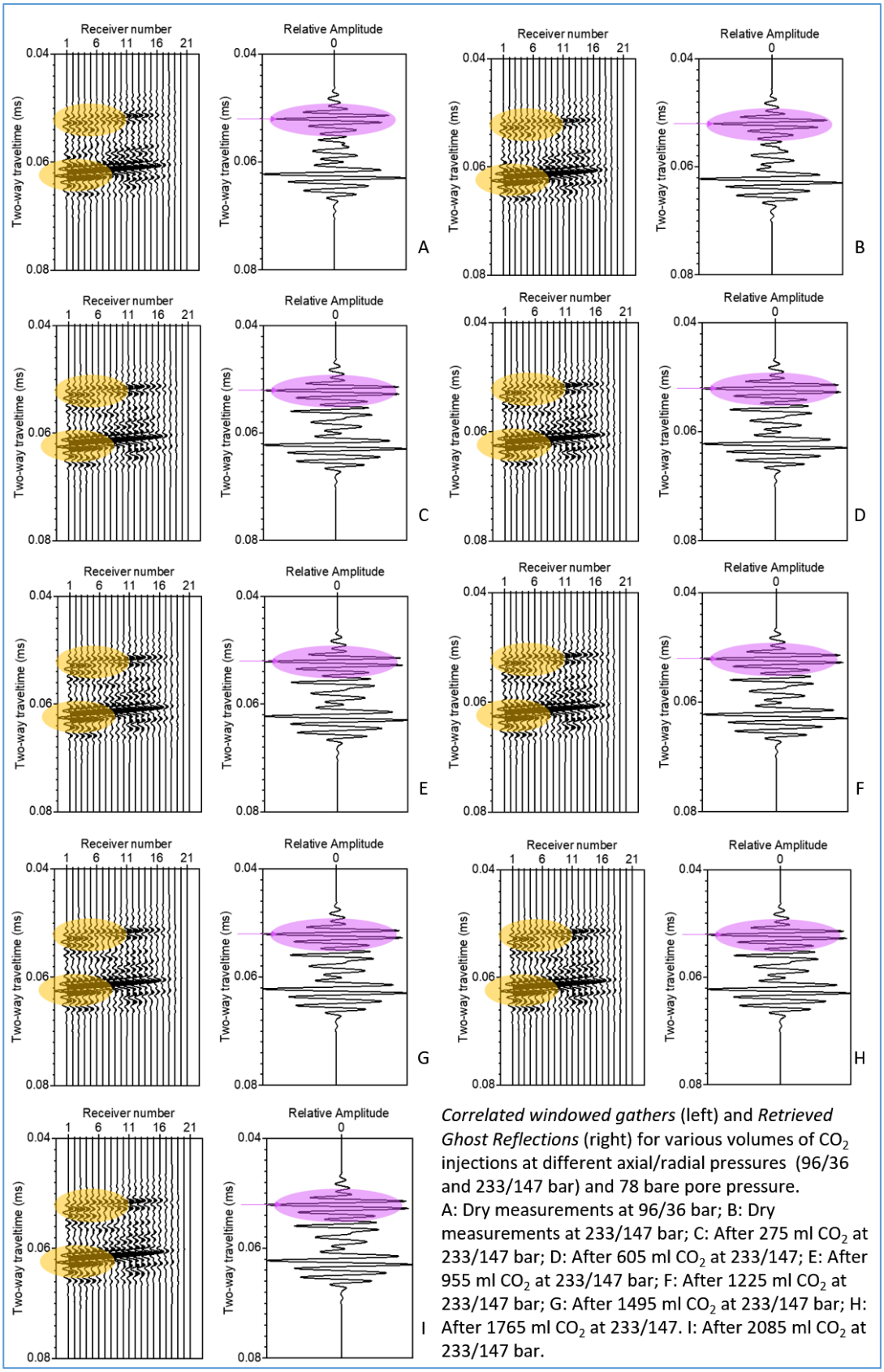

Correlated windowed gathers (left) and *Retrieved Ghost Reflections* (right) for various volumes of CO_2 injections at different axial/radial pressures (96/36 and 233/147 bar) and 78 bare pore pressure.
A: Dry measurements at 96/36 bar; B: Dry measurements at 233/147 bar; C: After 275 ml CO_2 at 233/147 bar; D: After 605 ml CO_2 at 233/147; E: After 955 ml CO_2 at 233/147 bar; F: After 1225 ml CO_2 at 233/147 bar; G: After 1495 ml CO_2 at 233/147 bar; H: After 1765 ml CO_2 at 233/147. I: After 2085 ml CO_2 at 233/147 bar.

Figure WP3.9: Overview of Correlated Window Gathers and Ghost Reflections for dry and CO_2 saturated rocks at different vertical and radial stresses, dry and under 78 bar pore pressures at 40°C. For details, see the graphs.

In figure WP3.9.C., the results for the retrieval of the ghost reflection after injection of 275 ml of CO_2 at 233 bar axial pressure and 36 bar radial pressure show that, again, the retrieved ghost reflection arrives at the same

time as in the figures WP3.9.A,B. When comparing those results with the figures WP3.9.D to I, for injections of 605 ml, 955 ml, 1225 ml, 1495 ml, 1765 ml, and 2085 ml of CO_2.

In conclusion can be stated that the method, by using the ultrasonic reflection measurements before injection of CO_2 and after injection of seven quantities of CO_2 to retrieve ghost reflections between the basalt/aluminum interface and the fracture, is valid. The procedure removed the kinematic influence of the metal plates and gave the possibility to interpret the results of volume changes unambiguously. The comparison of the retrieved ghost reflections for the before and after CO_2 injections shows that they arrive at the same two-wave travel time, i.e., that no velocity changes happened because of the CO_2 injection. This means that the CO_2 did not migrate from the fracture upward through the basalt sample.

The results also show that the method of ghost-reflection retrieval can be used for performing laboratory measurements with sources and receivers on top of the high-pressure installation and still monitoring for changes inside the target sample. This eliminates the need to use special transducers and special installation for placing the transducers directly on the sample inside the installation at high pressures.

The translation from lab to field scale is also valid for larger structures and can be applied to monitoring CO_2 dissemination during reinjection into a geothermal reservoir.

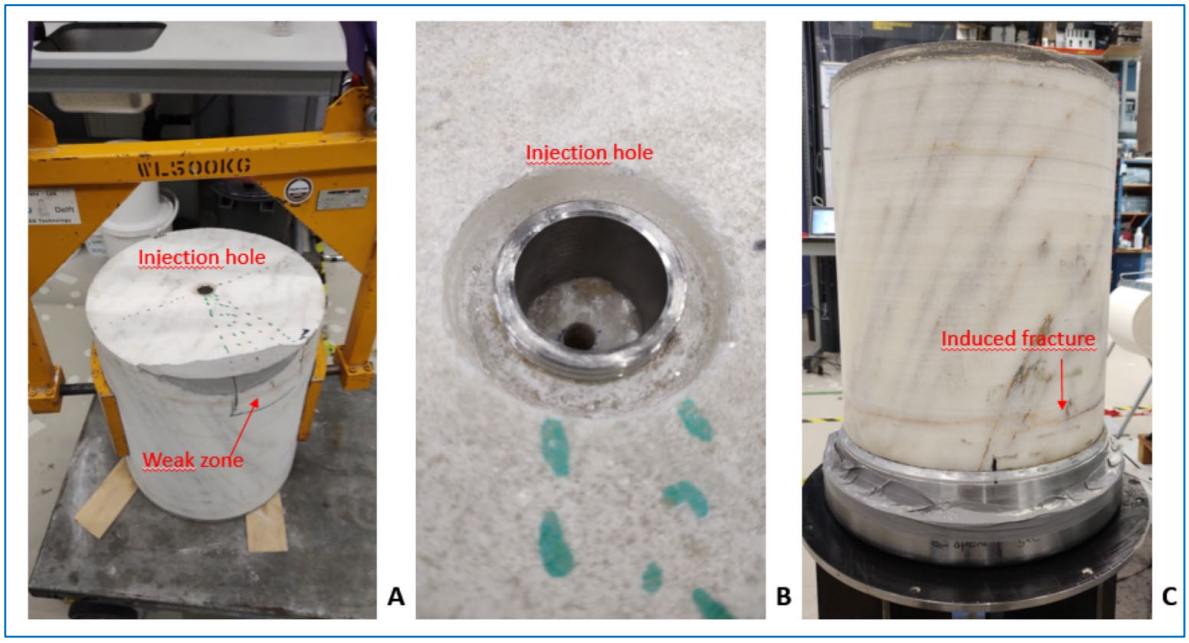

Figure WP3.10: The marble cylinder as used in the borehole simulator. A: the original sample with the weak zone (red streak) and position of the injection hole. B: detail of the injection hole and its depth up to the weak zone. C: The sample after the measurements with the induced fracture in the weak zone. Oil leaking out of the fracture.

The Turkish Marble Large Diameter Cylindrical Sample

As for the large basalt sample, we repeated the experiment with the Turkish marble sample. However, instead of an artificial fracture, here we use an inlet ending in a potential zone of weakness (Figure WP3.10.A, B). This former fracture zone was re-opened for the injection of brine and a brine-CO_2 mixture (Figure WP3.10.C). This large-scale experiment resulted into a successful acoustic dry measurement and a fully brine-saturated measurements of the reflector related to the fracture. A small perforation in the rubber sleeve prior to injecting CO_2, hindered the supercritical CO_2 measurements since it was not possible to create a fully saturated supercritical CO_2-filled fracture. The oil, used for confining pressure, already migrated into the fracture. Hence, we decided to saturate the fracture with it and since it has a comparable density as super-critical CO_2 at circa 250 bars, i.e. 0.95 ton/m3. So, we decided to perform seismic reflection measurements on a fully oil saturated

fracture. It is comparable and to a certain extent representative of supercritical CO_2 due to similar densities at the given pore pressures.

Summary of the experimental results

The unconfined and confined experiments on marble plugs for borehole experiments and seismic modelling:

Unconfined uniaxial trials (UCS).

- The temperature effect shows with increasing T a reducing V_p, thermal expansion of minerals and a larger effect at lower stress.
- The average V_p/V_s ratio for marble is 1.8 and for calcschist 1.7. There is no distinct temperature or σ_1 effect.
- The measurements done during unloading cycles are not different from the loading cycles, they suggest no permanent deformation.
- General trend is a reducing *E* with increasing temperature for both calcschist and marble. The thermal expansion of minerals, reduce the stiffness (loses elasticity) and thus *E*. A potential generation of micro-cracks is not expected at 100°C and without thermal shocks.

Confined uniform stress trials (CCS).

- There is an increasing V_p with stress due to closure of micro cracks. The $Vp_{uniform\ stress}$ is larger than the Vp_{UCS}, since the overall compaction is higher.
- The temperature effect at uniform stress is larger at lower stress. However, this effect is higher for UCS experiments since there is more room for expansion due to the absence of additional confining pressure.
- The V_p/V_s ratios for marble and calcschist are respectively 1.8 and 1,7 – 1.8.

Confined stresses under representative field conditions (CCS)-

- The Stress effect shows less variation in V_p due to initial stress condition of a $V_{p\text{-}reservoir\ stress} \approx V_{p\text{-}uniform\ stress}$ but larger than $V_{p\text{-}UCS}$. The impact of $\sigma_2=\sigma_3$ is negligible.
- The temperature effect is higher when compared to uniform stress results.
- The V_p/V_s ratio shows a negligible impact due to stress, i.e. ~1.75 for marble and 1.7-1.8 for calcschist.

Confined stresses on fully brine and CO_2 saturated fractured marble plugs.

The combined stress/P_{pore} effect as can be expected under in-situ conditions show:

- The results show an increasing V_p with increasing axial stress and P_{pore}.
- Fluid saturated fractures show a faster transit time than dry fractures $V_{p\text{-}fracture\_saturated} > V_{p\text{-}dry,\ intact,\ marble}$.
- The shear wave, V_s trend differs from dry-case due to the change in dry/wet fracture and by that presence/absence of pore pressure. In other words, a negative impact of absence of pore pressure gives a larger positive impact of the axial stress
- The combined stress and temperature effect shows that higher temperatures give slightly more room for compaction and by that an increasing V_p.
- The V_p/V_s ratio is over 2.0; higher than previous results due to the previously mentioned V_p,V_s behavior

Regarding the effect of pore fluid type (Supercritical CO_2 vs. brine) on seismic velocity ($V_{seismic}$), it is observed that:

- The first arrival, for both P- and S-waves, are very similar and cannot easily be used to distinguish brine from CO_2 in single fractures. The aperture is most probably too small (tens of µm) to observe any effect in transmission. We had wavelengths of ~31 (P-waves) and ~15 (S-waves) mm.

- However, the amplitude levels show differences, i.e. a lower maximum/minimum amplitude for the CO_2-case and the fluid type did affect overall elastic properties.

Given a constant radial stress with and pore pressure (P_p), the effect of the vertical stress (σ_1) on the seismic velocity ($V_{seismic}$) and fracture permeability (k_{fr}) shows:

- A similar V_p - stress trend as before with the largest increments at low stress.
- V_s increases slightly with stress at a constant Pore pressure (P_p), giving a $V_p/V_{s\text{-saturated}}$ of ca. 2.09. Note that the dry value is circa 1.75.
- The fracture permeability (K_{fr}) reduces with increasing stress from 176 mD to 165 mD, or 6.2%.This is caused by the fracture closure with increasing stress.
- The V_p – K_{fr} shows a good correlation fit. A V_p increase results into a $K_{fracture}$ decrease of $K_{fr} = -0.152 \cdot V_p + 1124.2$

The effect of the pore pressure (P_p) on seismic velocity ($V_{seismic}$) and fracture permeability (k_{fr}) at a constant radial and axial stress is as follows:

- Both primary and secondary speed decrease with increasing pore pressure. Increasing pore pressure reducing the forces that act on mineral contact surfaces and by that the total mineral contact area, resulting in reducing velocity reduction.
  The V_p/V_s is about 2.06.
- The fracture permeability increases with increasing pore pressure due to opening of the fracture aperture of the fracture; Where V_p decreases, K_{fr} increases.
  V_p – K_{fr} shows a good correlation fit.

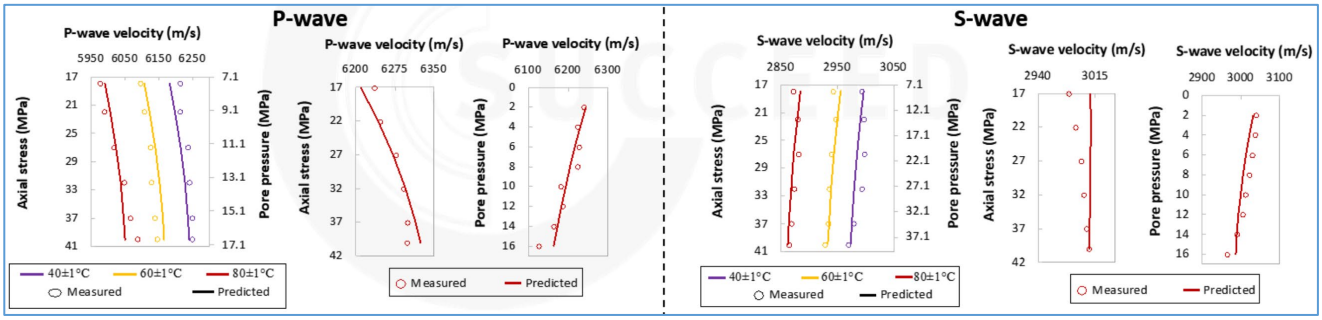

Figure WP3.11: Data integration of the Kizildere plug experiments performed for parameter definition as used in the borehole experiments and for prediction of Vp and Vs in vertical seismic profile estimation.

Quantifying previous results on the plugs providing an empirical relationship for a V_p and V_s prediction (Figure WP3.11).

- We applied multiple a nonlinear regression to the accumulated velocity dataset of all experiments where a 100% brine-saturated marble was used to estimate seismic velocities. Based on the variables: axial stress, pore pressure and temperature we obtained:
  - $V_p = 6105.62 + 10.17\sigma_1 - 7.78P_p + 1.43T - 0.09{\sigma_1}^2 + 0.11{P_p}^2 - 0.05T^2$
  - $V_s = 3019.22 + 0.28\sigma_1 - 5.99P_p + 1.80T - 0.01{\sigma_1}^2 + 0.16{P_p}^2 - 0.04T^2$

- The results are used for:
  - parameter definition as used in the borehole experiments.
  - prediction of V_p and V_s in vertical seismic profile estimation that can potentially be used for predicting seismic velocities at Kızıldere or similar sites.

The borehole experiments:

Turkish marble and Icelandic basalt 400x600 mm core samples were drilled from the large-scale reservoir blocks, made plan parallel on the end faces, equipped with injection and production tubing/grid foil and an artificial or induced fracture. Active-source acoustic reflection measurements were performed utilizing two separate transducers as seismic sources, and a total of 21 transducer places acting as receivers. With baseline measurements under dry and wet conditions with maximum axial and radial stress of 186 and 144 bars, respectively, were carried out reflection and refraction measurements to successfully identify the reflectors of interest.

The Icelandic basalt

- A complete series of experiment was conducted on Icelandic basalt. The wave-propagation parameters obtained during preliminary tests on small samples (e.g., optimal central frequency of 600 kHz) were used here.
- Reflection measurements were done at dry, brine-saturated, and CO_2-saturated fracture conditions.
- Several measurements were taken as function of the amount of supercritical CO_2 (80 bar and >33°C) injected.
- Results indicate that the velocity tend to decrease as function of amount of CO_2 injected.
- However, amplitude values, of the brine/CO_2-saturated fracture reflector, seem to be more sensitive to pore fluid changes.
- Generally, amplitude values reduce as function of injected CO_2, reaching maximum reductions of 12±1% with respect to the 100% brine-saturated amplitude value at near offset. Moreover, amplitude reductions (compared to the brine-saturated case) decrease as function of increasing offset.

The Kizildere Marble

- A partial complete series of experiment was conducted on the marble. As with the previous series, the wave-propagation parameters obtained during experiments on small samples (e.g., optimal central frequency of 600 kHz) as described here above, were used here for the base parameters.
- Hydraulic fracturing was conducted to initiate a semi-horizontal fracture. It has been used for the acoustic tests.
- Reflection measurements were successfully done at dry and brine-saturated.
- During CO_2-saturation leakage occurred and as an alternative, fracture was saturated with hydraulic oil. Then acoustic measurements were performed.
- All data have been gathered and are now analyzed.

Results of DUT as the contributions for partners to WP3.2: ICL and METU experiments

- We drilled and prepared cores and plugs from Kizildere and Hellisheiði reservoir rock, with various dimensions, to be used by ICL and METU (Figure WP3.12).
  - for geochemical related high P,T tests in autoclaves on Turkish and Icelandic material.
  - for rock mechanical tri-axial tests of Turkish reservoir and overburden.
- Rendered 3D-images have been made from all samples by using different CT-scanners. The scans have been created before and after the experiments at ICL and are analyzed on spatial characteristics.
  - The dual beam scanner for 200 micrometer resolution imaging.
  - Micro-scanners for 10 micrometer resolution imaging.
- When required, DUT made XRD/XRF analysis to explain textural issues on the scanned samples. Those analyses were also a base for the geochemical reference activities at ICL.

Figure WP3.12: Example. Various core dimensions, for rock mechanics and geochemical experiments by DUT, ICL and METU.

Literature referred to and created through WP2

- Draganov, D., K. Heller, and R. Ghose, 2012, Monitoring CO_2 storage using ghost reflections retrieved from seismic interferometry: International Journal of Greenhouse Gas Control, 11S, S35-S46, doi: 10.1016/j.ijggc.2012.07.026.
- Draganov, D., R. Ghose, K. Heller, and E. Ruigrok, 2013, Monitoring of changes in velocity and Q using non-physical arrivals in seismic interferometry: Geophysical Journal International, 192, 699-709, doi: 10.1093/gji/ggs037.
- Draganov, D., M. Janssen, M. Friebel, K. Heller, J. van den Berg, S. Durucan, K.-H. Wolf, and A. Barnhoorn, 2023, Direct monitoring of velocity changes due to CO2 injection in basalts under reservoir condition using seismic interferometry: 15th Euroconference on rock physics & rock mechanics (Euroconf23), Woudschoten, The Netherlands, 2023.
- Ma, X., A. Kirichek, K. Heller, and D. Draganov, 2022, Estimating P- and S-wave velocities in fluid mud using seismic interferometry: Frontiers in Earth Science, 10, 806721.
- Janssen, M., D. Draganov, J. Bos, B. Farina, A. Barnhoorn, F. Poletto, G. van Otten, K.-H. Wolf, and S. Durucan, 2022, Monitoring CO2 injection into basaltic reservoir formations in Iceland: laboratory experiments and preliminary simulation results: 83r EAGE Conference and Exhibition, Madrid, Spain, 2022, 1-5, doi: 10.3997/2214-4609.202210474.
- Janssen, M.T.G, Draganov, D., Barnhoorn, A. and Wolf, K.H.A.A., 2023. Storing CO_2 in geothermal reservoir rocks from the Kizildere field, Turkey: Combined stress, temperature, and pore fluid dependence of seismic properties. Geothermics, 108, p.102615.
- Shirmohammadi, F., D. Draganov, and R. Ghose, 2023, The utilisation of ghost reflections retrieved by seismic interferometry for layer-specific characterisation of near-surface field data: Near Surface Geophysics, revision submitted.

Work Package 4: Field monitoring of CO_2 injection operations, site performance and reservoir behavior at Kizildere and Hellisheiði sites.

Task 4.2: Development and field implementation of repeatable electric seismic-vibrator EM for semi-continuous seismic monitoring.
Task 4.4: Seismic monitoring data processing and interpretation using semi-continuous Electric seismic-vibrator and iDAS monitoring campaigns pre-during-post injection.

Task 4.2 and 4.4: the eVibe

Electric seismic-vibrator technology

Introduction of Seismic-Vibrator technologies

The need for innovations like electric seismic-vibrator or eVibe originates from the fact that conventional seismic sources like hydraulic vibrators and explosives are expensive, invasive, have data quality issues, and are based on technology and methods that are at least 60 years old, with very little advancement or innovation since inception.

Diesel hydraulic vibrators are overly complex and antiquated systems with maintenance issues inherent in the carrier vehicle chassis and drive train, the hydraulic system, the shaking masts, cylinders, baseplate, and vibrator electronics. An issue with any of these systems can cause lost production time or even unacceptable data quality that would require repeating the acquisition. Most seismic acquisition contractors maintain a 25% redundancy on each fleet to avoid lost time. The hydraulic system causes most of the failures on conventional vibrators. This usually brings a combination of data-quality problems, environmental cleanup requirements and maintenance downtime. The reason for these shortcomings is due to the intrinsic friction and harmonics that are at the core of the force generation. To generate seismic signals, oil is pumped from one chamber of the hydraulic valve to the other, causing friction and wear on components. Diesel hydraulic vibrators have a massive environmental footprint and CO2 emissions are high, these diesel vibrator trucks are also large and not capable of accessing many terrains without a large amount of clearing and site preparation. Safety standards are low due to high pressures and maintenance issues.

Explosives provide good signal for seismic acquisition but are costly and have a large environmental impact. Environmental permitting and transportation cause further issues and difficulty using this type of seismic source. Most importantly, explosives are a huge safety issue, which result in injury and costly HSE policies.

To conclude, conventional seismic source methods have Health, Safety and Environmental risks and shortcomings that no longer align with company policies and clients worldwide are actively looking for a solution.

The eVibe minimizes land disturbance due to the technology it adopts, direct drive motor technology. Direct drive motor technology generates high-quality and repeatable acoustic signals for seismic acquisition. The Direct drive motors generate a linear or rotary movement without the use of a transmission or gearbox. Instead, these motors use permanent magnets and coil windings to generate frictionless movements. Therefore, the motors are highly efficient (>90% IEC4/5) and result in reliable and high-quality seismic signals. As explained by Noordlandt et al. (2015), a direct drive motor is an electric motor that can produce large controllable forces and finely tuned frequencies that are suitable to drive a seismic reaction mass. This motor consists of two independent elements, a magnet track, and a coil track, allowing practically unlimited motor displacements. This makes the direct drive motor very suitable for expanding the source frequency band to the lower frequencies in which larger strokes are needed. In contrast to hydraulic engines, the direct drive motor performs equally well over the whole frequency range, making possible a smaller amount of signal distortion, especially at the low frequencies.

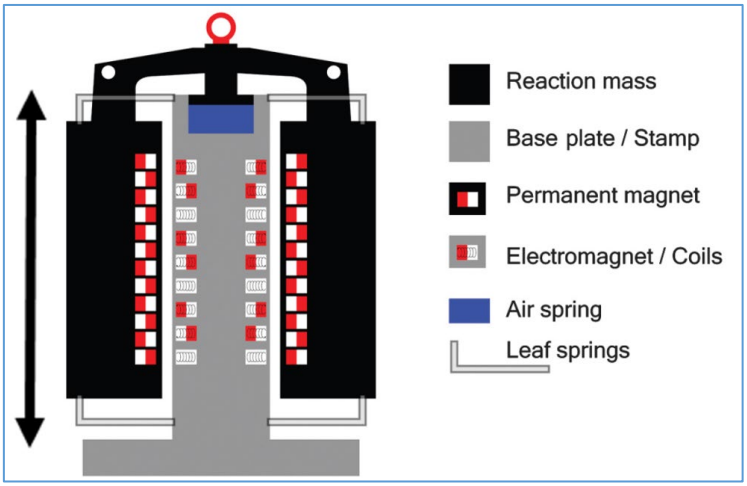

Figure WP4.1: eVibe principle

In more detail, the eVibe motor is an electric motor that can be seen as an unrolled permanent magnet synchronous motor (Figure 4.1). The motor used in the eVibe's consists of a U-shaped permanent magnet track with a coil track passing through the middle. The intercoil and intermagnet distances are chosen such that the same force can be made for any position of the tracks by controlling the current distribution over the different coils. The need for the synchronization of the track positions and the current, together with the fact that the resulting force acts along a line, is linear, thereby giving these types of motors their name (LSM, or,Linear Synchronous Motor). With this geometry, the motor can operate over any distance needed. Therefore, the eVibe can equally generate low frequencies with a large stroke as high frequencies with a relatively small stroke. This contrasts with hydraulic engines in which fluid flow and dynamics limit and distort the output at low and high frequencies or single-coil-magnet designs in which the linearity is lost for larger amplitudes.

As the direct drive motor is very efficient, frictionless and generates high forces over a broad bandwidth (especially at very low frequencies), very compact and light 'eVibe' seismic sources can be manufactured. This is well contrasted when compared to hydraulic seismic sources. Conventional seismic sources use hydraulic valves to generate acoustic signals. In principle, oil is being pushed from one chamber of the hydraulic valve to the other chamber at very high pressures. Consequently, a high magnitude of friction, viscous losses and harmonics are created within the hydraulic system. Therefore, much of the force generated by the hydraulic vibrator is lost in the design itself. In other words, very high forces are necessary to generate the desired seismic signals (although with a lot of harmonics), which result in massive diesel trucks with a high environmental footprint. As explained, the eVibe uses direct drive motors, which are frictionless, therefore, no force is lost in the system itself. Another important feature is the low noise (dB) of the eVibe due to the usage of the electric motors. This all ultimately results in near zero environmental impact (Brodic, 2019, 2021).

The eVibe solves the challenges of minimizing land disturbance and supplying exploration sectors long term and in a more sustainable and responsible manner. This is also proven based on our track-record of the TRL9 Lightning eVibe (Figure WP4.2.A). The Lightning eVibe is a P- and S-wave near-surface seismic source, which reaches depths of <1200 meters. Thereafter, a 3kN eVibe has been built, called the Synchro (synchronized Lightnings) a system capable of reaching <2000 meters (Figure WP4.2.B). Moreover, a 7kN prototype was built and extensively tested in relevant operational environments (Figure WP4.2.C). The 7kN prototype shows great potential for imaging deeper targets <3000 meters (Tranter, 2022).

Figure WP4.2: A. The Lightning eVibe, B. The Synchro eVibe, C. 7kN prototype eVibe, D. Linear-motor based vibrator 7kN (TU Delft, Seismic Mechatronics)

eVibe repeatability

For seismic acquisition for CCUS purposes or so-called 4D monitoring surveys or semi-continuous monitoring surveys, it is important to do these surveys with a high repeatability. The data must be acquired and processed in exactly same way throughout the monitoring project to be successful. This can be a challenging task considering all factors involved.
For hydraulic seismic sources the repeatability is low. The hydraulic piston or hydraulic valve is subject to wear and tear and viscous losses due to the high pressures used to pump oil between the chambers. Moreover, the repeatability is further reduced to dependence on temperature changes. This results in high internal harmonics distortion issues of >30% and low repeatability consequently. For the eVibe the repeatability is magnitudes better.
To quantify the so-called repeatability of the signals a vibratory source, an experiment was conducted near the town of Bant in the North-East polder of the Netherlands. As vibratory source, the linear-motor-based vibratory source called “Storm” was used, as shown in Figure WP4.1 and Figure WP4.2.D.

Repeatability.
For the measure of repeatability, the repeatability as defined in Kragh et al. (2002) is used but written slightly differently:

$$R_{NRMS}(a(t),b(t)) = \frac{2\sqrt{<[a(t)-b(t)]^2>}}{\sqrt{<a^2(t)>}+\sqrt{<b^2(t)>}}$$

where R_{NRMS} is the normalized root-mean-square repeatability of two signals a(t) and b(t), and <.> denotes the mean. Since the means on the right-hand side are over squared functions, they are root-mean-square (RMS) values. Often, R_{NRMS} given in percentages rather than fractions.

This measure of repeatability seems to capture the repeatability issue that we discuss here, but it should be realized that this measure is an attribute of the difference between the signals. This particular measure R_{NRMS} is sometimes not sensitive to the (repeatability) change in the signal that we are interested in; another measure, such as the predictability measure, may then be more appropriate. While R_{NRMS} is extremely sensitive to the smallest changes in signals, the predictability measure is not sensitive to overall static, phase or amplitude differences but is sensitive to noise and changes in the earth reflectivity (Kragh et al., 2002).

Repeatability of vibratory source,
To quantify the repeatability of a vibratory source, a suite of experiments was conducted, near the town of Bant. A spread of 96 geophones was laid out with a spacing of 2 m. 32 sweeps were sent out where the source remained at its position. The issue here is that the coupling of the source may change for those 32 sweeps, expecting that the soil beneath the baseplate will be more settled after many sweeps than in the beginning. This will affect the signal sent out and will affect measured acceleration on the reaction mass and the baseplate (mainly the latter) and therefore measured ground force of the vibrator. An important issue to note here is that on this vibratory, no feedback control is active.

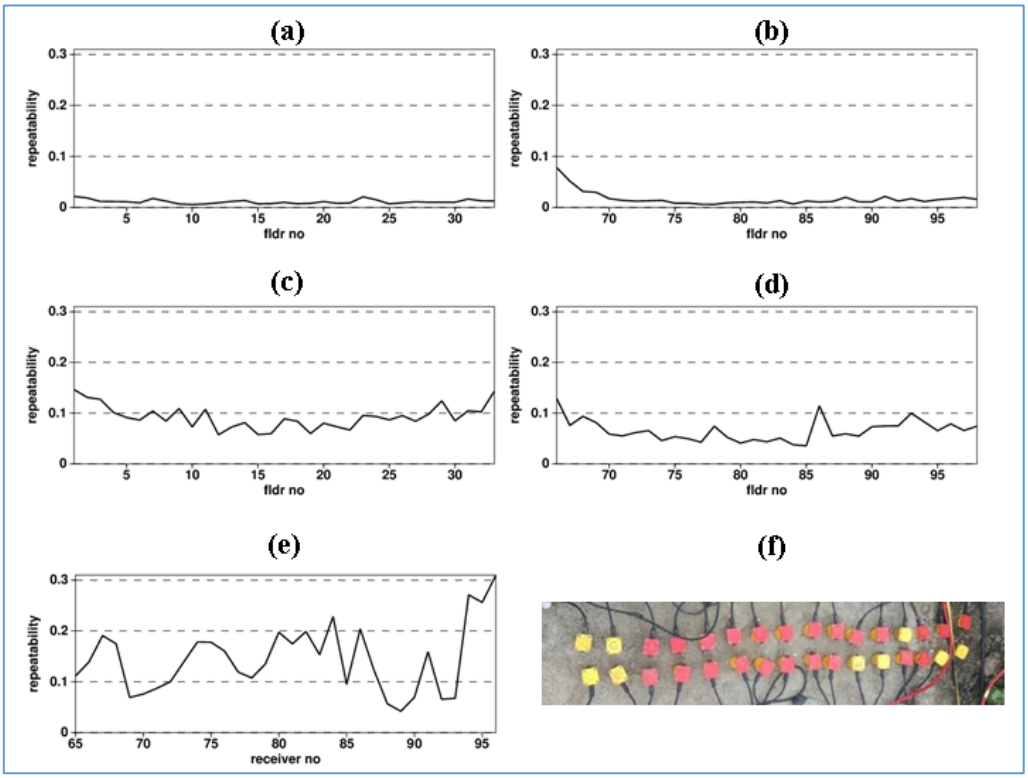

Figure WP4.3: Repeatability of ground force ((a) and (b)) and single-geophone recording ((c) and (d)), for a vibrator resting on one position ((a) and (c)) and lifting and lowering on the same position ((b) and (d)). Repeatability (e) of 32 geophones (f), perpendicular to the shot direction. All repeatability values are compared to their mean.

The results of this test can be seen in Figure WP4.3A for the measured ground force and in Figure WP4.3.C for the geophone data. For these figures, the function b(t) in the repeatability formula above has been taken as the mean of the ground forces and the mean shot for the geophone data, respectively. Also, for these data, correlation was done, using the mean of the measured ground forces of those 32 sweeps, so the same signal was used for the correlation with all the data. The repeatability of the correlated ground force in Figure WP4.3.A shows values around 1%, a good value for field data with a land seismic vibrator. This number includes the repeatability of the source itself and the repeatability of the coupling. When looking at the repeatability of the correlated geophone data in Figure WP4.3.C the values are an order of magnitude larger, more around 10%.

This shows that the variations of the geophone data are dominant, and the source variations are such that they have hardly any effect on the repeatability of the geophone data.
Then another experiment was carried out, namely by lifting the vibrator between each sweep, thereby affecting the source coupling. The source was placed at approximately the same position. These results are shown in Figure WP4.3.B for the measured ground force and Figure WP4.3.D for the geophone data. What is characteristic to see is that the repeatability of the correlated ground force is initially a bit large, just below 10%, but then reduces to the values when we did not lift the vibrator between the sweeps. This is typically an effect of source coupling. It also shows the effect of the settling of the ground beneath the vibrator. Later, the values reach the ones as before, namely around 1% repeatability.
When looking at the repeatability of the correlated geophone data, the values are like the ones when not lifting the vibrator in between. The values are even slightly lower, more below 10%; this is probably due to the environmental circumstances being slightly different, such as the noise/wind conditions (after half an hour).

Repeatability of geophone data.
Then one other experiment was carried out, namely by placing 32 geophones next to each other, as shown in Figure WP4.3.F; they are placed perpendicular to the shot position such that minimal time delays would be present between the different geophone recordings. What would be expected is that the signal would be very similar, the main differences being due to receiver coupling. It must be said that in the field, the coupling seemed to be nearly perfect since the geophones were placed in a sticky clayey soil. Still, the results for the repeatability look different, as shown in Figure WP4.3.E: some average value of 15% can be observed. This really shows that local soil variations are very important to consider when good-repeatable measurements are needed. It also shows why sometimes arrays of bunched geophones are being used, not only to boost the signal but also to average out the local soil variations.

Table WP4.1: The specifications of the developed 50kN eVibe.

Full force	min 43 kN (with added low freq motion for 50% Duty cycle) max 50 kN (mechanical stroke limit, @ 35 % Duty Cycle)
Frequency (full force, 0 taper)	4 – 145 Hz (min. 34 kN @ 200 Hz)
Frequency range	1 - >240 Hz
Operating Temp	-32 to +50 °C (chiller limiting, +43 °C might require lower full force)
Storage Temp	-40 to +80 °C (motor limiting)
Dimensions	1085 x 1210 x 1580/2000mm^3 (Top air bellow connection / HDM structure)
Usable stroke	68 mm
Total weight	3,400 kg
RM weight	2,400 kg
BP weight	1,000 kg
BP Area	1 m^2
RM suspension freq.	1.6 Hz
Hold down weight (excl vib of 3400 kg)	max 10,000 kg (air bellow limit);NOTE: max 5,000 kg for proto (Strenght lift interface)
HDW freq	1.5 -1.6 Hz
Generator power required	40 kW

Electric seismic-vibrator development

50kN eVibe development.

During the initial proposal of the project, it was proposed to develop a 50kN eVibe. This was the result of various discussions about the depth of penetration that the eVibe could achieve and what was necessary for the Succeed project, which was estimated at ca. 2500 meters. At that time, the force (kN) needed to reach the target depths was too conservatively determined, as will be explained in table WP4.1 here above.

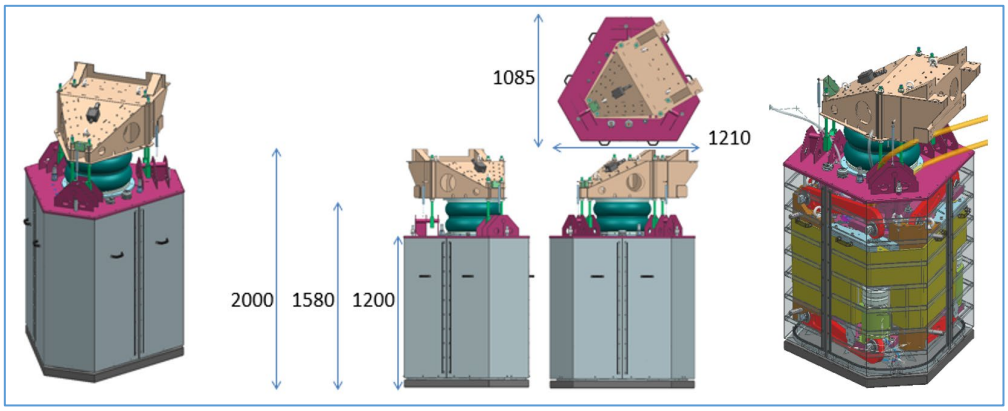

Figure WP4.4: 50kN eVibe

The 50kN eVibe comprises an electromagnetic actuator for generating a time-varying force, which enables a more reliable and/or robust operation. Figure WP4.4. shows the system which consists of:

- a base plate, with,
- a column mounted onto the base plate.
- a guiding mechanism, and,
- an electromagnetic motor arranged to generate a single force on the column in a first direction,
- wherein the column is provided with a single stator,
- and the electromagnetic motor is formed by a mover and the single stator arranged to interact with each other to generate the single force.

the guiding mechanism comprises a plurality of rods connecting the column to the mover, the guiding mechanism being configured to enable a displacement of the mover relative to the column in the first direction and restrict a displacement in a plane substantially perpendicular to the first direction.
The column is provided with the single stator, which means that there is only one stator on arranged on the column. Because there is only one single stator arranged on the column, the electromagnetic motor acts as a single motor to generate the single force on the column. Because only a single force is generated, the seismic shaker will shake the base plate more accurately and with improved robustness.

By providing the plurality of rods, the mover can be guided over a desired displacement relative to the stator. The rods provide an accurate guiding mechanism that can be arranged in a relatively small volume. In combination with the use of the single stator, this allows for a smaller seismic shaker. In comparison, some known seismic shakers use leaf springs as a guiding mechanism. The leaf springs need to have a sufficiently large thickness to withstand the stresses during operation of the seismic shaker. However, due to the large thickness, the leaf springs need to have a large length to allow the leaf springs to flex over the desired distance of the mover. Large leaf springs may have a good lifetime, but consume a large space, whereas short leaf springs fail after a short amount of time due to fatigue. The rods as implemented in the invention provide a guiding mechanism with a desired range in a small amount of space with an improved lifetime and robustness.

The resulting improvements are:

A: Repeatability:
to enhance geothermal performance as well as store the produced CO2, injected CO2 in the geothermal reservoir needs to be monitored very accurately by a repeatable source (with high controllability). The eVibe, like no other seismic source, is a highly repeatable source due to the use of electric linear motors combined with a leaf spring guiding system. Although, the earlier proposed eVibe would use linear motors, it would use a plurality of rods guiding system. Due to the high forces to be produced, a leaf spring guiding system would not be suitable. Unfortunately, the plurality of rods guiding system does not meet the repeatability requirements of the Succeed project. As a result, it is required to change the design back to a leaf spring design. Therefore, the peak force is adjusted as well.

B. Robustness and Icelandic survey line:
At the end of 2019/beginning of 2020, the location of the survey line is Iceland was determined. The reasons for choosing this line are related to the location/flow of the reservoir. Shooting seismics on this line would result in optimum seismic data. The line, however, is very narrow and steep. It is not possible to shoot the line with use of the earlier proposed eVibe. Simply because the eVibe (Vibrator, Electronics box, chiller, compressor), generator (>40kW), trailer and vehicle/telehandler are too large and heavy for this particular road. It would result in very dangerous operations with some environmental impact as well.

C. Depth of penetration (Figure WP4.5):
The depth requirement of the seismic data within the Succeed project is approximately 2000 meters. SM in cooperation with the TU Delft developed a ~1500 lbs eVibe that has shown to reach depths of ~3000 meters. Therefore, the 10kN / ~2500 lbs eVibe is able to achieve the project requirement.

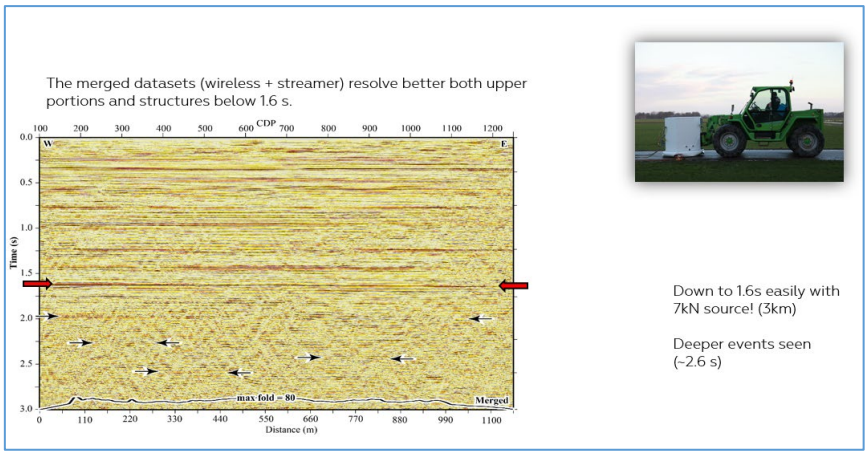

Figure WP4.5: 7kN eVibe test result.

D. P-wave + S-wave:
The 10kN eVibe is both a P-wave and S-wave vibrator. No other source of comparable power can provide both P- and S-wave generation as one instrument. Therefore, one can also use converted waves in the exploration and exploitation, something that now is hardly, if at all, used since there is hardly any S-wave source available for such depths. S-waves provides additional subsurface information to characterize mineralization. Therefore, it would be highly advantageous for the project – it will allow recording two types of data with the same source, something that was not planned in the project, but is highly desirable.

Seismic monitoring data processing and interpretation using semi-continuous Electric seismic- vibrator and iDAS monitoring campaigns pre-during-post injection.

10kN eVibe Field implementation and data interpretation results of the semi-continuous eVibe at the Hellisheiði geothermal field site in Iceland in 2021 and 2022.

The Hellisheiði 2021 active-seismic field acquisition campaign was performed using the fiber optic DAS HWC permanent installation also used for passive monitoring (Stork et al., 2020), integrated with a configuration of co-located different geophone lines with multicomponents, to investigate the wavefields obtained from the 10kN eVibe in P-wave mode. The depth target of the survey is around 2 Km. The vibration points follow the path of the iDAS fiber optics line installed. Among the DAS sensing line, other sensors have been deployed for auxiliary signal analysis, enhancing monitoring and quality control (Figure WP4.6).

Figure WP4.6: A. Survey overview, B. 10kN eVibe field implemented in Iceland.

During this survey the 10kN eVibe was installed on a Manitou telehandler (Figure WP4.6.B). The generator and control electronics were put at the back of the Manitou on a trailer. The seismic source was operated in "P-wave mode" (vertical vibration) with a source interval of 40 m. Per vibrating point 16 sweeps were performed and stacked. The total number of source points was 59. Initial source parameters have been set in the tuning phase, but the analysis during the ongoing survey suggested reducing the frequency to a range 2-150 Hz. Specifications for application are:

- Sweep type: upsweep linear, Sweep length (s): 15; Frequency range (Hz): Initial 2 – 240 (later 2-150).
- Taper type: cosine, Start taper (s): .300; End taper (s): .300 (later .600).
- Load force (kN): 10; Coupling surface (mm): 800 × 400.

Nevertheless, there are improvement points noticed during this project that need to be considered. Firstly, during the Iceland surveys a trailer was used for carrying the control electronics and generator. This influenced productivity and safety. This was recognized and therefore a platform was developed on top of the HDW frame to carry the control electronics and generator. This resulted in an improved setup but it was still not optimal. Therefore, SM is currently developing a battery pack that will replace the generator. The batteries will be placed on the HDW platform. This creates a "plug and play" setup that can be easily connected to local carriers. Moreover, SM has developed a HDW bracket for the 10kN eVibe that can be connected to electric telehandlers, resulting in a 100% electric system for seismic acquisition.

The project team provided in-field and remote support and technical instrumentation by a radio triggering system for triggering iDAS, to speed-up the collection of records during the early QC test phase (Figure WP4.7). The remote QC was performed in near-real time, i.e., relevant time to make prompt decisions on acquisition parameters (to optimize resources). QC included the choice of vibration parameters, energization interval, number of stacks, sweep mode, frequencies, and length, tuned during the survey based on the sweep and seismic result of initial and sample tests performed at the beginning of the survey. For this purpose, the pilots'

signals from the source were used and recorded shot by shot and made available at the end of the day in SEGY format.

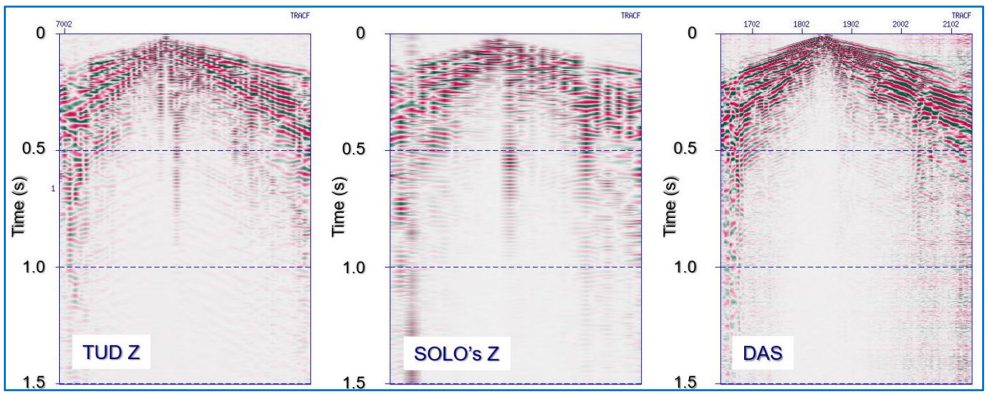

Figure WP4.7: 10kN Example of QC during acquisition. Shots obtained with different recording systems along the same main-line interval.

Also, the accelerometer signals were analyzed by looking at the amplitude frequency spectrums and time frequency plots (harmonics); see figure WP4.8. One could conclude that most of the harmonics are caused by the coupling and not by the LSM.

The Hellisheiði 2022 active-seismic field acquisition campaign was performed in a similar way as the campaign in 2021. The HDW frame was redesigned in a way that the control electronics and power source could be added to the front, which would prevent the usage of a trailer at the back. This ensures a safer and more efficient operation (Figure WP4.9).

Field implementation results of the semi-continuous Electric seismic-vibrator at the Kizildere geothermal field site in Turkey in 2022.

The Kizildere geothermal plant, Turkey, produces from a carbonate hydrothermal reservoir. Two existing wells have been equipped with fiber-optic monitoring cables to investigate the feasibility of injecting produced and captured CO2 into the reservoir as a supercritical fluid. Monitoring is required to investigate the geomechanical implications of this for the stability of operations. High temperatures, up to 245°C, in the reservoir pose a challenge for monitoring.

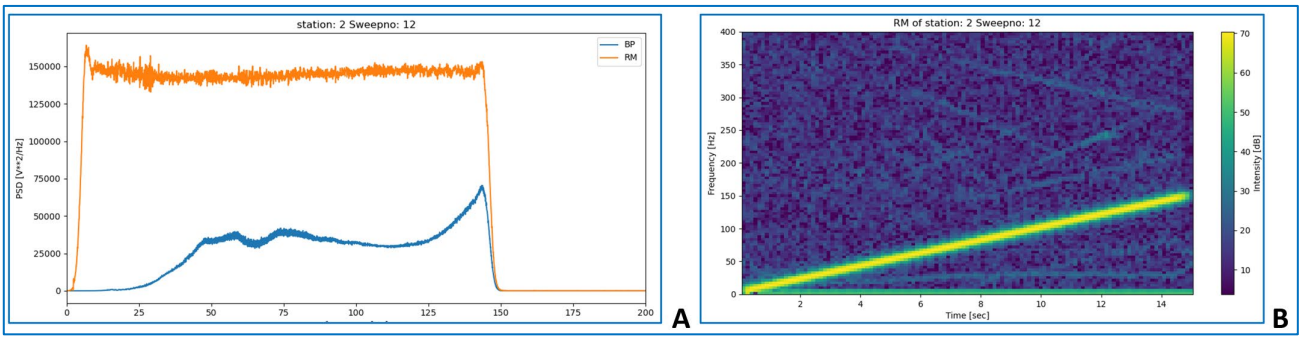

Figure WP4.8: A. Amplitude and frequency spectrum of baseplate and reaction-mass acceleration, B. Time frequency plot of the pilot signal reaction-mass acceleration.

A high temperature engineered (Constellation) cable has been deployed in two existing wells, to depths of 940 m and 900 m. In October 2022, a P-wave active seismic survey with the EVibe was carried out for Vertical Seismic Profiling (VSP) and seismic reflection imaging of the reservoir. The aim is to provide baseline and time-lapse monitoring of the injection process. The project involved 6 lines varying in length across the Kizildere geothermal plant.

Figure WP4.9: 10kN eVibe during 2022 Iceland survey

During this survey the 10kN eVibe was installed on a Manitou telehandler (Figure WP4. 9). The generator and control electronics were put at the top of the vibrator on the HDM platform. The seismic source was operated in "P-wave mode" (vertical vibration) with a source interval of 20 m. Per vibrating point 6 sweeps were performed and stacked. The total number of sweeps made was ca. 1000 and ca. 165 source points.

Initial source parameters have been set in the tuning phase, but the analysis during the ongoing survey suggested reducing the frequency to a range 2-180 Hz.

- Sweep type: upsweep linear, Sweep length (s): 16; Frequency range (Hz): 2 – 180Hz
- Taper type: cosine, Start taper (s): .380; End taper (s): .310
- Load force (kN): 10; Coupling surface (mm): 800 × 400.

Figure WP4.10: A. 2D selections for shot lines, B. Real shot locations.

Figure WP4.10: C: Field implementation of 10kN at Kilzildere geothermal plant.

Also, the accelerometer signals were analyzed by looking at the amplitude frequency spectrums and time frequency plots (harmonics). One could conclude again that most of the harmonics are caused by the coupling and not by the LSM (Figures WP4.11.a,b).

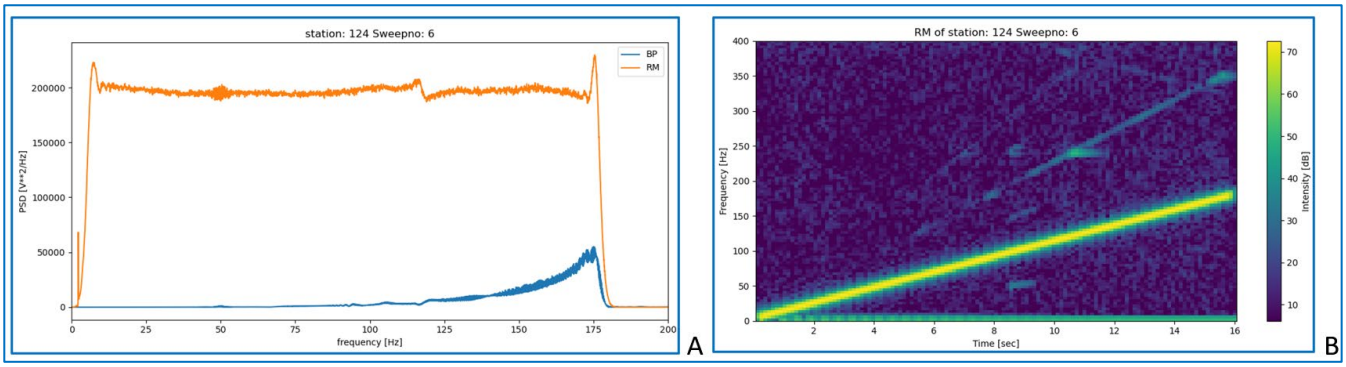

Figure WP4.11: A. Amplitude and frequency spectrum of baseplate and reaction-mass acceleration, B. Time frequency plot of the pilot signal reaction-mass acceleration

Implementation

The illumination (Figure WP4.13) of the source results as mentioned previously, and obtained by SILIXA and SM are analyzed for optimal placement of receivers and sources, respectively by DUT and OGS for the purposes of seismic interferometry, and which are used to design the acquisition geometries, solutions for the field plans. In WP1, DUT presented, as an example, based on the uni-axial lab results a vertical seismic profile for Hellisheidi. In WP3 DUT agreed and perform laboratory investigations into rock-fluid interactions: Geochemical, geomechanical and geophysical response of the reservoir to CO_2 injection and the response of reservoir rocks to the injection, seismic response and, impact on flow properties, geochemistry, integrity of the reservoir rock on change in strength. The resulting parameters are used as input for WPs 4 and 5 for interpretation and calibration of monitored data and numerical models used in field performance evaluation pre-and post- CO_2 injection, as well as long-term injection strategies planning (Figure WP4.12). During the second half of July 2021 and June 2022, the initial and final seismic surveys were performed before and after CO_2 injection. The site was near the OR-Reykjavìk Energy Geothermal Plant located at Hellisheidi, Iceland. These surveys are meant as the base active-source seismic surveys for monitoring, imaging, and reservoir characterization during the cumulative CO_2 sequestration, in the form of mineralization, at the site. As part of a cooperation agreement with ETH Zurich, we also performed a passive-source seismic survey using 148 three-component SmartSOLO seismic stations, provided courtesy of ETH Zurich and OR. The SmartSOLO stations were installed along two perpendicular lines – one of 92 stations and another of 56 stations. The longer line was laid along the helically wound optical cable of Silixa, which served as distributed acoustic sensing during the active-source survey. For Kizildere, Turkey, only the initial survey has been performed in February 2023.

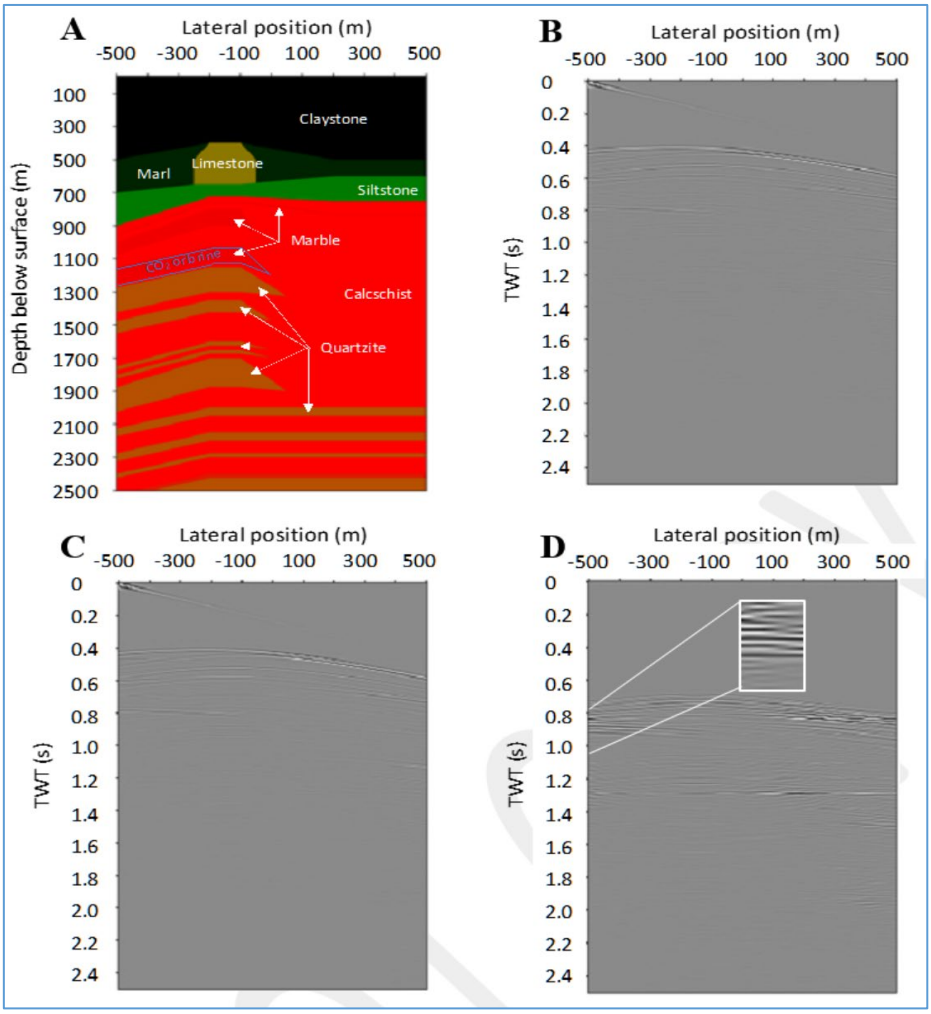

Figure WP4.12: A, Kızıldere subsurface model from earlier work (Janssen et al. 2021); basic concept. B, Special emphasis on the marble layer for CO_2- and brine-saturated velocities from the laboratory measurements (WP1, WP3) were used. Single shot gathers for the case of the marble layer saturated with CO_2 and (C) the same as (B) with brine. (D) Difference panel after subtraction of C from B. The amplitudes in the difference panel were increased with a factor 1,000 for visualization purposes. Here, only one source location was modelled, i.e., at x=-500 m. Receivers were placed at the surface with a spacing of 5 m. TWT stands for two-way travel time.

The passive survey at Hellisheid recorded continuously the ambient seismic noise, including the local, regional, and global seismicity, but also the active seismic shots, for about seven days. The passive data is meant to be used for imaging and reservoir characterization in the inline direction (along the helically wound optical cable) but most importantly in the crossline direction (perpendicular to the helically wound optical cable) to help obtain three-dimensional information of the subsurface structures. This would be achieved applying seismic interferometry to turn the passive recordings of the ambient noise into virtual-source reflection recordings with virtual sources at each SmartSOLO station. Results of data acquisition and processing has been gathered and disseminated in the reviewed article by Hassing et al. (2023).

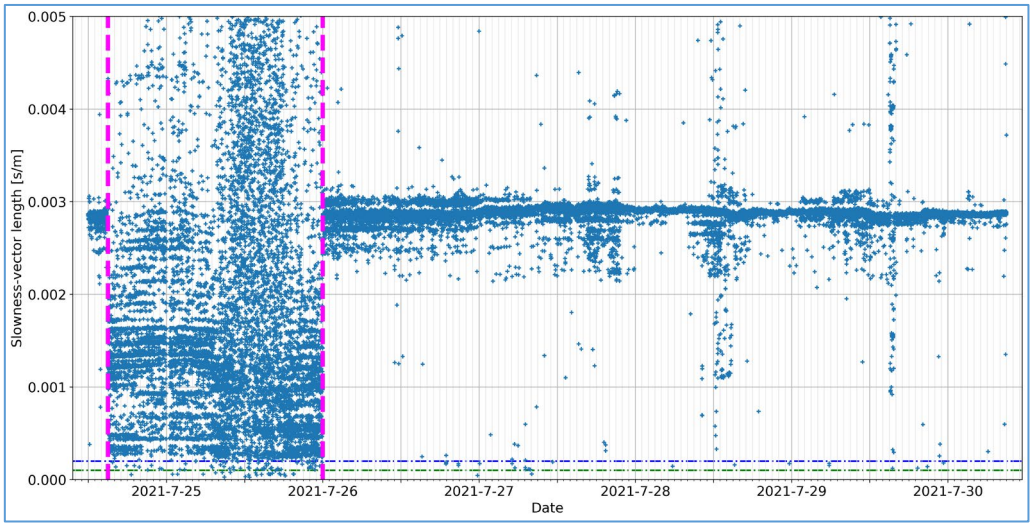

Figure WP4.13: From S.Hassing et al., 1923. Results of the illumination analysis as the length of the slowness vector plotted through time. Every marker indicates the dominant slowness of a single noise panel by using the results from each geophone line as a vector element. The figure shows a clear horizontal band around 0.0029 s/m. This pattern is broken up in the area between the vertical purple lines, where a larger spread in slowness values can be found. Horizontal blue and green dash-dotted lines indicate the selection criteria for panels in creating the stacked and zero-offset images, respectively.

Literature referred to and created through WP3

- Brodic, B., De Kunder, R., Ras, P., Van den Berg, J., and Malehmir, A., 2019a. Evaluation of signal properties of a prototype electromagnetic vibrator using MEMS-based landstreamer and wireless seismic recorders. 16th SAGA Biennial Conference & Exhibition 2019, Durban, South Africa, Extended Abstracts.
- Brodic, B., De Kunder, R., Ras, P., Van den Berg, J., and Malehmir, A., 2019b. Seismic Imaging Using Electromagnetic Vibrators-Storm versus Lightning. Near Surface Geoscience Conference & Exhibition EAGE, The Hague, Netherlands, Expanded Abstracts, Tu_25th_B04.
- Brodic, B., Ras, P., de Kunder, R., Guy, D., and Malehmir, A., 2021a. Seismic imaging using an E-vibe - A case study analyzing the signal properties of a seismic vibrator driven by electric linear synchronous motors (LSM's). Geophysics, 86, 1-49.
- Hassing, S.H.W. Deyan Draganov, Martijn Janssen, Auke Barnhoorn, Karl-Heinz A.A.Wolf, Jens van den Berg, Marc Friebel, Gijs van Otten, Flavio Poletto, Cinzia Bellezza, Erika Barison, Baldur Brynjarsson, Vala Hjörleifsdóttir, Anne Obermann, Pilar Sánchez-Pastor, Sevket Durucan. 2023. Imaging CO 2 reinjection into basalts at the CarbFix2 reinjection reservoir (Hellisheiði, Iceland) with body-wave seismic interferometry. In Geophysical Prospecting, Manuscript GP-2023-4339. DOI: 10.1111/1365-2478.13472 Open article.
- Hassing, S., Draganov, D., Barnhoorn, A. and Janssen, M., 2022, November. Imaging the CarbFix2 Reinjection Reservoir at Hellisheiði, Iceland, with Body-Wave Seismic Interferometry. In: 2nd EAGE Conf. on Near Surface in Latin America (Vol. 2022, No. 1, pp. 1-5). EAGE.
- Sverre Hassing, 2023. Body-wave seismic interferometry on passive seismic data for imaging CO2 reinjection at the Hellisheiði geothermal power plant, Iceland. MSc-thesis. http://resolver.tudelft.nl/uuid:f1baaf83-74c2-4438-8090-1dc01305c918
- Kragh, E., and P. Christie, 2002. Seismic repeatability, normalized rms, and predictability, The Leading Edge, vol. 21 (7), 640-647.
- Noorlandt, R., G. Drijkoningen, J. Dams, and R. Jenneskens, 2015, A seismic vertical vibrator driven by linear synchronous motors: Geophysics, 80, no. 2, EN57–EN67, doi:10.1190/geo2014-0295.1
- Tranter, Nick & Kunder, Richard & Turner, Ben & Drijkoningen, Guy. (2022). Acquiring Sustainable, Efficient High-Resolution Seismic Data for Geothermal Exploration in an Urban Environment. First Break. 40. 47-50. 10.3997/1365-2397.fb2022082.

Work Package 5: Reservoir modelling of alternative injection and reservoir performance scenarios.

Task 5.1: Development and update of a dynamic reservoir model of the Kizildere geothermal field using data from WP's 1, 3 and 4.

Practically all activities have been attributed to SM with contributions by DUT. Most of the results and already explained in WP4.
The hydrothermal system of the Kizildere geothermal field contains a convecting fluid mixture. It is heated at depth and then by buoyancy returned to the surface at dropping T,P in a non-isothermal and a continuous state of flow. Hence, a realistic predictions of reservoir performance under exploitation, needs a construction of the original geological system with P,T-distributions, and fluid flow. Hence the static model from the baseline seismic activities, well information and petrophysics, provides the basic elements for the determination of a reservoir configuration with in-situ conditions. Hence, the field calibration of the new eVibe, combined with the continuous data acquisition of Silixa and the petrophysical and geophysical interpretation by OGS, ICL, METU and DUT, created static reservoir models and defined the overburden. In the previous chapters with supporting data for model definition, we recommend you checking the *figures WP1.22,23,24,25,26, WP3.8, WP4.5,7,12 and 13. This description then is be used by ICL and METU as a set of initial conditions for history-matching, and for predictive time dependent calculations of the effects of fluid production and reinjection upon the reservoir.*

For more details, we refer to the Final Report and Periodical Reports with ERA-ACT and the SUCCEED website.

Work Package 6: Techno-economic assessment and optimization of a field-wide/regional CO_2 injection strategy for the Menderes Graben.

Task 6.1 Development of field and regional scale fluids and CO2 injection strategies.
Task 6.2 Well selection and injection rate optimization for long term pressure maintenance, geothermal fluids production and minimization of injected CO2 production.

The main objective of WP6 was the development of optimized field and regional scale fluids and CO_2 injection strategies for long-term reservoir pressure maintenance and CO_2 storage in the geothermal fields. The aim was to evaluate upscaling methods for single operation, and for the wider geothermal systems, i.e. the Büyük Menderes basin. Here DUT supported ICL.

Development of field and regional scale fluids and CO_2 injection strategies
During the project meetings in London (ICL) and in Kizildere (ZORLU), DUT and SM contributed by quantification of spatial characteristics for the interpretation of reservoir properties, overburden properties, geophysical imaging of the geological structure, extension of the reservoirs and overburden properties. At the first stage it was based on fieldwork and professional knowledge from previous project activities. However, after arrival of samples, preparations, and experimental work in Delft, ICL and METU and the first fieldwork results from Iceland by SM, OGS and Silixa, the creation of static and dynamic reservoir models were an added value for the well selection and injection rate optimization for long term pressure maintenance, geothermal fluids production and minimization of injected CO_2 production and maximization of CO_2 storage.

Well selection and injection rate optimization for long term pressure maintenance, geothermal fluids production and minimization of injected CO_2 production

During the project meetings in London (ICL) and in Kizildere (ZORLU), DUT and SM contributed by quantification of spatial well and reservoir rock characteristics for the interpretation of petrophysical reservoir properties, overburden properties, geophysical imaging of the geological structure, and, extension of the reservoirs.

For the report on economic model development and assessment of the economic performance of optimal strategies given market uncertainties and business development considerations. The lab and fieldwork data provided from WP1, WP3 and WP4, helped to improve well placement optimization algorithms to be considered by ICL and METU.

For more details, we refer to the Final Report and Periodical Reports with ERA-ACT and the SUCCEED website.

Work Package 7: Life-cycle environmental impacts, stakeholder/public communication, education, and training.

Task 7.2: Stakeholder/community perception and engagement.
Task 7.3: Training and educational activities.

Stakeholder/community perception and engagement
For DUT and SM, the understanding of public perception was embedded in demonstration activities showing researchers working in this project and bringing industry in contact with our findings.

For community:

- Internationally, the front window of SUCCEED by ICL was used, i.e. https://www.imperial.ac.uk/energy-futures-lab/succeed/
- For the Netherelands we used:
  A. For DUT, we used; *https://www.tudelft.nl/citg/over-faculteit/afdelingen/geoscience-engineering/research/geothermal/geothermal-science-and-engineering/research/succeed*
  B. For SM we used: https://seismic-mechatronics.com/ . Especially the topic “Zero-Carbon Seismic Acquistion Minizing environment impact by using the eVibe and enabling a zero-emission service.” Will be brought to the attention.
- We had interviews through “Delft Integral”, the newsletter of the University for the public and journalists.
  A. Dutch: https://www.tudelft.nl/delft-integraal/articles/bruiswater-voor-meer-stroom
  B. English: https://www.tudelft.nl/en/delft-outlook/articles/carbonated-water-for-steam-and-power
- For high school level it was visualized in visual presentation about Hellisheidi. One for Kizildere was never finished, since ZORLU never finished this project.
  A. Dutch: https://www.tudelft.nl/citg/onderwijs/student-stories/co2-problemen-oplossen-met-vulkanische-stenen
- B. English: https://www.tudelft.nl/en/ceg/education/student-stories/volcanic-rocks-solving-co2-problems

For Stakeholders:

- Various activities have been developed, where SM has been presenting their equipment and results in conferences and workshops of the EAGE, EGU, SGE, SPE, IPCC, COP as being the largest meetings (+10.000 members and conference attendants). The results are presented in conference papers (See the literature output section).
- SUCCEED workshop: presentations for the industrial reviewes through VEEGEO BV. By TUD and SM on the development of the EVib and Laboratory Georesults. Delft, October 2019.
-
- CO2GeoNet Open Forum, September 2022. Represented through ICL, +90 attendees. Presentation of the SUCCEED results in Iceland and Turkey.

- SM and DUT present environmental sustainability profile presentations, such as clean seismics in urban areas, through short communications to industry: https://pure.tudelft.nl/ws/portalfiles/portal/136166263/fb2022082.pdf
- 20 April 2022, The Hague. TU-Delft presented the SUCCEED program to the Dutch Petrophysical Society for professional geoscientists and engineers as being representatives for the sub-surface industry and government. Ca.25 attendees. K-H. Wolf: "The ACT-SUCCEED program, where CO_2-storage meets enhanced geothermal reservoir performance."
- In November 2022, DUT and SM presented their work in Kizildere/Denizli, Turkey, 46 attendees from the geothermal industry and central and local authorities.
- In the Chamber of Commerce, SM is the 12th out of top 100 of most innovative companies' https://www.kvkinnovatietop100.nl/site/Seismic-Mechatronics-Emissie-vrij-seismisch-onderzoek

Figure WP7.1 Stakeholders meeting and workshop at ZORLU-offices, November 2022.

For training and educational activities:

- In November 2022, DUT and SM presented their work in Ankara, Turkey, +35 attendees mostly from academia..

- DUT, has decided to apply the used methods and techniques of fieldwork, lab work, monitoring and reservoir activities in BSc-lectures, MSc-lectures and practical activities for:
  - BSc-Petrophysics, i.e. rock mechanics & acoustics.
  - BSc- field development course, i.e. cyclic storage.
  - MSc-Environmental engineering in the regular programs for Geo-energy and cross-over topics for sub-surface storage:
  https://filelist.tudelft.nl/TUDelft/Onderwijs/Opleidingen/Master/MSc_Applied_Earth_Sciences/Programme/Brochure%20Cross-Overs%20Final%20v2.pdf
- In Circextin, an Action2 ERASMUS+ program named "Cooperation for innovation and exchange of good practices" (Project nr: 2020-1-PL01-KA203-082089), aspects of the field activities, laboratory work and public awareness achievements have been implemented in a MOOC platform (Massive Online Open Course) in which the following two activities have been implemented and organized by DUT:
  1. Mining waste management/underground storage and circular storage of CO_2 and H_2.
  2. Waste storage and disposal.
  This MOOC was meant for strategic partnership building between European Universities and Industries and support for higher education for post-graduates. https://www.circextin.eu/
- Further, most of the educational and research output, what is not under embargo or IP-confidential, is available for common use from the SUCCEED website at ICL (https://www.imperial.ac.uk/energy-futures-lab/succeed/) and TU-Delft research portal (https://research.tudelft.nl/).

For the consortium management

- The following ACT Workshop and Reporting sessions have been attended and/or contributed to:
- 4th ACT knowledge sharing workshop in Athens, 6-7 November 2019.
- 5th ACT knowledge sharing workshop, virtual on 16 November 2020.
- 6th ACT knowledge sharing workshop in Rotterdam, 9-9 June 2022.
- SUCCEED workshop: presentations for RVO reviewers. By DUT and SM on the development of the EVib and laboratory georesults. Delft, Summer 2023.
- Quarterly Traffic Light Reports to ACT.
- Yearly Progress Reports to RVO.
- The regular TEAMS Meetings with partners are displayed in figure WP8.1.

Work Package 8: Project coordination and management.

Task 8.2: Project planning, monitoring, and execution.
Task 8.3: Technical Co-ordination of the activities at project level.
Task 8.5: Communication and dissemination.

Project planning, monitoring, and execution,
In close cooperation with ICL, DUT participated in the Project Management by the preparation of Project Periodic Meetings, minutes, and periodical reports. Here below, a copy of the meeting agenda is depicted, showing 20 gatherings organized by the consortium management.

Project Progress Meetings

- Meetings with Zorlu Energy Management on 03 September 2019 in Istanbul
- Project Kick Off Meeting on 25 – 26 September 2019 at Kızıldere
- Project Fieldwork and Meeting on 26 November 2019 at Hellisheiði
- Project Meeting on Kızıldere injection and monitoring wells on 23 December 2019 in Ankara
- Project Fieldwork and Progress Meeting on 26-28 February 2020 at Kızıldere
- Project Progress Meeting on 06 June 2020, Virtual
- Project Progress Meeting on 04 September 2020, Virtual
- Project Progress Meeting on seismic monitoring planning on 19 October 2020, Virtual
- Project Annual Progress Meeting with ACT on 23 October 2020, Virtual
- Project Progress Meetings on each Work Package during May 2021, Virtual
- Data sharing arrangements with the Swiss Seismological Service at ETH Zurich and the Coseismiq project early in 2020 and arrangements to share field resources with the ERA-NET Geothermica project DEEPEN around the Hengill volcano and the geothermal field during July 2021 SUCCEED field seismic survey
- Project Mid Term Review Meeting 15 June 2021 and organisation towards that, Virtual
- Virtual meetings between partners throughout to planning of the July 19-31 2021 field work in Iceland, reporting and collaboration
- Project Progress Meeting with ACT on Wednesday 17th November 2021, Virtual
- Virtual meetings between Imperial, METU and Zorlu every fortnight planning CO2 injection infrastructure at Kizildere
- Virtual meetings between Imperial, TUDelft, OGS, Silixa, OR, Mechatronics planning the June 2022 field survey
- Project meeting at Hellisheiði during 2nd seismic survey in June 2022
- Virtual meetings between Imperial, Zorlu, METU, TUDelft, OGS, Silixa, Mechatronics planning the October 2022 field FO cable installations and 1st seismic survey
- Meetings between ALL to organise the Stakeholder Workshop at Kizildere and a technical seminar at METU in Ankara on 01 and 04 November 2022
- Regular meetings between partners and the Coordinator since November 2022

Figure WP8.1: SUCCEED Project Progress Meetings over the entire program.

The minutes contain information and project results, monitoring agreements on the dissemination of project results after establishing a review procedure for all project deliverables before their submission in the public domain. Reports have been made for:

1. through ICL, for ERA-ACT. Those reports according to the contract; monitoring the time planning, progress and tracking of deliverables, milestones, and dissemination activities through the monitoring tool; Milestones and delays are reported, ensuring that the project execution is carried out in line with the work plan, the ERA-ACT contract, and the Consortium Agreement. Deviations from the work description and

implement remedial processes are explained. The reports, as far not under embargo or withheld by IP can be requested.

2. By DUT and SM for RVO. This reporting involves the Dutch part of the activities that has been supported by RVO. Here we follow the content of the previous and place the results within the framework of cooperation with the other European partners in the program. Further, our peer partner VEEGEO-BV was informed when requested through the entire course of the project. Moreover, until November 2022, research meeting for RVO-DIMOPREC and RVO-SUCCEED were a monthly occasion to inform about and discuss technical results and project continuation. This was on a voluntary base.

The technical co-ordination of the activities at project level.
DUT cooperated with the organization of steering and meeting events mostly through TEAMS or ZOOM sessions with Work Package Leaders for the technical progress on:

- Preparations of site inspections, geological fieldworks, rock sampling and transport.
- Preparations on the production of experimental rock samples for DUT, ICL and METU, following the guidelines and checking the specific types of laboratory experimental work.
- Review and integration of technical progress on the geological, petrophysical, geophysical and geochemical output, such that the activities in WP1, WP3 and WP4, were available and implemented in WP5, WP6 and WP7.
- Interaction of SM with OGS, DUT and Silixa for parameter definition for the construction and trial of the eVibe and the reciprocal data transfer of the initial demonstration and field results. This interaction has been essential for the arrangements needed to perform the geophysical fieldwork in Iceland and Turkey. Among others, lay outs for source and sensor distributions, transport of materials, choice and preparation of monitoring and injection wells and data storage, data handling and interpretation distribution for modelling, have been arranged.

Communication and dissemination.
DUT, as presented in WP7, assisted as the coordinator for The Netherlands, with the introductions for the kick-off meeting and sessions for external stakeholders and project support, i.e. RVO, ERA-ACT.

The coordinator prepared activities for the design of project branding through the websites, interviews, publications, dissemination of publications and presentations and communication. The results are described in WP7 and the literature section. For all but the final fieldwork, the reporting has been compiled and translated to reviewed articles, presentations and conference abstracts that are publicly available (See the literature list here below).

□ Results of the project (B)

Results of the project for spin-off and follow-up activities

Results of the project for spin-off

The development and implementation of the eVibe.
The entire fieldwork program provided most of the parameters to construct a new type of eVibe by SM.

- This seismic vibrator has an electric linear synchronous motor (LSM) and can be considered as a promising result for sustainable geothermal exploration in urban regions and protected nature conservations settings across Europe and the world. It has a very small and clean footprint. Minimal or no emission, higher quality and lower amplitude vibrations, constrained noise and by that minimal or no impairment make it easy to use almost everywhere.
- Unlike hydraulic vibrators, the eVibe maintains consistent performance across the entire frequency spectrum, reducing signal distortion, particularly at lower frequencies. This advancement has led to high-resolution imaging.
- The repeatability of the eVibe system surpasses that of hydraulic systems, resulting in superior imaging in both shallow and deep surfaces, as well as significant improvements in surface-wave analysis, despite hydraulic vibrators exerting five to fifteen times more force. Consequently, this has led to enhanced drilling and production assessments.

As a spin-off, the eVibe is useful for sustainable project development and monitoring.

- The motor is supported by electric power generation, which could be a CO_2-emitting generator. However, the construction of a powerful battery makes it possible to run the source generator for a full working day. At night, the battery will be recharged, and by that increasing the energy efficiency of the entire fieldwork.
- Transfer: The eVibe is easily moved by small carriers through living areas and rough landscapes, through the entire season and in extreme climate conditions. So, the damaging of infrastructure and harming of natural habitats is minimal.
- Position: Because of its ability to provide continuous repeatable and constant signals, the eVibe, as a source, can be used for constant monitoring of in-situ processes, such as dissemination of CO_2 in storage projects; CO_2-EOR/EGR activities; Geothermal enthalpy production and return water injection; Cyclic H_2-storage; Sub-surface movements from volcanic activities; and other initiatives where human interaction with the in-situ geological structures create time depending petrophysical changes.
- The economical advantage. Now, after the development, the development and building of eVibes is financially very attractive, since the running costs are much lower than those of conventional methods. The quality of the signals generated and the resulting data acquisition, proves that a risk reduction in data-quality and improved repeatability provides superior imaging and better appraisal results for enhanced drilling and production assessments. Costs are considerably lower than those from conventional systems.

Commercial Spin-off.

For SM, this project helped to launch monitoring and imaging activities in the following 8 projects in various countries.

- Sustainable projects: 1. Geothermie Eindhoven; 2. Geothermie Breda; 3. Geothermie Amsterdam; 4. Geothermie Lelystad.
- Environmental and research projects: 5.CCUS, North Dakota; 6.The Einstein Telescope 2D (potentieel 3D); 7.TNO VSP.
- Conventional exploration projects: 8.Nothern Australia Oil&Gas.

The laboratory work and field activities as a spin-off to imaging and modelling.

- The petrographical, petrophysical and geophysical experiments in the laboratory have been done on various scales and under various temperature, stress, and pore pressure conditions and with both brin and CO_2. In cooperation with ICL (geochemistry) and METU (Rock mechanics), a database was created for a volcanic and intrusive geological environment on the prediction rock fluid interaction characteristics and associated geophysical response changes. Moreover, it resulted into datasets that that have been used to create acoustic speed models.
- These acoustic representations were used to determine the field lay-out for monitoring systems, i.e., the iDAS fiber-optic surface lines and in wells, the stand alone three-component SmartSOLO geophones and station and the conventional recording by two-component cabled geophones (10 Hz). Then the three results have been compared to each other to verify the quality, and robustness of the continuous passive seismic results of the iDas system. The reporting by S. Hassing (2023) is the base for the working method to perform time lapse imaging during an injection period.
- The resulting images for Hellisheidi and Kizildere where the base for the reservoir model configurations of the reservoirs and overburden. Results on stress and temperature related rock/fluid interactions and the related petrophysical and petrological results, were the base for scenario modelling and life-cycle impact predictions.

As a spin-off, the method of working proved to be effective and ready for dissemination in journals and for implementation in future storage projects or cyclic exploitation of the sub-surface.

- As figure AP1 shows, all work packages within SUCCEED reveal that in an enhanced approach, novel equipment, and data-acquisition methods, result into a time related continuous geophysical monitoring with higher resolution geological images as a base for geological reservoir building. By using relevant laboratory input, prediction of the sub-surface processes and associated environmental occurrences, it leads to better continuous supervising of the operation.
- The environmentally friendly approach provides tools for a better assessment of the life-cycle prediction during and after the entire operation.
- The combined suite of newly developed equipment and monitoring tools, provide less time-consuming procedures to perform appraisal, production, and reclamation activities. Hence, cost may reduce considerably for the entire life cycle of the exploitation.

Discussion

The energy sector and mineral exploration industry are faced with the challenge of supplying sustainable energy and crucial raw materials for the long term. To guarantee this offer, cost-effective, sustainable, CO_2-low or free innovations are needed. In addition, CO_2 storage is one of the better options for compensation in cases where industrial production of CO_2 cannot be avoided. For partly sustainable opportunities, such as geothermal energy, the long-term assurance of green energy production may be supported by improvement of the reservoir integrity through CO_2 injection. The origin of the CO_2 then can be the original reservoir steam or captured from flue gas or air. SUCCEED was able to prove this concept.

The project results here presented show that large steps can be made to reduce emission. However, the economical, geographical, and geological conditions must be such that the demonstrated method can be applied. Consequently, for any of the conditions previously mentioned being not available, the system needs to be adapted by a realistic replacement. However, the content of the other conditions still can be applied directly or in a modified way. Examples are not always preferred CO_2 enhanced oil/gas recovery; cyclic system developments for underground CO_2 heat pumps; sub-surface hydrogen storage cushioning; and CO_2-storage in

aquifers/water drive. For other areas with other geological signatures, like low heat flow, opportunities have been discussed with VEEGEO BV. Thinking of enthalpy mining of warm water, as abundantly available in the Netherlands, the return water might be enriched with local CO_2 for storage and improvement of reservoir pressure. As already investigated by Salimi et al. (2012), for the Ammerlaan concession geology, a model explained the possibilities for temporary and permanent storage of CO_2 in a cyclic enhanced geothermal system.

In all, the SUCCEED program proved that for high temperature geo-systems it is possible to produce steam for electricity generation with the reinjection of CO_2 with the return water and that with

1. a new electrical vibrator and newly developed continuous monitoring,
2. it is possible to image and predict the origin of the reservoir for production and injection, and
3. the monitoring of large-scale processes in the sub-surface over the entire appraisal, exploitation and close-off period is feasible.
4. With the new equipment and tools, both timelines for active interference and related costs most probably will be reduced.
5. Moreover, the integrated approach of this project as a whole or in parts can be used under other geographical and geological conditions, with or without adaption of the project components.

Salimi, H., Wolf, K.H., Bruining, J., 2012. Negative Saturation Approach for Non-Isothermal Compositional Two-Phase Flow Simulations. In: Transport in Porous Media, 91 (2), 2012, Springer Science+Business Media B.V. https://doi.org/10.1007/s11242-011-9851-5

□ Conclusions and recommendations

Conclusions for the project per WP

All project parts have been completed or almost realized, which means for the Netherlands, i.e. DUT and SM that:

In WP 1, mostly *DUT with SM*, performed all geotechnical fieldwork on the sites of Hellisheiði and Kizildere have been surveyed. At the surface, the locations for the by two-component cabled geophones (10 Hz) along and the helically wound cable have been determined. Where possible, options for additional recording was also prepared with two perpendicular lines of three-component stand-alone geophones (Iceland) and fiber optics cables in two monitoring wells. In addition, geological surveys in the vicinities of the test sites made it possible to characterize the reservoir and overburden rocks. For Turkey, two tons of representative samples have been collected and transported to Delft. *For Iceland, the sampling and transport of rocks was delayed by 16 months and done after the Covid lock downs and snow period.* All samples have been cored and petrographically. geomechanically, geophysically and petrophysically analyzed and also sent to partners in METU and ICL for further research win WP2 and WP3. Further, a part of the DUT samples was used for uni-axial acoustic measurements under high P,T for the determination of acoustic speed in the reservoirs and overburden. The results have been shared with the partners involved in geophysical imaging and fieldwork activities. In addition, the outcomes were used for the first imaging of the static profile for determination of source and receiver spacings of the 1st seismic field work.

In WP2, *SM and DUT*, in interaction with the partners, reviewed for both sites the geomorphological situation for the choices to be made for outlays of the surface monitoring lines in Hellisheiði and on the first choice for surface lines and monitoring wells in Kizildere. Regarding the development of technical and operational procedures, it was decided to implement the additional two-component cabled geophones (10 Hz) and place those along the fiber optics lines. To get cost neutral as possible, SM and DUT merged the shipping activities for

both, the vibrator and monitoring equipment and implemented it in the operational procedures, monitoring lay-outs and infrastructure planning.

In WP3, *DUT* has contributed to the rock mechanics and geochemical rock characterizations by the preparation and quantification of the provided cores. In addition, pre-, syn-, and post- analysis CT-scanning quantified the volumetric alterations of the ICL geochemical experiments. In addition, (DUT and ICL) determined the effects of injected CO_2 on the reservoir rock at Kizildere and Hellisheiði, and mobility of the geothermal fluid in the wellbore region/reservoir, and the enhancement of the production conditions such as pressure and mobility. Reservoir and overburden rocks have been triaxially tested under stress with P_{pore}, high T, alternating H_2O/CO_2 saturations. With artificial fractures we recognized changes in seismic signatures and permeability. In the meantime, and parallel to the small-scale experiments (*and with many months of Covid delays*), the large-scale HPHT borehole-simulator has been reconstructed with existing and renovated parts, borrowed peripheral data acquisition equipment and additional need for techtime. Experiments have been performed by using seismic response in an changing basalt and a marble reservoir rock when fractures were saturated by alternating CO_2/brine compositions at different P,T and Sw/Sg. Seismic interferometry have been used to follow the replacement of brine by CO_2. The results of all laboratory experiments are used for the construction of vertical seismic profiles from the surface to reservoir depth, both in original conditions and after reservoir saturation. In addition, the outcomes were used for the first imaging of the static profile for determination of source and receiver spacings of the 2nd seismic field work.

In WP4, *SM* built a repeatable eVibe. The apparatus has been developed, built, and tested in the workshop and field. Thereafter it was successfully used during the two field campaigns in Iceland and in Turkey. Since the Silixa-iDAS system also was innovative, it was decided to add reference measurements by *DUT* in all fieldworks, by using two-component cabled geophones in all monitoring activities. As part of this WP, the seismic-data acquisition campaigns were carried out**.** During the 2021 acquisition, whenever the active source was not utilized, the stand-alone three-component geophones (temporarily lent from the DEEPEN project) also acquired passive-source data (i.e., ambient-noise seismic signals such as local, regional, and global seismicity). Student Sverre Hassing used the passive data for his MSc thesis. He created a passive image of the subsurface, by using seismic interferometry. This is especially relevant for the crossline. As the active source was only located along the inline, no high-quality active image could be obtained for the crossline. *DUT* tried to fill this gap with the construction of a passive image. In November 2022 the baseline, i.e., prior to CO_2 injection, monitoring acquisition was conducted at Kizildere, Turkey. The data was acquired using the seismic vibrator from SM as a source and the fiber-optic helically wound cable from Silixa as 'continuous' receivers. Moreover, conventional geophones from *DUT* were also used, to verify the results obtained with the fiber-optic cable. The goal of this monitoring acquisition is to have a baseline, which we can compare later with data acquired when substantial amounts of CO_2 have been injected. The field data has been disseminated between all partners involved in geophysical monitoring activities. Here, intensive input by *DUT and SM* and in close cooperation with OR, ZORLU, ICL, OGS and Silixa, two successful seismic fieldworks for the Hellisheiði and one for Kizildere. The data-acquisition resulted into good (micro-) seismic data processing for injection induced seismicity (Hellisheiði)and progress of CO_2 injection in the reservoir. For Kizildere, only the baseline activities have been monitored and processed.

In WP5 and WP6, the results of WP1, 2, 3 and 4 produced by *DUT and SM* have been used for reservoir modeling of alternative injection and reservoir performance scenarios. *DUT* and OGS prepared the Kızıldere subsurface model for which the velocity model was taken from our earlier work (Janssen et al. 2021). Now the 3rd marble layer (shown by the blue outline in figure WP4.12), for which CO_2- and brine-saturated velocities from the laboratory measurements can be used with the visualization of the CO_2 dissemination. Thereafter, all previous results have been applied to techno-economic assessment and optimization of a field-wide or regional CO_2 injection strategies, where possible, for the Kizildere region.

In WP7, *DUT and SM* contributed to stakeholder involvements in Denizli and Ankara (Turkey) and The Hague (Netherlands), through the Dutch CATO-program and through public communication such as the Newsletters of DUT and newspapers. Furthermore, various conferences and reviewed publications with regards to the CO_2 injection/storage have been integrated with geothermal technology. In cooperation with the partners, a blueprint was developed and applied to validation of monitoring, modelling and verification methodologies applicable to other high enthalpy geothermal systems.

In WP8, *DUT* was responsible for the project planning, monitoring, and execution, in close cooperation with ICL and participated in the Project Management by the preparation of Project Periodic Meetings, minutes, and periodical reports. Periodical reports were prepared. through ICL, for ERA-ACT on monitoring the time planning, progress and tracking of deliverables, milestones, and dissemination activities through the monitoring tool; Deviations from the work description and implement remedial processes are explained. By *DUT and SM*, similar activities have been reported for RVO. They do involve the Dutch part of the activities that has been supported by RVO. *DUT* cooperated with the organization of steering and meeting events mostly through TEAMS or ZOOM sessions with Work Package Leaders for the technical progress in the laboratory, for fieldwork, for interpretation, modeling and scenario building and particularly the development, construction, calibration and implementation of the eVibe by *SM*. In addition, the Dutch dissemination of results via websites, interviews, (conference) presentations, stakeholder meetings and reviewed publications, have been monitored and processed through the procedures of the SUCCEED program.

Output activities with the involvements of DUT and SM.
Reviewed Literature SUCCEED:

- Janssen M.T.G., Barnhoorn A., Draganov D., Wolf K-H.A.A., Durucan S. 2021. Seismic Velocity Characterisation of Geothermal Reservoir Rocks for CO_2 Storage Performance Assessment. *Applied Sciences*. 11(8), 3641. *https://doi.org/10.3390/app11083641*. Article is Open Access: *https://www.mdpi.com/2076-3417/11/8/3641*.
- Parlaktuna, M., Durucan, Ş., Parlaktuna, B., Sinayug, Ç., Janssen, M.TG., Şenturk, E., Tongic, E., Demircioglu, Ö., Poletto, F., Bohm, G. and Bellezza, C., 2021. Seismic velocity characterisation and survey design to assess CO2 injection performance at Kızıldere geothermal field. Turkish Journal of Earth Sciences, 30(9), pp.1061-1075.
- Janssen, M.T.G, Barnhoorn, A., Draganov, D., Wolf, K. H. A., & Durucan, S. (2021). Seismic Velocity Characterisation of Geothermal Reservoir Rocks for CO2 Storage Performance Assessment. Applied Sciences, 11(8), 3641.
- Janssen, M.T.G., Draganov, D., Barnhoorn, A. and Wolf, K.H.A.A., 2023. Storing CO2 in Geothermal Reservoir Rocks from the Kizildere Field, Turkey: Combined Stress, Temperature, and Pore Fluid Dependence of Seismic Properties. *Geothermics, 108,* p. 102615.
- Sverre H.W. Hassing, Deyan Draganov, Martijn Janssen, Auke Barnhoorn, Karl-Heinz A. A. Wolf, Jens van den Berg, Marc Friebel, Gijs van Otten, Flavio Poletto, Cinzia Bellezza, Erika Barison, Baldur Brynjarsson, Vala Hjörleifsdóttir, Anne Obermann, Pilar Sánchez-Pastor, Sevket Durucan. 2023. Imaging CO 2 reinjection into basalts at the CarbFix2 reinjection reservoir (Hellisheiði, Iceland) with body-wave seismic interferometry. In Geophysical Prospecting, Manuscript GP-2023-4339. DOI: 10.1111/1365-2478.13472 Open article.

Conference meetings and Presentations

- Karl-Heinz Wolf: SUCCEED - Synergetic Utilisation of CO2 storage Coupled with geothermal EnErgy Deployment. CATO-3 meeting, ACT - RVO presentations to the CATO-3 Consortium. 26 November 2019, Utrecht, the Netherlands
- Durucan S., Korre A., Parlaktuna M., Şenti. irk E., Wolf K-H.AA, Chalari A, Stork AL., Nikolov S., de Kunder R., Sigfusson B., Hjorleifsd6ttirg V., Andersen N., Poletto F., 2021. SUCCEED: A CO2 storage and utilization

project aimed at mitigating against greenhouse gas emissions from geothermal power production. Proc. 15th Int. Conf. Greenhouse Gas Control Technologies, 15-18 March, Abu Dhabi, UAE, http://dx.doi.org/10.2139/ssrn.3819789.

- Janssen, M., Russel, J., Barnhoorn, A., Draganov, D., Wolf, K., & Durucan, S. (2020, November). Seismic Velocity Characterization and Modelling for Synergetic Utilisation of CO2 Storage Coupled with Geothermal Energy Extraction. In *1st Geoscience & Engineering in Energy Transition Conference* (Vol. 2020, No. 1, pp. 1-6). European Association of Geoscientists & Engineers. The Extended abstract can be found online: *https://www.earthdoc.org/content/papers/10.3997/2214-4609.202021053*.
- Janssen, M.T.G., Draganov, D., Bos, J., Farina, B., Barnhoorn, A., Poletto, F., Van Otten, G., Wolf, K. and Durucan, S., 2022a, June. Monitoring Co2 Injection into Basaltic Reservoir Formations at the Hellisheidi Geothermal Site in Iceland: Laboratory Experiments. In 83rd EAGE Annual Conference & Exhibition (Vol. 2022, No. 1, pp. 1-5). European Association of Geoscientists & Engineers.
- Janssen, M.T.G., Barnhoorn, A., Draganov, D., and Wolf, K.H.A.A., 2022b. CO2 Storage in Geothermal Reservoir Rocks: A Seismic Velocity Characterization Study. In European Geothermal Congress 2022, Berlin, 17-21 October 2022.
- Janssen, M.T.G., Garcia, E.R., Barnhoorn, A., Draganov, D., and Wolf, K.H., 2022. Storing CO_2 in Geothermal Reservoir Rocks: A Laboratory Study on Acoustic and Mechanical Properties (No. EGU22-4396). Copernicus Meetings. Presentations on baseline seismic response characterization study on Icelandic formations.
- Stork, A.L., Poletto, F., Draganov, D., Janssen, M.T.G. et al. Monitoring CO_2 Injection with Passive and Active Seismic Surveys: Case Study from the Hellisheidi Geothermal Field, Iceland. In 16th International Conference on Greenhouse Gas Control Technologies.
- Hassing, S., Draganov, D., Barnhoorn, A. and Janssen, M., 2022, November. Imaging the CarbFix2 Reinjection Reservoir at Hellisheiði, Iceland, with Body-Wave Seismic Interferometry. In Second EAGE Conference on Near Surface in Latin America (Vol. 2022, No. 1, pp. 1-5). European Association of Geoscientists & Engineers.
- Athena Chalari, Anna L. Stork, Mike Spence, David Boon, Alison Monaghan, Flavio Poletto, Walter Boehm, Erdinç Şentürkh, Mahmut Kaan Tüzen, Richard de Kunder, Ismael Vera Rodriguez, Joseph Wolpert. Jens van den Berg, Deyan Draganov. 2024. Distributed Fiber Optic Sensing for Geothermal Applications. 3rd EAGE Geotech., 2024.
- Athena Chalari, Anna L. Stork, Flavio Poletto, Fabio Meneghini, Cinzia Bellezza, Biancamaria Farina, Ari David, Gualtiero Böhm, Andrea Schleifer, Sevket Durucan, Baldur Brynjarsson, Gijs van Otten, Deyan Draganov, Vala Hjörleifsdóttir, Auke Barnhoorn, Karl-Heinz Wolf, Anna Korre, Anne Obermann, Pilar Sánchez-Pastor, Erdinç Şentürk, Mahmut Parlaktuna. Monitoring CO2 injection with Distributed Acoustic Sensing (DAS) passive and active seismic surveys.

Thesis work:

- Sverre Hassing, 2023. Body-wave seismic interferometry on passive seismic data for imaging CO2 reinjection at the Hellisheiði geothermal power plant, Iceland. MSc-thesis. *http://resolver.tudelft.nl/uuid:f1baaf83-74c2-4438-8090-1dc01305c918*
- Elara Redondo Garcia, 2023. Petrophysical and Mechanical Characterization of the Volcanic Rocks in the Hellisheiði Geothermal Field and implications of Thermal Fracturing in CO2 mineralization. MSc-thesis. *https://repository.tudelft.nl/islandora/object/uuid%3A641e5df2-c411-450d-9095-342673a225a7*

□ Explanation of the method of knowledge dissemination.

During the entire project line, activities and results have been coordinated and disseminated through SUCCEED, mostly via presentations, (reviewed) Journal Articles and online activities:

- Existing dissemination programs such as CO2GeoNet Open Forum and various Professional Societies with conferences involved in CO_2-storage, sustainable energy, and climate.
- The SUCCEED website is the base for all public/open information. Either directly available on the site, or by request, data is available. For the Netherlands, all data is available in Delft-PURE and at a later stage, after project approval, the report is handed over to CATO-II.
- For utilization and education, the Dutch results of the program are implemented in (online) courses at Highschool-, BSc-, MSc- and Post Academic level as (partly online) educational program items, videos and social media. In addition, elements have been used in a MOOC for an Erasmus+ program.

In this way, the public, stakeholders, authorities, and environmental bodies have been informed and educated.

For detailed results, we refer to the activities in WP7.

□ Explanation PR project and further PR possibilities

- For community interaction DUT used and use the international front window of SUCCEED by ICL.
- For the Netherlands DUT uses the Delft Project Site, Delft-PURE and CATO-II.
  Specific for the eVibe activities, the website of SM provides all information required.
- News media, like radio, television, web casts and university periodicals are to be used for interviews.

For Stakeholders interaction, DUT had and will develop opportunities to explain the lab, field and equipment activities.

- Technical and environmental fairs and conferences are attended through stand demonstrations, workshops, and presentations. Here, IPPC, COP, EAGE, EGU, SGE, SPE are important options either for DUT or for SM. Moreover, CO2GeoNet Open Forum occasions are very relevant for continuity of the CO_2 storage commercially related activities.
- For SM and DUT, the environmental sustainability profile presentations, for clean seismics in urban areas, is to be displayed through short communications to industry through business communication channels, regional environmental public bodies and professional geoscience/engineering organizations.
- DUT has decided to apply the used methods and techniques of fieldwork, lab work, monitoring and reservoir activities in BSc-lectures, MSc-lectures and practical activities for BSc/MSc/PhD-lectures and practical activities, but also post graduate courses for Industry. Here we may think of Summerschools and Special Topic Meetings.

□ Acknowledgements

“Het project is uitgevoerd met subsidie van het Ministerie van Economische Zaken, Nationale regelingen EZ-subsidies, Topsector Energie uitgevoerd door Rijksdienst voor Ondernemend Nederland.”

“The project was carried out with subsidy from the Ministry of Economic Affairs, National regulations for Economic Affairs subsidies, Top Sector Energy implemented by the Netherlands Enterprise Agency.”

Acknowledgements II

SUCCEED is funded through the ACT programme (Accelerating CCS Technologies, Horizon 2020 Project No 294766). Financial contributions made by the Department for Business, Energy & Industrial Strategy UK (BEIS), the Rijksdienst voor Ondernemend Nederland (RVO), the Scientific and Technological Research Council of Turkey (TUBITAK), and our research partners Orkuveita Reykjavíkur/Reykjavik Energy Iceland (OR) and Istituto Nazionale di Oceanografia e di Geofisica Sperimentale Italy (OGS) are gratefully acknowledged.